GEM TN-93-292

Technical Note on Fast Calorimeter Simulation for GEM

S. Peter, Yu. Fisyak, K. McFarlane
SSC Laboratory

February 10, 1993

Abstract:

This note describes a first approach to establish a fast and precise calorimeter simulation for the GEM detector within the framework of SIGEM, which is based on GEANT. The note consists mainly of a loose collection of related papers. Its idea is to establish a basis suitable for future development.

++

T E C H N I C A L N O T E O N

F A S T C A L O R I M E T E R S I M U L A T I O N F O R G E M

February, 10th 1993

S. Peters, Yu. Fisyak, K. McFarlane

++

This note describes a first approach to establish a fast and precise calorimeter simulation for the GEM detector within the framework of SIGEM, which in turn is based on GEANT. The note consists mainly of a loose collection of related papers. Its idea is to establish a basis suitable for future development.

C O N T E N T S

- Introductory Remarks
- 'The Fast H1 Detector Monte Carlo' by M. Kuhlen
- Draft 'The Parameterized Simulation of Electromagnetic Showers in Homogenous and Sampling Calorimeters' by G. Grindhammer and S. Peters
- 'The Fast Simulation of Electromagnetic and Hadronic Showers' by G. Grindhammer, M. Rudowicz and S. Peters
- H1 Software note on ' "Calibrated Energies" in the H1 Detector Simulation' by G. Bernardi, W. Hildesheim, M. Kuhlen and M. Rudowicz
- GFLASH 1.4 Users Manual
- Current Status of GFLASH 1.4 in SIGEM

++

I N T R O D U C T O R Y R E M A R K S

++

The aim of interfacing GFLASH 1.4 with SIGEM is to provide GEM with a fast but nevertheless precise program for calorimeter simulation within GEANT.

GFLASH 1.4 is a package for fast calorimeter simulations in the framework of GEANT. It is based on H1FAST, the detector simulation program for the H1 detector at the ep collider HERA (DESY,FRG). The features covered include a proper handling of individual particle tracking in coarse geometries (GEANT mixtures), electromagnetic shower parameterization, optional hadronic shower parameterization, so-called particle terminators, and a very detailed book keeping of all energy losses. Geometrical constraints may be applied to the parameterizations and terminators (eg. prohibit shower parameterization in the vicinity of cracks).

The following topics are covered in the notes included here:

'The Fast H1 Detector Monte Carlo' gives a general overview of the H1FAST approach to a detailed and accurate detector simulation.

The Draft 'The Parameterized Simulation of Electromagnetic Showers in Homogenous and Sampling Calorimeters' reflects the actual status of electromagnetic shower parameterization as used in H1FAST and GFLASH 1.4.

Hadronic shower parameterizations are described in 'The Fast Simulation of Electromagnetic and Hadronic Showers'. The algorithms for both electromagnetic and hadronic shower parameterizations described there are actually part of the fully parameterized detector Monte Carlo GEMFAST.

The H1 Software Note ' "Calibarated Energies" in the H1 Detector Simulation' describes how the detailed book keeping of all energies is used in H1.

The GFLASH 1.4 Users Manual contains a detailed description of GFLASH and its main user interfaces. The corresponding source code is available at SSCL. Please contact one the authors.

Finally the GEM-specific changes to the original code are sketched and the current status is summarized. Recommended future activities are outlined.

THE FAST H1 DETECTOR MONTE CARLO

Michael Kuhlen*†
Max-Planck-Institut für Physik
Werner-Heisenberg-Institut
Föhringer Ring 6
8000 München 40, Germany

Abstract

The simulation of large samples of physics events in the HERA detectors requires special techniques for the time consuming simulation of showers in the calorimeters. The fast H1 detector Monte Carlo is based on shower parametrization where possible without sacrificing precision, and the replacement of the complicated sampling structures of the calorimeter stacks by homogeneous averaged media. This scheme has been implemented in the general framework of GEANT and results in an acceptable simulation time, about a factor 10 faster than the detailed GEANT simulation for typical HERA neutral current events. Comparisons with e and π test beam data show good agreement in those aspects which are typically important for analysis.

INTRODUCTION

In calorimeter simulation three different purposes can be distinguished: calorimeter studies, physics analysis, and feasibility studies. With decreasing accuracy requirements an increasing simulation speed can be achieved. A very detailed calorimeter geometry description with shower tracking down to very low cut-offs is used for calorimeter studies. It is able to predict the absolute response and resolution "from first principles". The CPU time needed is of the order of 1 s/GeV and scales linearly with the shower energy. This is prohibitively slow for event simulation in physics analysis (e.g. acceptance calculation). Here the CPU time has to be reduced substantially, and the simulation has still to be accurate in those features on which the analysis relies. Finally, for feasibility studies rather crude approximations are possible, and a speed of 0.1 s for 100 GeV showers with a logarithmic scaling law can be reached.

In the following, the H1 concept for fast and accurate event simulation in physics analysis will be presented. The precision is being checked against e and π test beam data, and information on the implementation and timing performance is given.

SIMULATION CONCEPT

A lot of time can be saved by simplifying the geometry description of the detector. The sampling structures of the different H1 calorimeters - alternating layers of absorber and read out material - is replaced by homogeneous volumes filled with mixed media. In

*representing the H1 working group on fast simulation: G. Bernardi, G. Grindhammer, W. Hildesheim, M.K., S. Peters and M. Rudowicz

†Bitnet H1KMKU@DHHDESY3

Talk given at the *XXVI International Conference on High Energy Phyiscs*, Dallas 1992.

these media energy depositions are simulated - no longer the signal itself -, and then mapped onto the actual read out geometry. The signal ("e/mip","e/h" effects) and the desired resolution (sampling fluctuations) are generated in a second step via external response functions.

Most of the signal in the read out layers is produced from low energy shower particles. High cut-offs for low energy particle tracking can be introduced, because the signal (charge) is no longer simulated directly. In addition, particles are terminated when they are likely not to contribute to the signal outside of the current read out cell.

Electromagnetic showers have a high particle multiplicity, making their parametrization advantageous. Hadronic showers on the other hand have lower multiplicity, are more irregular in shape and generally larger in size, usually extending over detector inhomogeneities. Therefore only electromagnetic subshowers in the cascade are being parametrized, and only if they do not extend over cracks between calorimeter modules. Parametrization over cracks is not allowed because it leads to an incorrect description of the amount of energy lost in dead materials. Punch through is simulated naturally because the hadrons in the cascade are tracked individually.

A general e.m. shower parametrization has been developed[1], which simulates longitudinal and lateral shower shapes as well as their fluctuations and correlations. It can be applied to all homogeneous and sampling calorimeters, and depends explicitly only on the radiation length X_0, the Molière radius R_M, the critical energy E_c, the nucleus charge number Z and the sampling frequency in the case of sampling calorimeters.

IMPLEMENTATION

The fast Monte Carlo (MC) is implemented in the general framework of GEANT[2] for geometry description and particle tracking, while GHEISHA[3] or FLUKA[4] produce hadronic interactions. On an HP 9000-720 workstation, the average simulation time is about 2 s/evt. for e^- of 100 GeV, 7 s/evt. for 100 GeV π^-, and 50 s/evt. for a typical sample of HERA neutral current events.

A complete book keeping of all energy depositions (e.m., hadronic and "invisible", i.e. energy lost in a nuclear reaction) in all parts of the detector allows to reconstruct the response *after* simulation with simple response functions, which are basically sums over the smeared true energy depositions[5,6]. This flexible scheme offers the possibility of quick retuning with different response functions, including a perfect one to check reconstruction algorithms. In addition, the absolute energy scale of the MC is intrinsically correct, because energy is simulated directly.

COMPARISON WITH DATA

Extensive checks of the simulation program against test beam data of different H1 liquid argon calorimeter modules with electrons and pions of energies ranging from 5 to 200 GeV have been carried out[1,6], of which only a selection can be shown here. The modules consist of an e.m. section (lead/liquid argon) followed by a hadronic section (iron/l.ar.).

In figs. 1 and 2 lateral and longitudinal shower profiles for 10 GeV electron showers are shown for the MC and the data. The lines represent at each point the mean of the energy distribution plus its RMS, giving a measure for the shower to shower fluctuations. Not only the average shapes agree well, but also the shape fluctuations are well reproduced, in fact data and MC are hard to distinguish. A good description of the measured resolution was almost trivially achieved with a simple resolution function applied to the stored true energy depositions (not shown here). With the

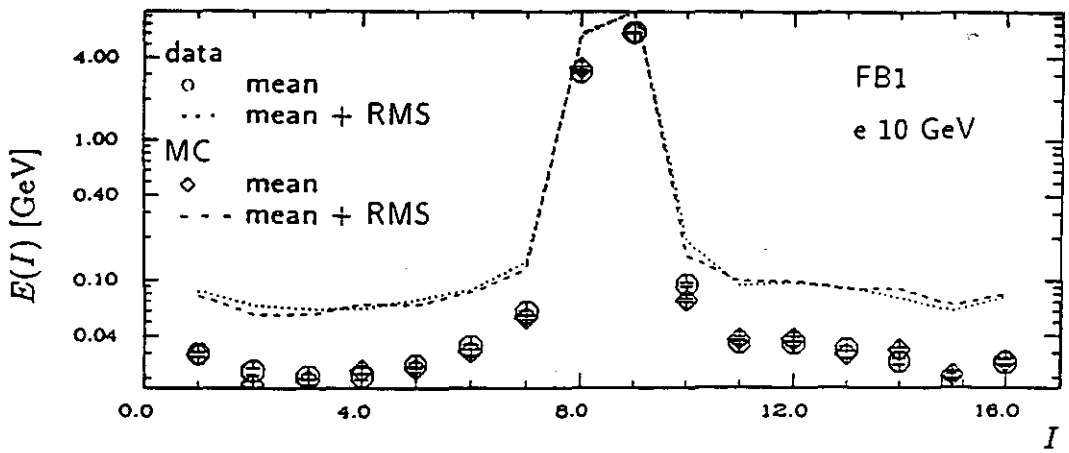

Figure 1. Lateral profile for 10 GeV e^- showers. The coordinate I corresponds to the transverse pad number.

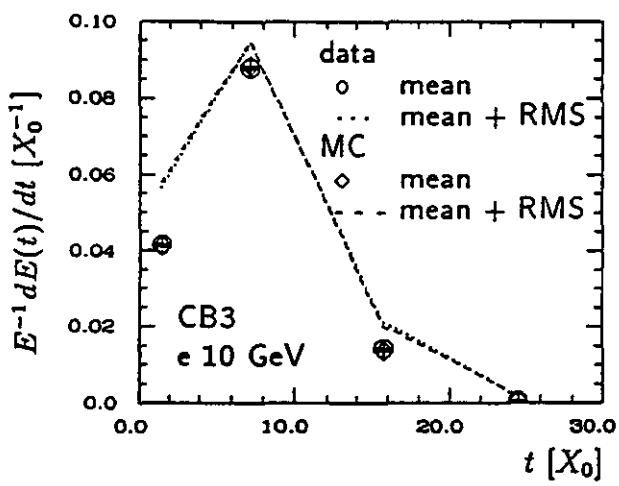

Figure 2. Longitudinal profile for 10 GeV e^- showers. The depths t of the readout layers are given in units of X_0.

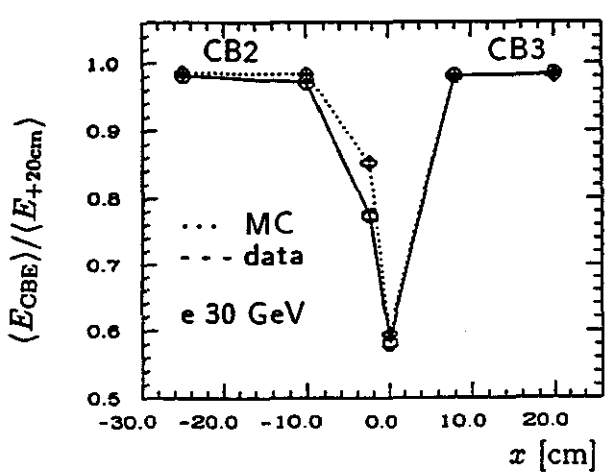

Figure 3. Electron scan over crack between modules. The coordinate x gives the impact point of the beam. Plotted is the energy in the e.m. section, normalized to the total energy seen at $x = 20$ cm.

concept of conditional shower parametrization also the reduced response over the uninstrumented region between two adjacent calorimeter modules can be modelled (fig. 3).

The energy depositions of 30 GeV pions in the e.m. and hadronic sections of the calorimeter as well as the sum of both are shown in fig. 4. In general, the distribution of energy across the discontinuity between the two different modules is well simulated, though at closer look GHEISHA can be seen to generate too many events which are almost completely absorbed in the e.m. section, in contrast to FLUKA. The sum of both modules yields the right response ("h/e") for the non-compensating H1 calorimeter, and also a good description of the π^0 and sampling fluctuations.

Among other quantities, H1 plans to use for e/π separation the energy of the hottest cell in a shower, plus the energy of its three most energetic neighbors. This estimator E_{H4} is expected to be large for compact e.m. showers, where most of the energy is deposited in a few cells, while for pionic showers of the same energy E_{H4} is much smaller, as shown in fig. 5 for e and π data. The fast MC is able to reproduce these features in detail, and in particular allows a reliable estimate of the π background under the e peak.

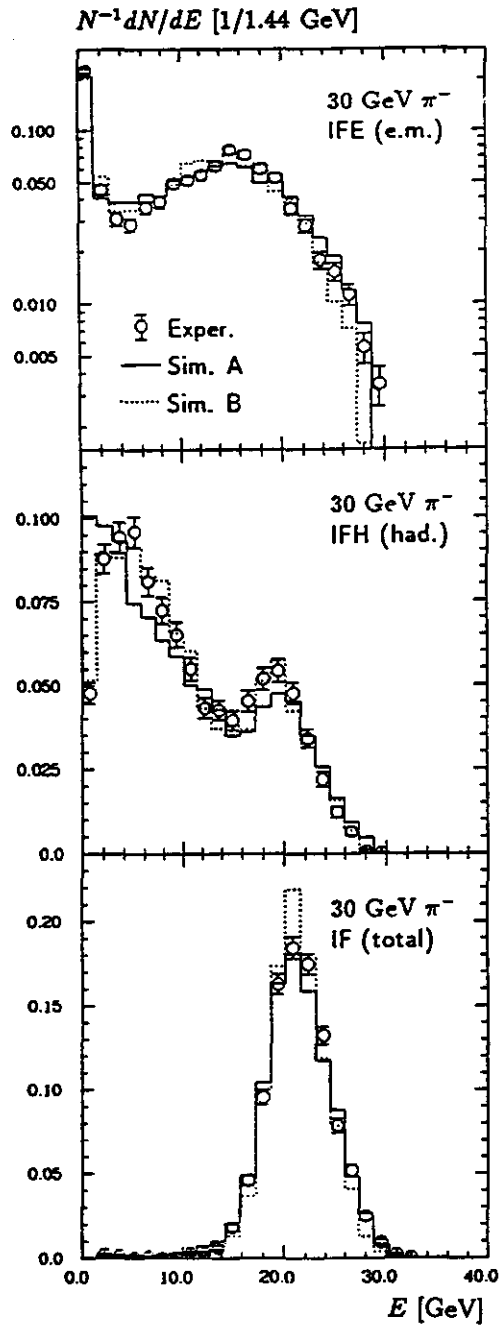

Figure 4. Energy deposition of 30 GeV pions in a l. ar. module: e.m. section, hadronic section and total. The data are compared to the fast simulation based on GHEISHA (A) and FLUKA (B).

To conclude, the fast MC is now the standard choice for massive event simulation in H1, and our results demonstrate its validity for the extraction of physics from HERA events.

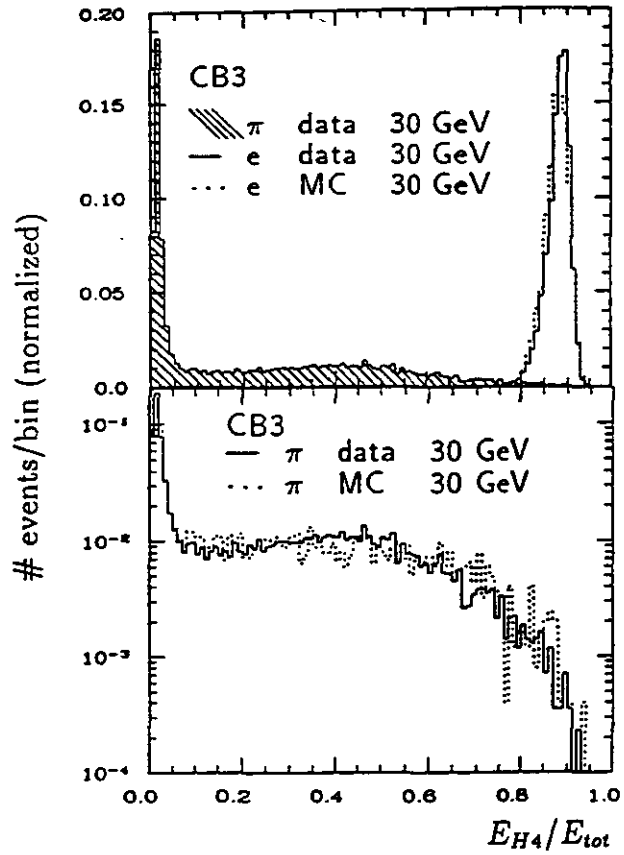

Figure 5. Estimator for electron/pion separation.

REFERENCES

1. S. Peters, *Die parametrisierte Simulation elektromagnetischer Schauer.* Thesis, Universität Hamburg, 1992.
2. R. Brun et al., "GEANT3 User's GUIDE", CERN-DD/EE 84-1, Geneva 1984.
3. H. Fesefeldt et al., "The Simulation of Hadronic Showers, Physics and Applications", PITHA 85/02, Aachen 1985.
4. P.A. Aarnio et al., "FLUKA 89 User's Guide", Geneva 1990.
5. G. Bernardi et al., " 'Calibrated Energies' in H1 Detector Simulation," *H1 Software Note* 26, (1991).
6. M. Rudowicz, *Hadronische Schauersimulation für den H1-Detektor.* Thesis, Universität Hamburg, 1992.

The Parameterized Simulation of Electromagnetic Showers in Homogenous and Sampling Calorimeters

G. GRINDHAMMER[a] and S. PETERS[a,b]

[a] *Max-Planck-Institut für Physik, Werner-Heisenberg-Institut, D-8000 München 40, FRG*

[b] *Deutsches Elektronen-Synchrotron DESY, D-2000 Hamburg 52, FRG*

DRAFT 27.01.93

Abstract

A general approach to a fast simulation of electromagnetic showers using parameterizations of the longitudional and radial profiles in homogenous and sampling calorimeters is described. The dependence of the shower development on the used materials and the sampling geometry is taken into account explicitly. Comparisons with detailed simulations of various calorimeters and data from the H1 liquid argon calorimeter are made.

. Introduction

n calorimeter simulation different tasks can be distinguished: calorimeter studies, physics analysis nd feasibility studies. A detailed simulation where all secondary particles are tracked individually .own to some minimum energy is requiered for accurate calorimeter studies. For physics analysis and easibility studies large number of Monte Carlo events have to be produced. Using individual particle racking, the computing time needed for such kind of simulations increases approximately linear with he energy absorbed in the detector and can easily become prohibitive. Using parameterizations for lectromagnetic (sub)showers can speed up the simulations considerably, without sacrificing precision. The high particle multiplicity in electromagnetic showers as well as their compactness and the good nderstanding of the underlying physics makes their parameterization advantegoues.

Jsing an Ansatz by Longo and Sestili [1], a simple algorithm for the description of longitudinal hower profiles has been used succesfully for the simulation of the UA1 calorimeter [2]. Later, this Ansatz has been extented to the simulation of individual showers, taking their shower-to-shower luctuation and correlations consistently into account [3, 4, 5]. For the parameterized simulation of adial energy profiles no conclusive procedure has been established until now.

n homogenous media, a scaling of the longitudinal and radial profiles in radiation lengths rsp. Molière adii does not lead to a material independent description of electromagnetic shower development. In ampling calorimeters, the shower shapes depend in addition on the geometrical design. We have xtented the above Ansatz for parameterized simulation of longitudinal profiles by taking the material nd geometry dependence of the parameters into account and developed a new algorithm to simulate adial energy distributions [6]. Correlations between longitudinal and radial shower development are lso considered.

2 Procedure

To arrive at a general description of electromagnetic shower development, we studied detailed Monte Carlo simulations of various homogenous media and sampling calorimeters, performed with the GEANT package [7]. In a first step only average shower profiles in homogenous Media have been analyzed, from which scaling laws for the material and energy dependence of the parameters have been extracted. Starting from the relations which describe the average behaviour of the parameterized quantities, we developed parameterizations for individual electromagnetic showers in homogenous calorimeters, taking fluctuations and correlations into account.

The parameterizations in homogenous media are a first approximation for electromagnetic shower development in sampling calorimeters, if they are viewed as consisting of one single, effective medium. The inhomogenoues material distribution in sampling calorimeters has, however, influence on the exact behaviour of the shower shapes, eg. the depth of the shower maximum in longitudinal profiles.

This is explained mainly by the transition effect, which turns out to be sensitive to the shower depth [6, 8, 9]. These effects have been considered by adding geometry dependent terms to the parameterizations for homogenous media, which can easily be calculated from the calorimeter design.

3 Parameterization in homogenous media and sampling calorimeters

In the parameterized simulations the spatial energy distribution of electromagnetic showers is given by three propability density functions (pdf),

$$dE(\vec{r}) = E\, f(t)dt\, f(r)dr\, f(\phi)d\phi, \tag{1}$$

describing the longitudinal, radial and azimuthal energy distributions. Here t denotes the longitudinal shower depth in units of radiation lenghts, r measures the radial distance from the shower axis in Molière units, and ϕ is the azimuthal angle. The start of the shower is defined by the space point, where the first electron or positron bremsstrahlungs process occurs. A gamma distribution has been used for the parameterization of the longitudinal shower profile, f(t). The radial distribution, f(r), is described by a two-component Ansatz. And it has been assumed that the energy is distributed uniformly in ϕ: $f(\phi) = 1/2\pi$.

3.1 Longitudinal shower profiles – homogenous media

It is well known, that average longitudinal shower profiles can be described by a Gamma-distribution [1]:

$$\left\langle \frac{1}{E}\frac{dE(t)}{dt} \right\rangle = f(t) = \frac{(\beta t)^{\alpha-1}\beta \exp(-\beta t)}{\Gamma(\alpha)}. \tag{2}$$

The center of gravity, $\langle t \rangle$, and the depth of the maximum, T, can be calculated from the shape parameter α and the scaling parameter β according to

$$\langle t \rangle = \frac{\alpha}{\beta} \tag{3}$$

$$T = \frac{\alpha - 1}{\beta}. \tag{4}$$

Longitudinal electromagnetic shower development in homogenous media has been studied analytically some time ago [10]. An important result of calculations using "Rossis Approximation B" [10] has been, that longitudinal shower moments will be equal in different materials, provided one measures all lengths in units of ratiation lengths (X_0), and energies in units of critical energies (E_c). Numerically, E_c can be calculated according to

$$E_c = 2.66 \left(X_0 \frac{Z}{A} \right)^{1.1} \tag{5}$$

11], and determines the kinetic energy of electrons, where the energy lost in bremsstrahlung equals approximately the ionization loss. For the depths of the shower maximum

$$T \propto \ln y = \ln \frac{E}{E_c} \tag{6}$$

is predicted [10].

It is therfor desirable to use T in the parameterization. This is demonstrated in figure 1, where the average depths of the shower maximum in various homogenous media[1], T_{hom}, is plottet versus y in the energy range from 1 to 100 GeV. As a second variable, α can be used. In this case a parameterization depending on the charge number Z of the material has to be used (figure 2). The lines in both figures correspond to fits to GEANT simulations according to

$$T_{hom} = \ln y + t_1 \tag{7}$$

$$\alpha_{hom} = a_1 + (a_2 + a_3/Z) \ln y. \tag{8}$$

The exact numbers are given in the Appendix (A.1.1), where all formulae and numbers which will be mentioned in the following are summarized.

Assuming that also individual profiles can be approximated by a gamma-distribution, the fluctuations and correlations can be taken into account consistently (for details refer also to [5]). For each single GEANT-simulated shower T and α is determined by fitting a gamma-distribution. We have used the logarithms of T and α for parameterization, because these quantities were found to be approximately normal distributed. For the parameterization of the expectations $\langle \ln T_{hom} \rangle$ and $\langle \ln \alpha_{hom} \rangle$ the logarithms of equations 7 and 8 have been used. The y-dependence of the fluctuations can be described according to

$$\sigma = (s_1 + s_2 \ln y)^{-1} \tag{9}$$

and the correlation between $\ln T_{hom}$ and $\ln \alpha_{hom}$ is given by

$$\rho(\ln T_{hom}, \ln \alpha_{hom}) \equiv \rho = r_1 + r_2 \ln y. \tag{10}$$

The dependence of these quantities on y is shown in figure 3 for various materials together with the parameterizations (see numbers in Appendix A.1.2).

From these formulae, corellated varying parameters α_i and β_i can be produced according to

$$\begin{pmatrix} \ln T_i \\ \ln \alpha_i \end{pmatrix} = \begin{pmatrix} \langle \ln T \rangle \\ \langle \ln \alpha \rangle \end{pmatrix} + C \begin{pmatrix} z_1 \\ z_2 \end{pmatrix} \tag{11}$$

with

$$C = \begin{pmatrix} \sigma(\ln T) & 0 \\ 0 & \sigma(\ln \alpha) \end{pmatrix} \begin{pmatrix} \sqrt{\frac{1+\rho}{2}} & \sqrt{\frac{1-\rho}{2}} \\ \sqrt{\frac{1+\rho}{2}} & -\sqrt{\frac{1-\rho}{2}} \end{pmatrix}$$

[1]The index "hom" in the following formulas indicates the validity for homogenous media. For sampling calorimeters the index "sam" will be used.

and $\beta_i = (T_i - 1)/\alpha_i$. z_1 and z_2 are standard normal distributed random numbers. The longitudinal energy distribution is evaluated bei integration in steps of $\Delta t = t_j - t_{j-1} = 1X_0$,

$$dE(t) = E \int_{t_{j-1}}^{t_j} \frac{(\beta_i t)^{\alpha_i - 1} \beta_i \exp(-\beta_i t)}{\Gamma(\alpha_i)} dt \,,$$

using eg. the GAMDIS function of the CERN computer library.

It is worthwhile to mention that only one ($\langle \ln \alpha_{hom} \rangle$) of the five quantities needed depends explicitly on the material while for the other four this dependence is absorbed by using y instead of E.

In figure 4 longitudinal profiles of GEANT and parameterized simulations in a leadglass calorimeter (SF5) are compared. Shown are the mean profiles and the mean + 1 RMS in each X_0 interval. While the mean is in perfect agreement, the fluctuations are underestimated by the parameterized simulations at low energies, indicating that the description of individual profiles by gamma-distributions becomes a better approximation with increasing shower energy. Comparisons for other materials (Fe, Cu, W, Pb, U) are of comparable quality as in figure 4 [6]. In the next sections we will show, how the sampling fluctuations in sampling calorimeters can be used to get a better estimation for the shape fluctuations at low energies.

3.2 Sampling fluctuations

In fast simulations, sampling calorimeters consisting of a complicated but repetitive sampling structure are usually described by one single effective medium (the formulas we used to compute effective material parameters are summarized in Appendix A.2.1). The *effect* of the sampling, sampling fluctuations and scaling with sampling fractions down to visible signals, has to be considered for in parameterized simulations explicitly.

The simulation of sampling fluctuations can be done in a comfortable way, using again a gamma distribution:

$$G(a,b) = \frac{x^{a-1} b e^{-bx}}{\Gamma(a)} \tag{12}$$

with

$$\langle x \rangle = \frac{a}{b} \,,\; \sigma^2(x) = \frac{a}{b^2}. \tag{13}$$

The energy in each longitudinal intergration step, $dE(t)$, is fluctuated according to equation 12 choosing

$$a = \frac{dE(t)}{c^2} \text{ and } b = \frac{1}{c^2} \tag{14}$$

using eg. the RANGAM function of the CERN computer library. It is easy to show, that the central limit theoreme will ensure the total energy to be normal distributed obeying the usual law:

$$\frac{\sigma}{E} = \frac{c}{\sqrt{E}}. \tag{15}$$

Using this procedure the occurence of negative energies is automaticaly protected and additional fluctuations are introduced to the longitudinal shape, leading to a better agreement in the shape fluctuations. In addition, this method can be used to fluctuate energy depositions of real particle (electrons, hadrons) if they are tracked individually through an effective homogenous volume.

3.3 Longitudinal shower profiles – sampling calorimeters

Aside of scaling and sampling fluctuations, the inhomogenous material distribution in sampling calorimeters influences the exact behaviour of the shower shapes. In the first stages of electromagnetic shower development the signal is dominated by electrons and positrons. Behind the shower maximum low energetic photons become more and more importend. The transition effect, beeing explained mainly by the absorption properties of low energetic photons, must in turn depend on the shower depth. Consequently, the signal ratio of electrons to minimum ionizing particles (mip's), e/mip, decreases continuously as the shower propagates longitudinally. Averaging over the whole shower, e/mip remains energy independent for $E \gtrsim 1$ GeV. As a consequence of the decreasing e/mip the signal maximum in a specific sampling calorimeter occurs at earlier depth than expected for a homogenous calorimeters with the same effective material properties. This can be seen from figure 5 (left upper corner), where $\langle \ln T \rangle$ for homogenous media is compared to the values in five different sampling calorimeters. In addition the amount of shifting turns out to depend on the exact geometrical arrangement.

The parameterizations of the longitudinal shape as given in section 3.1 for homogenous media can therfor not be used for sampling calorimeters directly. Instead it may be understood as first approximations, to which geometry dependent corrections have to be added. We have used the sampling frequency

$$F_S = \frac{X_{0,eff}}{d_a + d_p} \tag{16}$$

and the value of e/mip (averaged over the shower) to account for the shower depth dependence of the transition effect. d_a and d_p denote the thickness of the active and passive layers, respectivly. If the exact number of e/mip is not known,

$$\hat{e} = \frac{1}{1 + 0.007(Z_p - Z_a)} \approx \frac{e}{mip} \tag{17}$$

gives a sufficient approximation for many calorimeters [12] with charge numbers Z_p and Z_a.

The average longitudinal profiles can now be parameterized according to

$$T_{sam} = T_{hom} + t_1 F_S^{-1} + t_2(1 - \hat{e}) \tag{18}$$

$$\alpha_{sam} = \alpha_{hom} + a_1 F_S^{-1} \tag{19}$$

and the quantities used for simulations of individual showers are given by

$$\langle \ln T_{sam} \rangle = \ln\left(\exp(\langle \ln T_{hom} \rangle) + t_1 F_S^{-1} + t_2(1 - \hat{e})\right) \tag{20}$$

$$\langle \ln \alpha_{sam} \rangle = \ln \left(\exp(\langle \ln \alpha_{hom} \rangle) + a_1 F_S^{-1} \right). \tag{21}$$

$\sigma(\ln T_{sam})$, $\sigma(\ln \alpha_{sam})$ and $\rho(\ln T_{sam}, \ln \alpha_{sam})$ are described with the help of the same formulas as in the case of homogenous media. (See Appendix A.2.2 and A.2.3).

Figure 5 summarizes the parameterizations for sampling calorimeters. The expectation of $\ln T$ does not longer scale with y. The expectation of $\ln \alpha$ depends on the material and the geometry ($\hat{e}$). The fluctuations and correlations of the parameters can still be approximated without any explicit material or geometry dependence.

Figures 6 to 8 compare GEANT simulations and parameterized simulations of the H1 lead liquid argon calorimeter (IFE). The GEANT simulations have been performed with low cuts and a very detailed geometry description, including eg. copper pad plates and G10 layers. These simulations have *not* been used to tune the parameterizations. Both, average longitudinal profiles and their fluctuations (including sampling fluctuations) are in very good agreement (figure 6). The energy containment (figure 7) and the energy resolution (figure 8) as a function of the longitudinal calorimeter length is also well predicted. Comparisons with detailed simulations of other calorimeter (Fe-LAr, Cu-Sc, W-LAr, Pb-LAr, U-Sc) showed a comparable performance [6].

3.4 Radial shower profiles – homogenous media

Figure 9 shows average radial energy profiles,

$$f(r) = \frac{1}{dE(t)} \frac{dE(t,r)}{dr}, \tag{22}$$

at different shower depths in Uranium. The profiles show a distinct maximum in the core of the shower which vanishes with increasing shower depth. In the tail ($r \gtrsim 1 R_M$) the distribution looks nearly flat at the beginning ($1 - 2X_0$), becomes steeper at moderate depths ($5 - 6X_0$, $13 - 14X_0$), and becomes flat again ($22 - 23X_0$). A big variety of different functions have been used to describe radial profiles. We have used the following two component Ansatz:

$$\begin{aligned} f(r) &= p f_C(r) + (1-p) f_T(r) \\ &= p \frac{2 r R_C^2}{(r^2 + R_C^2)^2} + (1-p) \frac{2 r R_T^2}{(r^2 + R_T^2)^2} \end{aligned} \tag{23}$$

with

$$0 \leq p \leq 1.$$

Here R_C (R_T) is the median of the core (tail) component and p is a propability, giving the relative weight of the core component. In the shower depth $1 - 2X_0$ $f(r)$, $p f_C(r)$ and $(1-p) f_T(r)$ are also shown in figure 9.

The evolution of R_C, R_T and p with increasing shower depth is shown in figure 10 for 100 GeV showers in Iron and Uranium. We have used the variable $\tau = t/T$ which measures the shower

depth in units of the depth of the shower maximum to generalize the radial profiles. This made the parameterization more convenient and separated the energy and material dependence of various parameters. The median of the core distribution, R_C, increases linearly with τ. The weight of the core, p, is maximal at around the shower maximum and the width of the tail, R_T, is minimal at $\tau \approx 1$. This behaviour can be traced back to the radial profiles shown in figure 9.

The following formulas have been used to parameterize radial energy density distribution for a given energy and material:

$$R_{C,hom}(\tau) = z_1 + z_2\tau \tag{24}$$

$$R_{T,hom}(\tau) = k_1\{\exp(k_3(\tau - k_2)) + \exp(k_4(\tau - k_2))\} \tag{25}$$

$$p_{hom}(\tau) = p_1 \exp\left\{\frac{p_2 - \tau}{p_3} - \exp\left(\frac{p_2 - \tau}{p_3}\right)\right\} \tag{26}$$

The parameters $z_1 \cdots p_3$ are either constant or simple functions of $\ln E$ or Z (see Appendix A.1.3 for details). The complicated evolution of R_T and p with the shower depth and the dependence of the material can be explained mainly with the propagation of low energetic photons [6]. The offset in R_T between Iron and Uranium (figure 10) for example, indicating a wider distribution in Iron, reflects the difference in the mean free path which for 1 MeV photons is approximately twice as much in iron as in uranium, if lenghts are measured in Molière units.

We found a good agreement of mean radial profiles between parameterized and detailed simulations in Fe, Cu, W, Pb and U absorbers for energies between 0.4 and 400 GeV. This is demonstrated in figure 12 where radial profiles in various shower depths are compared for 40 GeV showers in lead and 100 GeV showers in Uranium.

The introduction of radial shape fluctuations has to be considered with some care. Even if no fluctuations are simulated on $f(r)$ explicitly, radial energy profiles at a given shower depths will fluctuate, because the shower maximum T, and though τ, varies from shower to shower. Another source of radial fluctuations arise from the method which we have adopted for the simulation of radial distributions: The energy content of a longitudinal interval of length 1 X_0, $dE(t)$, is calculated from the actual longitudinal energy density distribution as described in section 3.1. This energy is splitted into N_S discret spots of Energy $E_S = dE(t)/N_S$ which are distributed radially according to $f(r)$ with the help of a Monte Carlo method. This can be done very easy, because the pdf's $f_C(r)$ and $f_T(r)$ can be integrated and inverted:

$$F(r) = \int_0^r \frac{2r'R^2}{(r'^2 + R^2)^2} dr' = \frac{r^2}{r^2 + R^2} \tag{27}$$

$$F^{-1}(u) = R\sqrt{\frac{u}{1-u}}. \tag{28}$$

With the help of two uniform distributed random numbers, $v_i, w_i \in [0, 1[$, random radii according to

$f(r)$ are generated according to:

$$r_i = \begin{cases} R_C\sqrt{\frac{v_i}{1-v_i}}, & \text{if } p < w_i \\ R_T\sqrt{\frac{v_i}{1-v_i}}, & \text{else.} \end{cases}$$

This method leads to additional fluctuations in the energy content of every radial interval which follow a binomial distribution. Thus, the relation

$$\frac{\sigma^2(\epsilon)}{\langle\epsilon\rangle(1-\langle\epsilon\rangle)} = const = N_S^{-1} \tag{29}$$

describes the contribution to radial shape fluctuations produced by the Monte Carlo method in each longitudinal intergration interval. Here ϵ denotes the energy quota in a given radial interval at a given shower depths:

$$\langle\epsilon\rangle \equiv \int_{r_1}^{r_2} f(r)dr = \frac{dE(t,r)}{dE(t)}. \tag{30}$$

We have investigated the possibility to tune N_S in each longitudinal interval to match the radial shape fluctuations observed in detailed GEANT simulations[2]. As an example the quantity $\sigma^2(\epsilon)/(\langle\epsilon\rangle(1-\langle\epsilon\rangle))$ is displayed at $t = 5 - 6X_0$ in figure 11 for detailed simulations and parameterized simulations without any radial shape fluctuations. The difference of these curves, which is also shown in figure 11, is approximately constant and determines N_S^{-1} in equation 29 (note that the variance is additiv). We found, that a constant contribution to $\sigma^2(\epsilon)/(\langle\epsilon\rangle(1-\langle\epsilon\rangle))$ can be used to match the total radial shape fluctuations to a good approximation at all shower depths.

Summing N_S over all shower depths, the total number of spots N_{spot} needet for one shower can be optained and parameterized according to

$$N_{spot} = 93\ln(Z)E^{0.876}. \tag{31}$$

To parameterize the spot numbers in each longitudinal integration interval it is convenient to parameterize the density distribution, $1/N_{spot}\, dN_S(t)/dt$ in figure 11, which follows a gamma distribution which parameters are given by the parameterizations of the corresponding longitudinal energy profile:

$$T_{Spot} = T_{hom}(0.698 + 0.00212Z) \quad \text{and} \tag{32}$$

$$\alpha_{Spot} = \alpha_{hom}(0.639 + 0.00334Z). \tag{33}$$

The total fluctuations optained with this method are also compared in figure 12 by adding 1 RMS to the mean profiles.

Additional correlations between longitudinal and radial shower development are taken into account by introducing a correlation between the radial pdf's and the actual center of gravity,

$$\langle t\rangle_i = \frac{\alpha_i}{\beta_i} = T_i\frac{\alpha_i}{\alpha_i - 1},$$

[2]De Angelis et al. have used a similar method to reproduce shape fluctuations [13].

of an individual shower. This is done by calculating τ in equation 24, 25 and 26 from $\langle t \rangle_i$ instead of T. Thus:

$$\tau = \frac{t}{T} \longrightarrow \tau_i = \frac{t}{\langle t \rangle_i} \frac{\exp(\langle \ln \alpha \rangle)}{\exp(\langle \ln \alpha \rangle) - 1} . \tag{34}$$

The need to introduce these correlations is demonstrated in figure 13, where integrated radial profiles are shown, which were optained by summing over all longitudinal layers. Note that the mean integrated profiles,

$$\left\langle \frac{1}{E} \frac{dE(r)}{dr} \right\rangle ,$$

is independent of energy, which is well reproduced by the parameterized simulations. The relative fluctuations on this distributions,

$$\hat{\sigma}(r) \equiv \frac{\sigma_{RMS}}{\left\langle \frac{1}{E} \frac{dE(r)}{dr} \right\rangle}$$

is shown using both, τ and τ_i in calculating the radial profiles. Only the simulations using τ_i are able to predict the fluctuations observed in the GEANT simulations correctly.

Finaly, the completed algorithm is summarized as follows: Determine the energy $dE(t)$ within one longitudinal integration interval as described in section 3.1. In case of sampling calorimeters apply sampling fluctuations on $dE(t)$. In the same loop evaluate the number of spots needet to reproduce radial shape fluctuations in this interval according to

$$N_S(t) = N_{spot} \int_{t_{j-1}}^{t_j} \frac{(\beta_{Spot} t)^{\alpha_{Spot}-1} \beta_{Spot} \exp(-\beta_{Spot} t)}{\Gamma(\alpha_{Spot})} dt .$$

Distribute the spots radially according to $f(r)$ as described above. Distribute the spots uniformly in the longitudinal interval and in ϕ. Transform the spot coordinates $(E_S, t[X_0], r[R_M], \phi)$ into the detector reference system (E_S, x, y, z).

3.5 Radial shower profiles – sampling calorimeters

The influence of the exact geometry on radial energy profiles is rather small. At the start of the shower the profiles look a bit smoother as in homogenous media. With increasing shower depth they approach the shapes that are expected for homogenous media with the same effective material quantities. These small deviations have been taken into account by the following corrections to the mean profiles:

$$R_{C,sam} = R_{C,hom} + z_1(1 - \hat{e}) + z_2 F_S^{-1} \exp(-\tau_i) \tag{35}$$

$$R_{T,sam} = R_{T,hom} + k_1(1 - \hat{e}) + k_2 F_S^{-1} \exp(-\tau_i) \tag{36}$$

$$p_{sam} = p_{hom} + (1 - \hat{e})(p_1 + p_2 F_S^{-1} \exp(-(\tau_i - 1)^2)) \tag{37}$$

using again the sampling frequency and e/mip (see numbers in Appendix A.2.4).

The total number of spots needet to simulate the radial shape fluctuations is much smaller than in the case of homogenous media and does no longer depend sensitivly on the used materials. Instead, the spot number can be parameterized according to

$$N_{spot} = \frac{10.3}{c} E^{0.959} \tag{38}$$

where c measures the sampling fluctuations according to

$$\frac{\sigma}{E} = \frac{c}{\sqrt{E}}$$

(see figure 14). The density distribution of the spot numbers is parameterized in analogy to the homogenous media:

$$T_{Spot} = T_{sam}(0.831 + 0.0019Z) \quad \text{and} \tag{39}$$

$$\alpha_{Spot} = \alpha_{sam}(0.844 + 0.0026Z) \tag{40}$$

Figure 15 and 16 compares GEANT simulations and parameterized simulations of mean radial profiles and their relative fluctuations,

$$\hat{\sigma}(t,r) = \frac{\sigma_{RMS}}{\left\langle \frac{1}{dE(t)} \frac{dE(t,r)}{dr} \right\rangle}, \tag{41}$$

in the H1 liquid argon calorimeter at various energies. The influence of radial leakage on containment and energy resolution is demonstrated in figure 17 and 18. The energy independence of the energy contained in a cylinder of radius r_C is well reproduced by the parameterized simulations. The energy resolution as defined in figure 18 does not depend on radial leakage. This is correctly predicted by the parameterized simulations only if the correlations between longitudinal and radial shower development is taken into account (usage of τ_i).

4 Comparison with Data

We have compared parameterized simulations with test beam data from the H1 calorimeter, which is made of lead and liquid argon in the electromagnetic sections [14]. Moduls of the inner forward (IFE), the forward barrel (FB1) and the central barrel (CB2/CB3) calorimeter have been studied. The electron beams in the energy range between 5 and 80 GeV entered the stacks under angles of 11° in the IFE and CB3, and under 35° in the FB1 calorimeter.

The energy resolution of the data can be described by

$$\frac{\sigma(E)}{\langle E \rangle} = \sqrt{\frac{c^2}{\langle E \rangle} + \frac{b^2}{\langle E \rangle^2} + \left(\frac{\sigma(p)}{p}\right)^2}. \tag{42}$$

Here c describes the sampling fluctuations, b consideres the noise, and $\sigma(p)/p$ denotes the momentum resolution of the beam. In the Monte Carlo the momentum resolution has been simulated explicitly, the electronic noise was taken into account by adding random trigger events to the simulated cell energies, and c, which is approximately 11% for all moduls, has been used to simulate the sampling fluctuations.

The simulations, denoted by "MC" in the following figures, have been carried out with the H1 detector simulation program H1FAST [15, 16]. The algorithms described so far are part of this program, which is used for the mass production of Monte Carlo events in the H1 detector at the HERA collider at DESY (Hamburg, FRG), requiering a high precision also in complicated detector regions (eg. cracks). If a shower developes partly inside cracks between adjacent moduls, which in general can not be approximated by a single effective medium, parameterizations will in general fail to reproduce measured signals. In H1FAST we therefor do not parameterize showers if they cross such boundaries. Only electromagnetic (sub)showers are parametrized, which fit into one single stack.[3]

During analysis, a 3σ noise cut has been applied to both the data and the Monte Carlo at the cell level, and energy clusters were built from cells cointaining energies above the threshold. Energy distributions in the clusters with maximum channel numbers are compared in figure 19 for all three moduls considered. In addition the energy in all other cells, not belonging to the selected clusters, are also shown.

Longitudinal profiles are shown in figure 20 for various energies in the IFE calorimeter. The mean profiles, as well as the fluctuations, are nearly indestinguishable in the data and the Monte Carlo. Energy distribution in individual longitudinal layers are compared in figure 21 at 30 GeV in the CB3 calorimeter, showing that not only the mean and fluctuations but also the shape of the distributions are predicted correctly by the parameterized simulations.

Figure 22 compares lateral profiles in different shower depths in the IFE calorimeter at one energy, and in figure 23 lateral profiles, summed over all longitudinal sections are shown at various energies in the FB1 calorimeter. There is good agreement in the peek distributions. The tails of the profiles are dominated by electronic noise.

As shown so far, parametrized simulations can predict measured calorimeter signals very precisly, if the shower development is confined within one single calorimeter stack. Using the concept of partial parametrization as described above, the influence of cracks on the measured signal can be reproduced as shown in figure 24. We have used testbeam data scanning the crack between H1-CB2 and H1-CB3, consisting of two electromagnetic (CB2E, CB3E) and two hadronic stacks (CB2H, CB3H). The width of the crack is aprroximately 1 cm. Shown are the energies in the electromagnetic moduls (E_{CB2E}, E_{CB3E}), the sum of both ($E_{CBE} = E_{CB2E} + E_{CB3E}$), and the sum measured in the electromagnetic and hadronic moduls ($E_{CB} = E_{CBE} + E_{CBH}$) as a function of the beam impact position. All energies are normalized to $E_{+20} \equiv E_{CB}(x_{calo} = 20cm)$. The energy lost while scanning the crack with a 30

[3] A stand alone version (called GFLASH 1.4) running with GEANT and covering the same functionality is available for distribution. Please contact one of the authors.

GeV test beam extents to around 40%, if only the electromagnetic sections are considered, and is still around 20% if the hadronic moduls are also taken into account. The agreement between data and partial parametrization is quit satisfactory.

Out of the various comparisons we made, only a limited number is presented here. We have studied carefully quantities, which are relevant for physics analysis with the H1 detector and found good capabilities of the (partial) parameterization for eg. e/π separation.[6]

5 Timing

The CPU time reduction depends on the complexity of the geometry description and the cut off parameter in the detailed simulation as well as on the type of simulated events. Fully parameterized simulations of electromagnetic showers in a simple (box) geometry are arround 7000 times faster at 100 GeV (900 at 1 GeV) compared with GEANT simulations of a very detailed geometry and with low cuts (e^--cut 200 keV, γ-cut 10 keV).

In the framework of the H1 simulation program partial parameterization of electromagnetic showers is performed as described above together with individual tracking of hadrons and employment of particle terminators (see also [15, 16]). The gain factors for 30 GeV showers in the H1 detector (including detailed simulations of tracker volumes) are 200 for electrons and 25 in case of hadronic showers. Medium cuts (e^--cut 1 MeV, γ-cut 200 keV) were used in in the corresponding detailed simulations. Complete detector simulations of HERA events (ep scattering at $\sqrt{s} = 314$ GeV) require 10 times less CPU time using partial parameterization.

6 Conclusions

We have developed parameterizations of electromagnetic showers, which take the material and geometry dependence explicitly into account. Shower to shower fluctuations and correlations are taken into account consistently, as well as correlations between longitudinal and radial shower development. Comparisons with data have shown, that parameterized simulations are able to predict measured calorimeter signals with an acceptable precision. Using the methods described above the energy resolution is reproduced at the level of $\pm 0.5\%$. The energy deposited in longitudinal and lateral layers is predicted with a precision of typically $\pm 1.5\%$ for both, the means and the fluctuations. Using partial parameterizations the energy measured in electromagnetic (all) moduls differs by an amount of 1.7% (9%) if the beam enters directly into a crack. Parameterizations can therefor provide fast and precise algorithms to be used for Monte Carlo mass production for physics analysis.

Acknowledgement

somebody to acknowledge?

A Summary of formulae

A.1 Homogenous Media

A.1.1 Average longitudinal profiles

$$
\begin{aligned}
T_{hom} &= \ln y - 0.858 \\
\alpha_{hom} &= 0.21 + (0.492 + 2.38/Z)\ln y
\end{aligned}
$$

A.1.2 Fluctuated longitudinal profiles

$$
\begin{aligned}
\langle \ln T_{hom} \rangle &= \ln(\ln y - 0.812) \\
\sigma(\ln T_{hom}) &= (-1.4 + 1.26 \ln y)^{-1} \\
\langle \ln \alpha_{hom} \rangle &= \ln\left(0.81 + (0.458 + 2.26/Z)\ln y\right) \\
\sigma(\ln \alpha_{hom}) &= (-0.58 + 0.86 \ln y)^{-1} \\
\rho(\ln T_{hom}, \ln \alpha_{hom}) &= 0.705 - 0.023 \ln y
\end{aligned}
$$

A.1.3 Average radial profiles

$$
\begin{aligned}
R_{C,hom}(\tau) &= z_1 + z_2\tau \\
R_{T,hom}(\tau) &= k_1\{\exp(k_3(\tau - k_2)) + \exp(k_4(\tau - k_2))\} \\
p_{hom}(\tau) &= p_1 \exp\left\{\frac{p_2 - \tau}{p_3} - \exp\left(\frac{p_2 - \tau}{p_3}\right)\right\}
\end{aligned}
$$

with

$$
\begin{aligned}
z_1 &= 0.0251 + 0.00319 \ln E \\
z_2 &= 0.1162 + -0.000381 Z \\
k_1 &= 0.659 + -0.00309 Z \\
k_2 &= 0.645 \\
k_3 &= -2.59 \\
k_4 &= 0.3585 + 0.0421 \ln E \\
p_1 &= 2.632 + -0.00094 Z \\
p_2 &= 0.401 + 0.00187 Z \\
p_3 &= 1.313 + -0.0686 \ln E
\end{aligned}
$$

A.1.4 Fluctuated radial profiles

$$
\begin{aligned}
\tau_i &= \frac{t}{\langle t \rangle_i} \frac{\exp(\langle \ln \alpha \rangle)}{\exp(\langle \ln \alpha \rangle) - 1} \\
N_{Spot} &= 93 \ln(Z) E^{0.876} \\
T_{Spot} &= T_{hom}(0.698 + 0.00212 Z) \\
\alpha_{Spot} &= \alpha_{hom}(0.638 + 0.00334 Z)
\end{aligned}
$$

A.2 Sampling Calorimeters

A.2.1 Material and geometry parameters

$$
\begin{aligned}
w_i &= \frac{\rho_i d_i}{\sum_j \rho_j d_j} \quad (\rho = \text{density}) \\
Z_{eff} &= \sum_i w_i Z_i \\
A_{eff} &= \sum_i w_i A_i \\
\frac{1}{X_{0,eff}} &= \sum_i \frac{w_i}{X_{0,i}} \\
\frac{1}{R_{M,eff}} &= \frac{1}{E_s} \sum_i \frac{w_i E_{c,i}}{X_{0,i}} \\
E_{c,eff} &= X_{0,eff} \sum_i \frac{w_i E_{c,i}}{X_{0,i}} \\
F_S &= \frac{X_{0,eff}}{d_a + d_p} \\
\hat{e} &= \frac{1}{1 + 0.007(Z_p - Z_a)}
\end{aligned}
$$

A.2.2 Average longitudinal profiles

$$
\begin{aligned}
T_{sam} &= T_{hom} - 0.59 F_S^{-1} - 0.53(1 - \hat{e}) \\
\alpha_{sam} &= \alpha_{hom} - 0.444 F_S^{-1}
\end{aligned}
$$

A.2.3 Fluctuated longitudinal profiles

$$
\begin{aligned}
\langle \ln T_{sam} \rangle &= \ln\left(\exp(\langle \ln T_{hom} \rangle) - 0.55 F_S^{-1} - 0.69(1-\hat{e})\right) \\
\sigma(\ln T_{hom}) &= (-2.5 + 1.25 \ln y)^{-1} \\
\langle \ln \alpha_{sam} \rangle &= \ln\left(\exp(\langle \ln \alpha_{hom} \rangle) - 0.476 F_S^{-1}\right) \\
\sigma(\ln \alpha_{hom}) &= (-0.82 + 0.79 \ln y)^{-1} \\
\rho(\ln T_{hom}, \ln \alpha_{hom}) &= 0.784 - 0.023 \ln y
\end{aligned}
$$

A.2.4 Average radial profiles

$$
\begin{aligned}
R_{Z,sam} &= R_{Z,hom} - 0.0203(1-\hat{e}) + 0.0397 F_S^{-1} \exp(-\tau) \\
R_{T,sam} &= R_{T,hom} - 0.14(1-\hat{e}) - 0.495 F_S^{-1} \exp(-\tau) \\
p_{sam} &= p_{hom} + (1-\hat{e})(0.348 - 0.642 F_S^{-1} \exp(-(\tau-1)^2))
\end{aligned}
$$

A.2.5 Fluctuated radial profiles

$$
\begin{aligned}
\tau_i &= \frac{t}{\langle t \rangle_i} \frac{\exp(\langle \ln \alpha \rangle)}{\exp(\langle \ln \alpha \rangle) - 1} \\
N_{Spot} &= \frac{10.3}{c} E^{0.959} \\
T_{Spot} &= T_{hom}(0.813 + 0.0019 Z) \\
\alpha_{Spot} &= \alpha_{hom}(0.844 + 0.0026 Z)
\end{aligned}
$$

References

[1] E. Longo and I. Sestili, Nucl. Instr. and Meth. 128, 283, (1975)

[2] R. K. Bock et al., Nucl. Instr. and Meth. 185, 533, (1981);
M. della Negra, Scripta Phys. 23, 469, (1981).

[3] Y. Hayashide et al., CDF Note 287, Batavia, IL (1985).

[4] J. Badier and M. Bardadin-Otwinowska, ALEPH 87–9, EMCAL 87–1, Geneva (1987).

[5] G. Grindhammer, M. Rudowicz and S. Peters, Nucl. Instr. and Meth. A290, 469, (1990)

[6] S. Peters, PhD thesis at the University of Hamburg; MPI–PhE/92–13 (1992).

[7] R. Brun et al., GEANT3 User's Guide. CERN–DD/EE 84–1, Geneva (1986).

[8] W. Flauger, Nucl. Instr. and Meth. A241, 72, (1985)

[9] R. Wigmans, CERN/EP 86-141, Geneva (1986)

[10] B. Rossi, Prentice Hall, New York, (1952)

[11] O. I. Dovzhenkko and A. A. Pommanskii, Soviet Physics Jetp Vol. 18, Numb. 1, (1964)

[12] J. del Peso and E. Ros, DESY 90–045, (1990)

[13] A. de Angelis and P. A. Palazzi, NIM A271, 455, (1988)

[14] H1 collaboration, Technical Proposal for the H1 Detector, DESY, (1986)

[15] M. Kuhlen, To be published in: Proceedings of the XXVI International Conference on High Energy Physics, Dallas (1992).

[16] M. Rudowicz, PhD thesis at the University of Hamburg; MPI–PhE/92–14 (1992).

Figure Captions

1 Depths of the shower maxima as a function of y. 20

2 Shape parameter α as a function of y. 21

3 Parameters of individual longitudinal profiles in homogenous media. 22

4 Mean longitudinal profiles and their fluctuations in a leadglass calorimeter. 23

5 Parameters of individual longitudinal energy profiles in sampling calorimeters. 24

6 Mean longitudinal profiles and their fluctuations in the H1 lead liquid argon calorimeter IFE. 25

7 Energy containment vs calorimeter depth in H1-IFE. 26

8 Energy resolution vs calorimeter depth in H1-IFE. 27

9 Mean radial profiles in U at various calorimeter depth. The two component Ansatz is indicated for the depth $1 - 2X_0$. 28

10 Shower depth and material dependence of radial shower parameters. 29

11 Tungsten, 40 GeV. Left figure: Decomposition of the two sources of radial shape fluctuations. Right figure: Comparison of energy and spot density distributions. . . . 30

12 Mean radial profiles and their fluctuations in Pb (40 GeV) and U (100 GeV). 31

13 Top: Mean integrated radial profiles in leadglass. Bottom: Corresponding shape fluctuations: — (· · ·) with (without) long./rad. correlations. 32

14 Total number of spots required for sampling calorimeters. 33

15 Mean radial profiles in the H1 lead liquid argon calorimeter IFE. 34

16 Radial shape fluctuations in the H1 lead liquid argon calorimeter IFE. 35

17 Energy containment vs calorimeter radius in H1-IFE. 36

18 Energy resolution vs calorimeter radius in H1-IFE. 37

19 Energy distributions of the cluster with maximum channel number (E_{max}) and in all other channels (E_{rest}) for 30 GeV showers in three different moduls of the H1 Pb LAr calorimeter. 38

20 Mean longitudinal profiles and fluctuations in H1-IFE. 39

21 Energy distributions in 4 subsequent layers in H1-CB3 (30 GeV). 40

22 Mean lateral profiles and fluctuations at different depths in H1-IFE (10 GeV). The coordinates J correspond to transverse pad numbers. 41

23 Mean lateral profiles and fluctuations in H1-FB1. The coordinates I correspond to transverse pad numbers. 42

24 Normalized energies as measured across a crack between the moduls H1-CB2 and H1-CB3. 43

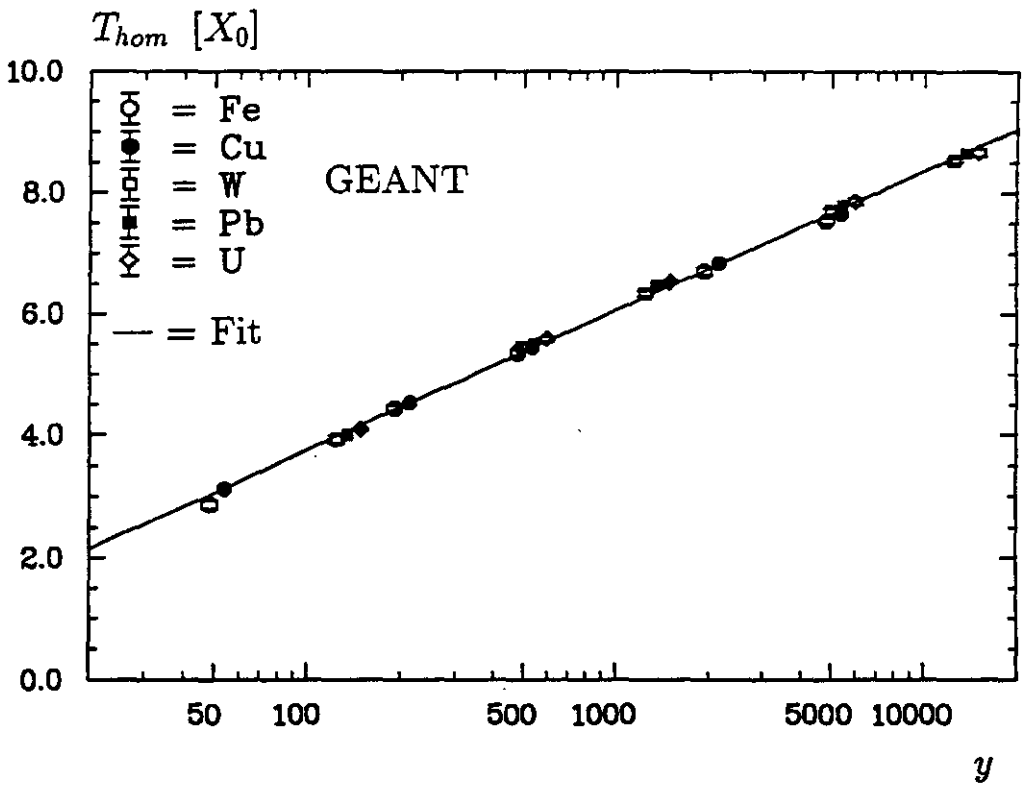
T_{hom} $[X_0]$
10.0
8.0
6.0
4.0
2.0
0.0
= Fe
= Cu
= W
= Pb
= U
= Fit
GEANT
50
100
500
1000
5000
10000
y

Figure 1:

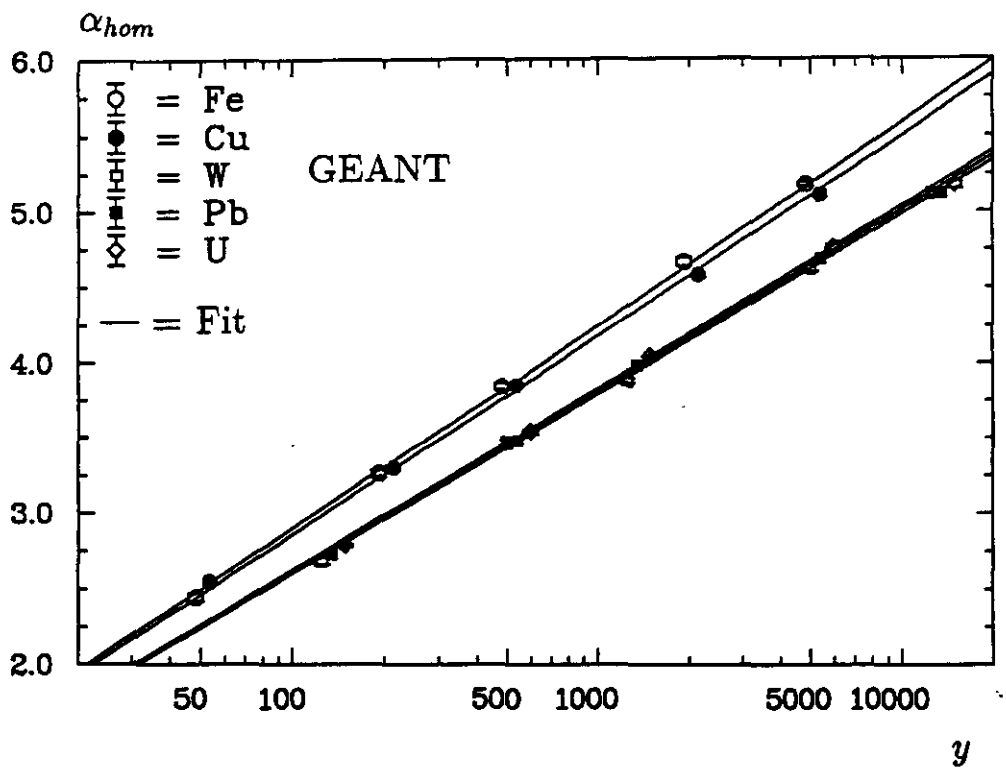
α_{hom}
6.0
5.0
4.0
3.0
2.0
= Fe
= Cu
= W
= Pb
= U
= Fit
GEANT
50
100
500
1000
5000
10000
y

Figure 2:

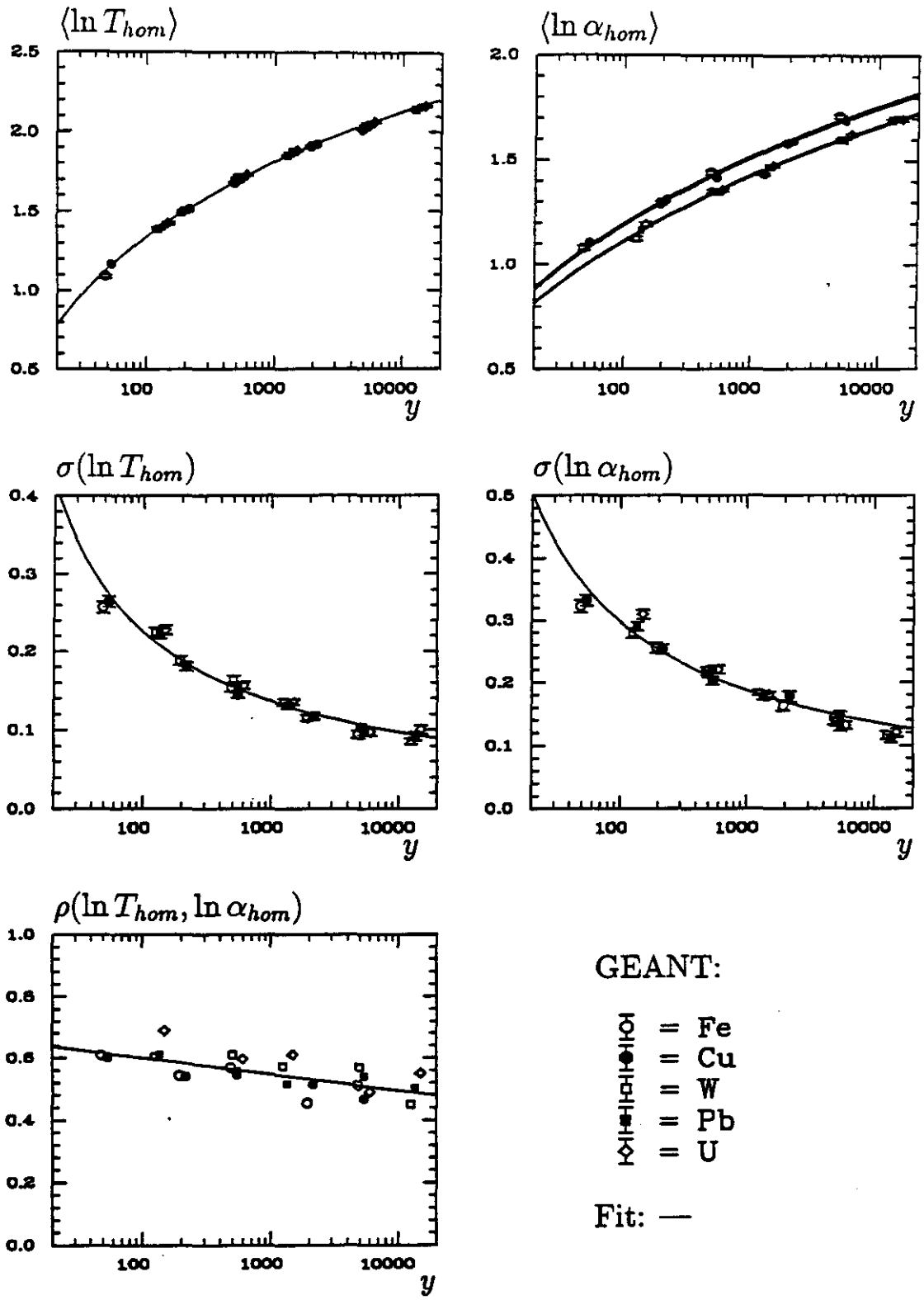
$\langle \ln T_{hom} \rangle$
$\langle \ln \alpha_{hom} \rangle$
$\sigma(\ln T_{hom})$
$\sigma(\ln \alpha_{hom})$
$\rho(\ln T_{hom}, \ln \alpha_{hom})$
y
GEANT:
= Fe
= Cu
= W
= Pb
= U
Fit: —

Figure 3:

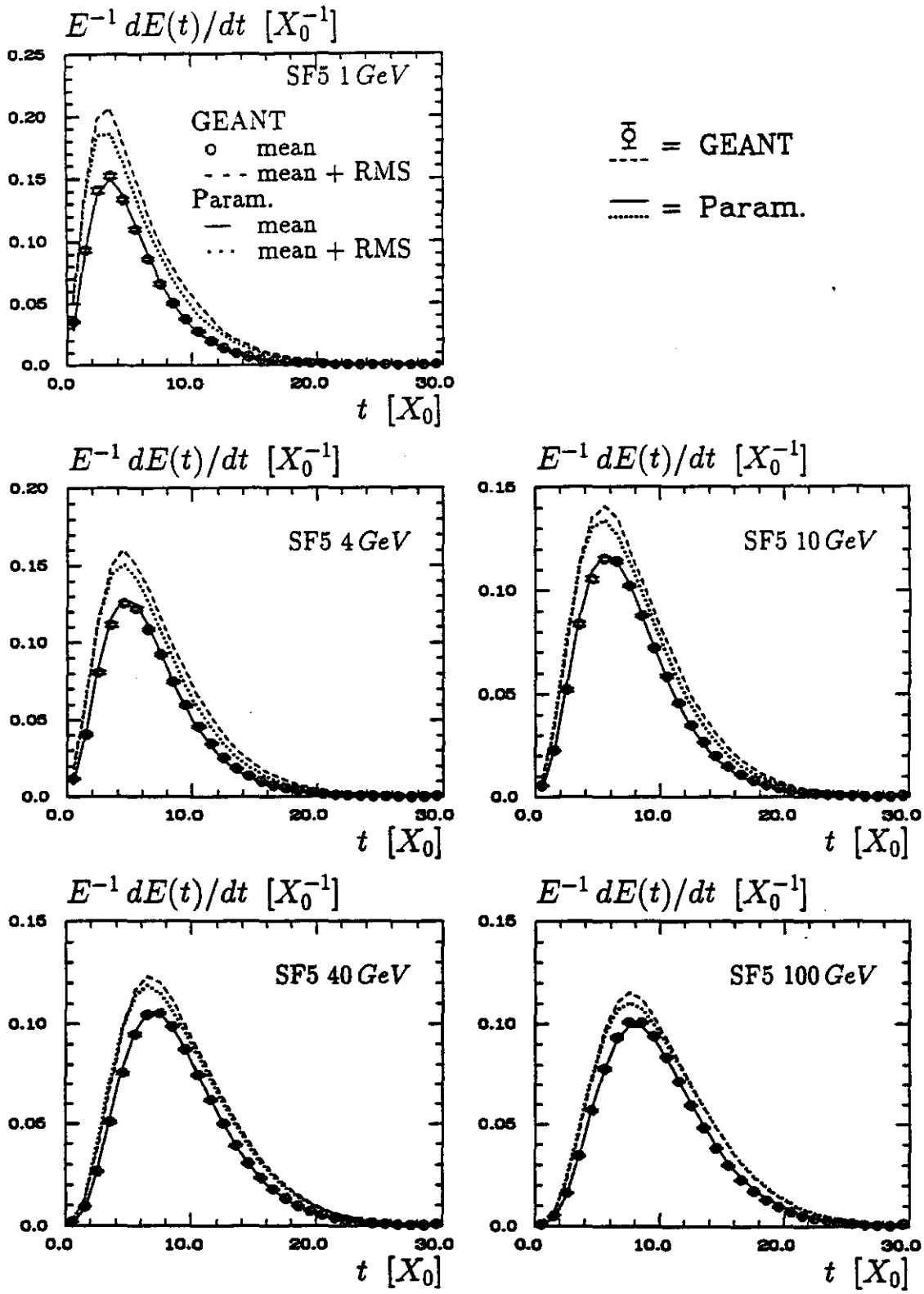
$E^{-1}\,dE(t)/dt\ [X_0^{-1}]$
SF5 1 GeV
GEANT
o mean
- - - mean + RMS
Param.
— mean
··· mean + RMS
= GEANT
= Param.
SF5 4 GeV
SF5 10 GeV
SF5 40 GeV
SF5 100 GeV
$t\ [X_0]$

Figure 4:

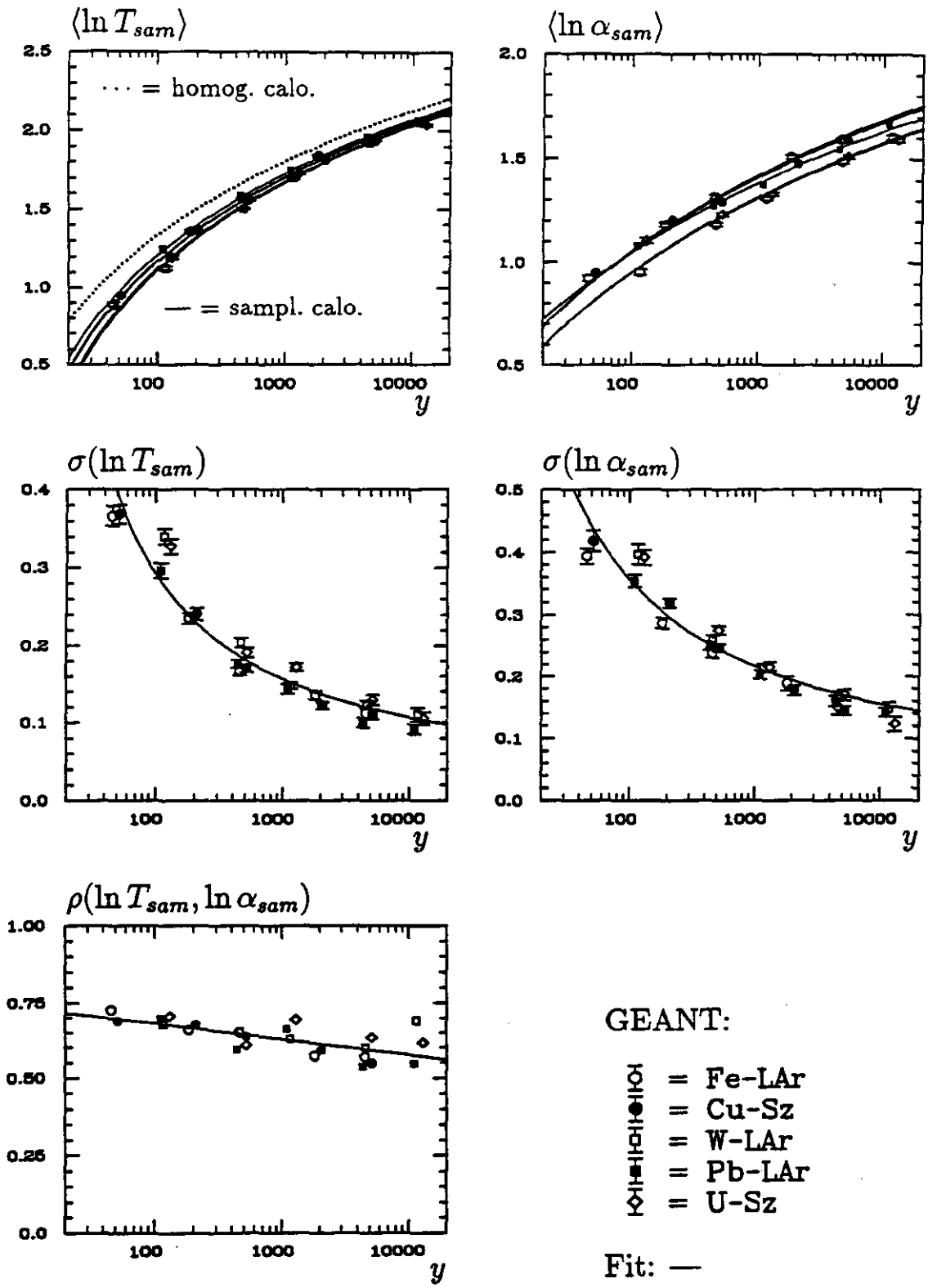
$\langle \ln T_{sam} \rangle$
··· = homog. calo.
— = sampl. calo.
$\langle \ln \alpha_{sam} \rangle$
$\sigma(\ln T_{sam})$
$\sigma(\ln \alpha_{sam})$
$\rho(\ln T_{sam}, \ln \alpha_{sam})$
y
GEANT:
= Fe-LAr
= Cu-Sz
= W-LAr
= Pb-LAr
= U-Sz
Fit: —

Figure 5:

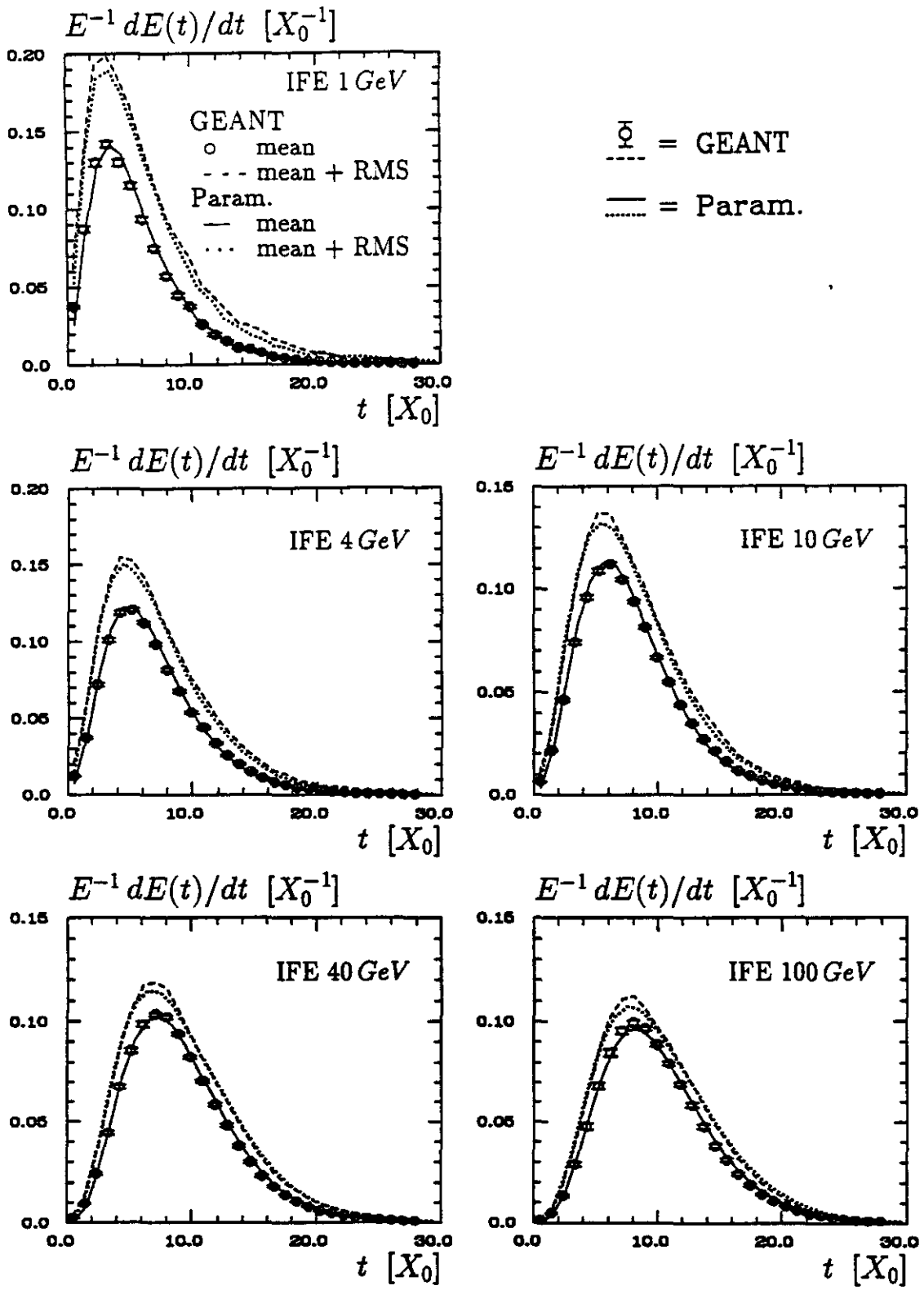
$E^{-1}\,dE(t)/dt\ [X_0^{-1}]$
IFE 1 GeV
GEANT
mean
mean + RMS
Param.
mean
mean + RMS
= GEANT
= Param.
IFE 4 GeV
IFE 10 GeV
IFE 40 GeV
IFE 100 GeV
$t\ [X_0]$
0.0
0.05
0.10
0.15
0.20
10.0
20.0
30.0

Figure 6:

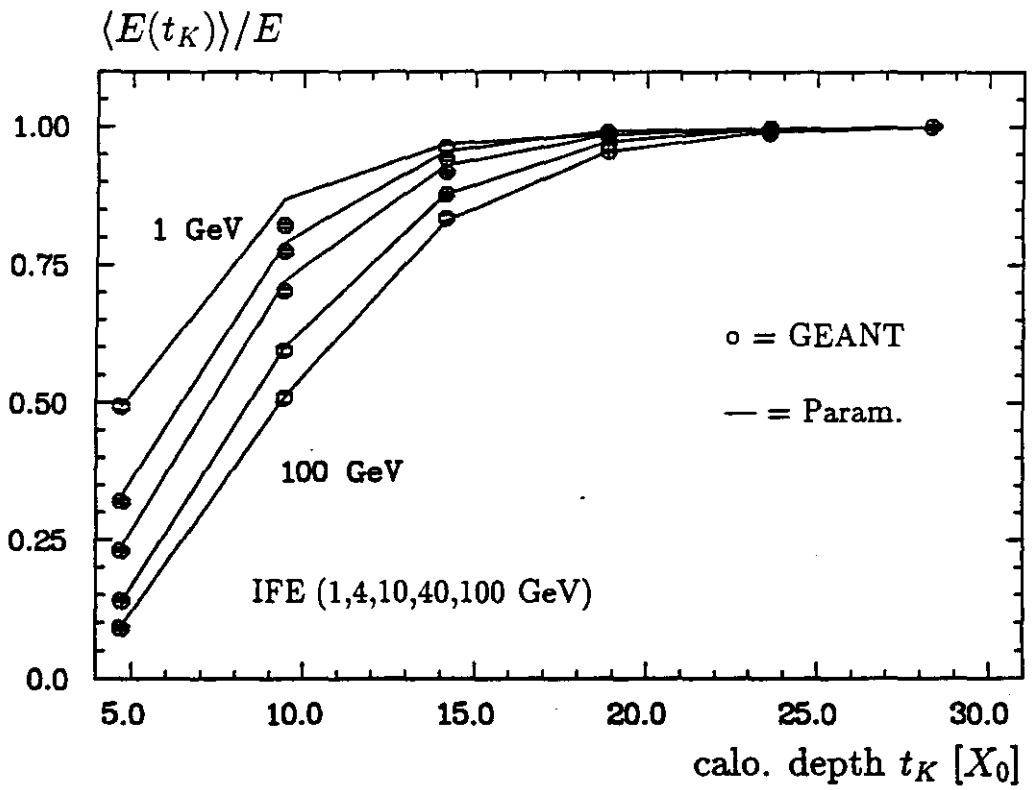
$\langle E(t_K)\rangle/E$
1.00
0.75
0.50
0.25
0.0
5.0
10.0
15.0
20.0
25.0
30.0
calo. depth t_K $[X_0]$
1 GeV
100 GeV
IFE (1,4,10,40,100 GeV)
o = GEANT
— = Param.

Figure 7:

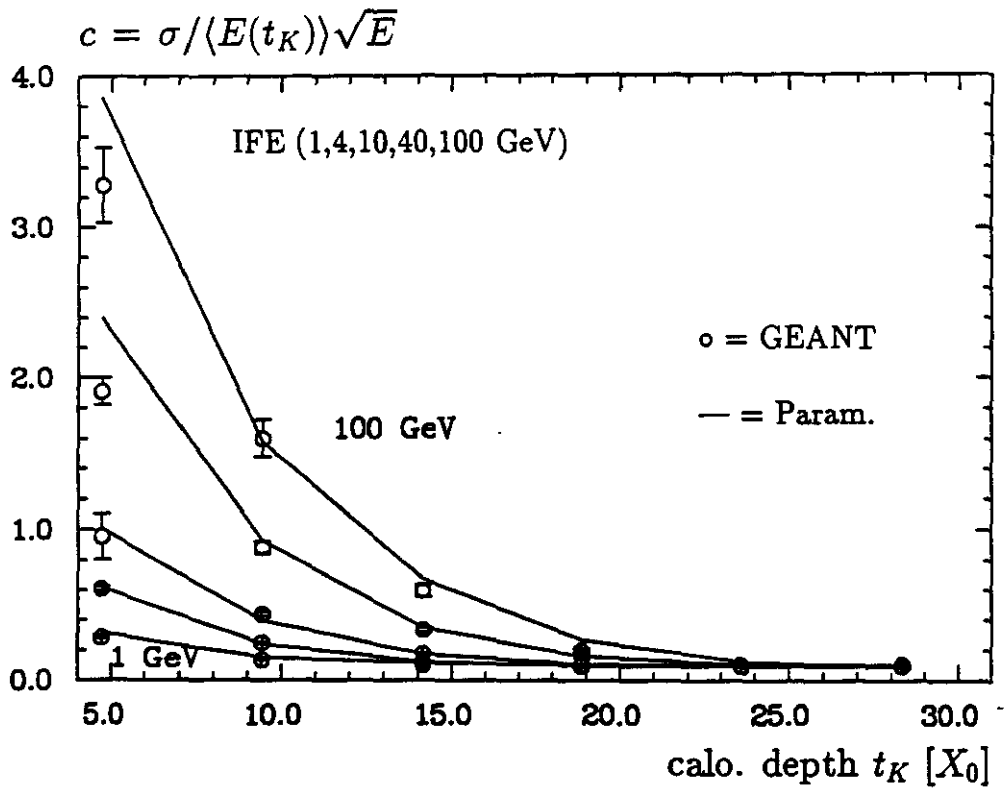
$c = \sigma/\langle E(t_K)\rangle\sqrt{E}$
4.0
3.0
2.0
1.0
0.0
IFE (1,4,10,40,100 GeV)
o = GEANT
— = Param.
100 GeV
1 GeV
5.0
10.0
15.0
20.0
25.0
30.0
calo. depth t_K $[X_0]$

Figure 8:

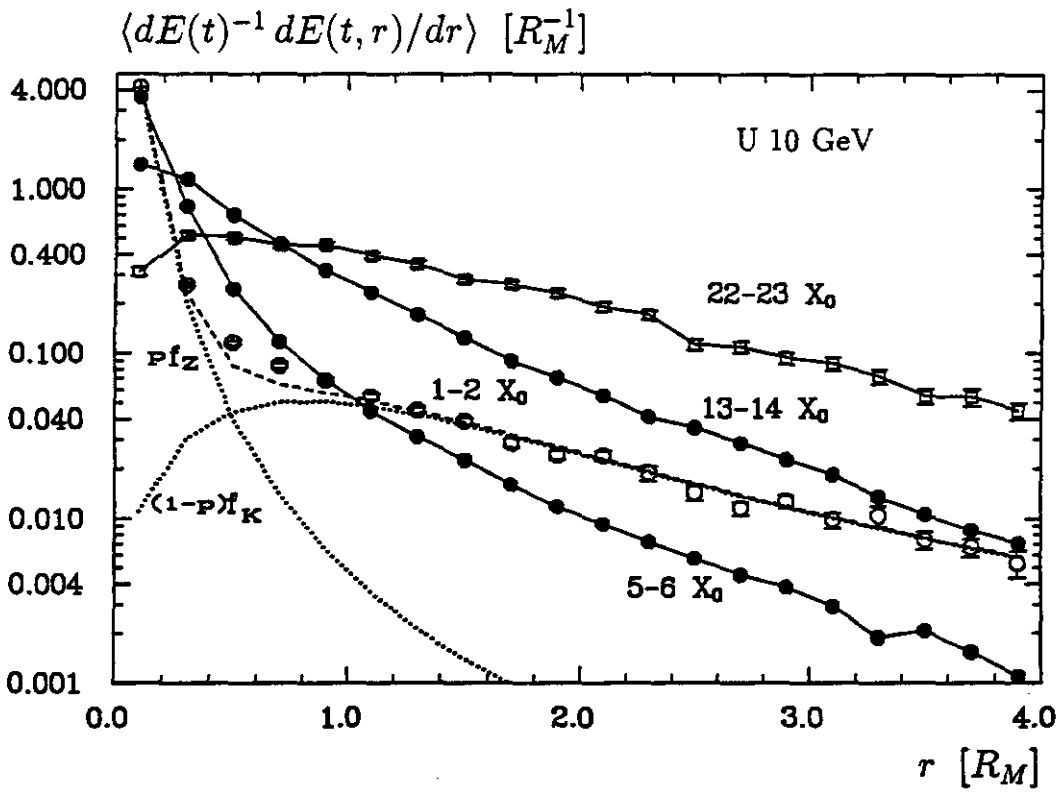
$\langle dE(t)^{-1}\, dE(t,r)/dr \rangle$ $[R_M^{-1}]$
U 10 GeV
22-23 X_0
13-14 X_0
1-2 X_0
5-6 X_0
pf_Z
$(1-p)f_K$
4.000
1.000
0.400
0.100
0.040
0.010
0.004
0.001
0.0
1.0
2.0
3.0
4.0
r $[R_M]$

Figure 9:

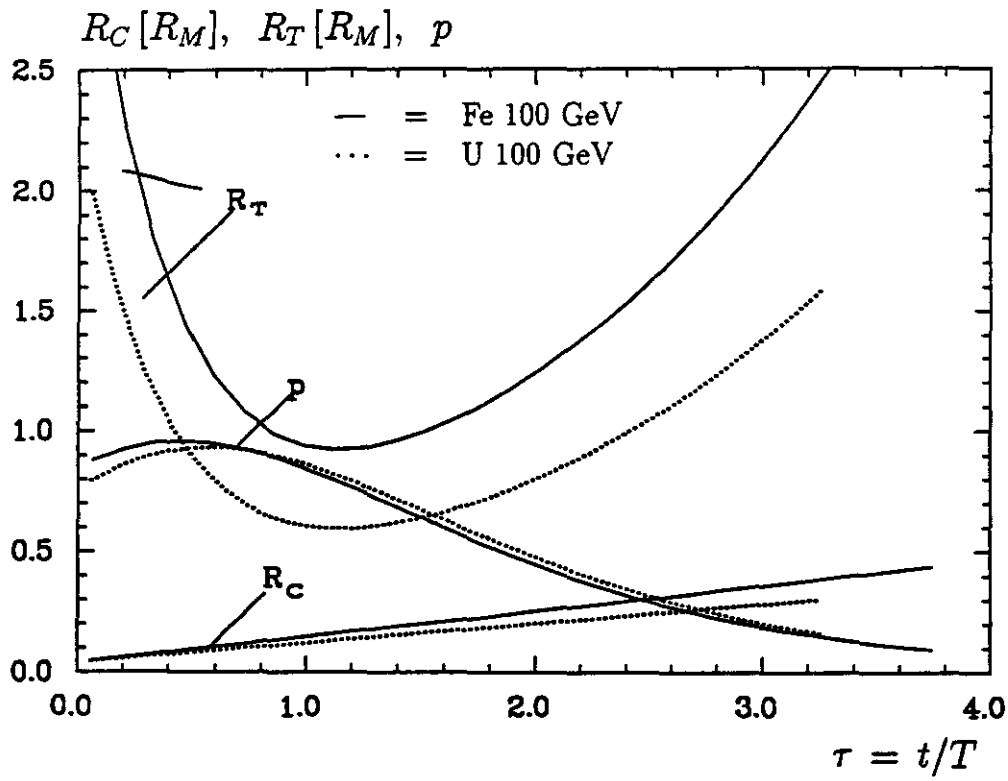
$R_C\,[R_M],\ \ R_T\,[R_M],\ \ p$
— = Fe 100 GeV
··· = U 100 GeV
R_T
p
R_C
2.5
2.0
1.5
1.0
0.5
0.0
0.0
1.0
2.0
3.0
4.0
$\tau = t/T$

Figure 10:

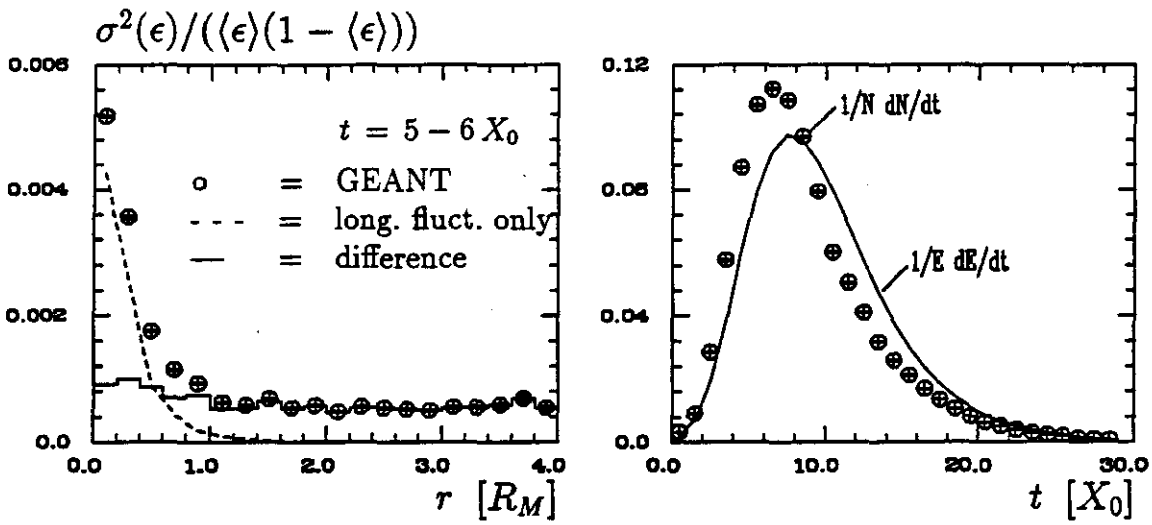
$\sigma^2(\epsilon)/(\langle\epsilon\rangle(1-\langle\epsilon\rangle))$
0.006
0.004
0.002
0.0
$t = 5 - 6\,X_0$
o = GEANT
- - - = long. fluct. only
— = difference
0.0
1.0
2.0
3.0
4.0
r $[R_M]$
0.12
0.08
0.04
0.0
1/N dN/dt
1/E dE/dt
0.0
10.0
20.0
30.0
t $[X_0]$

Figure 11:

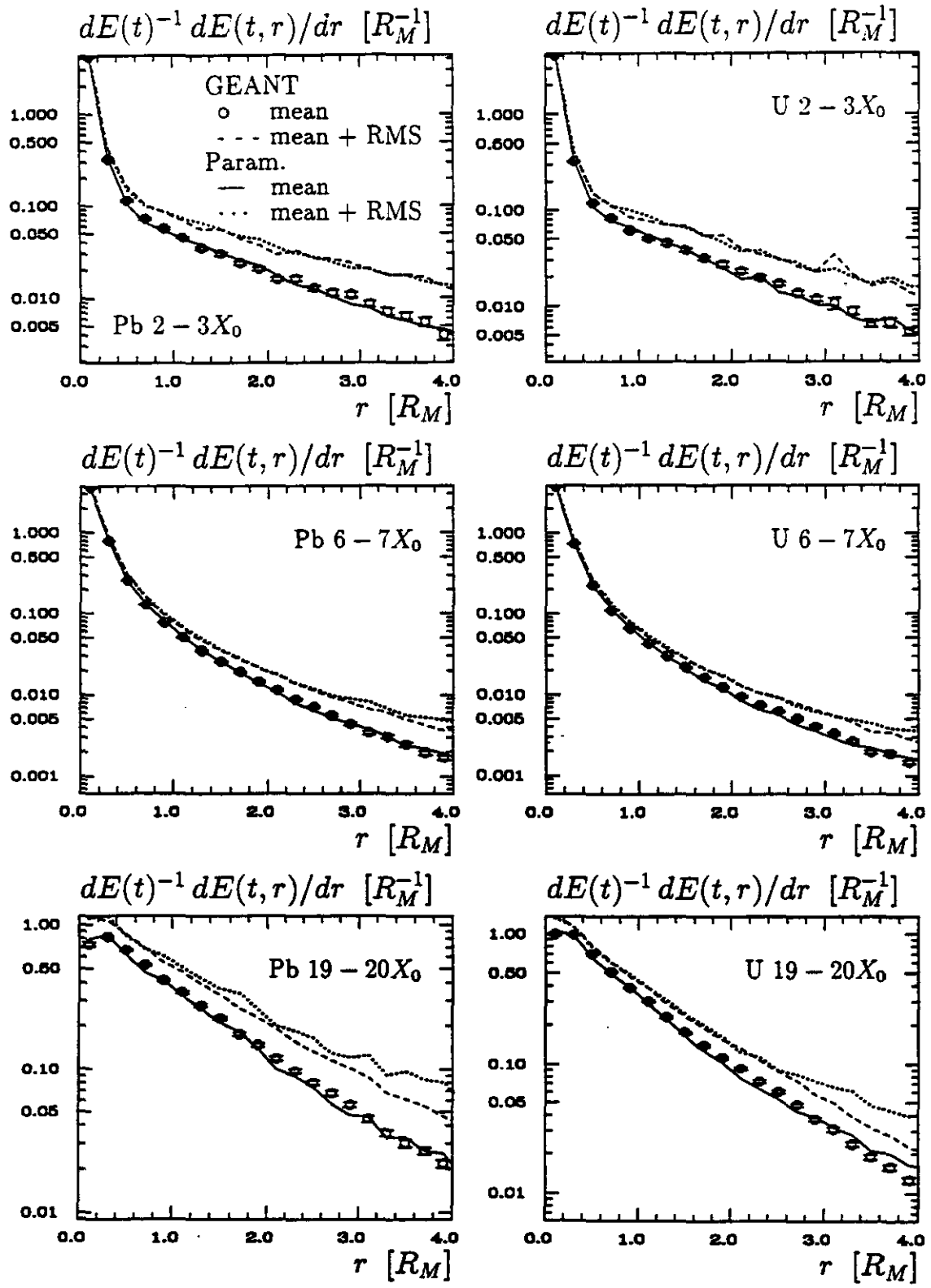
$dE(t)^{-1}\,dE(t,r)/dr\ \ [R_M^{-1}]$
GEANT
o mean
- - - mean + RMS
Param.
— mean
··· mean + RMS
Pb $2-3X_0$
U $2-3X_0$
Pb $6-7X_0$
U $6-7X_0$
Pb $19-20X_0$
U $19-20X_0$
$r\ \ [R_M]$

Figure 12:

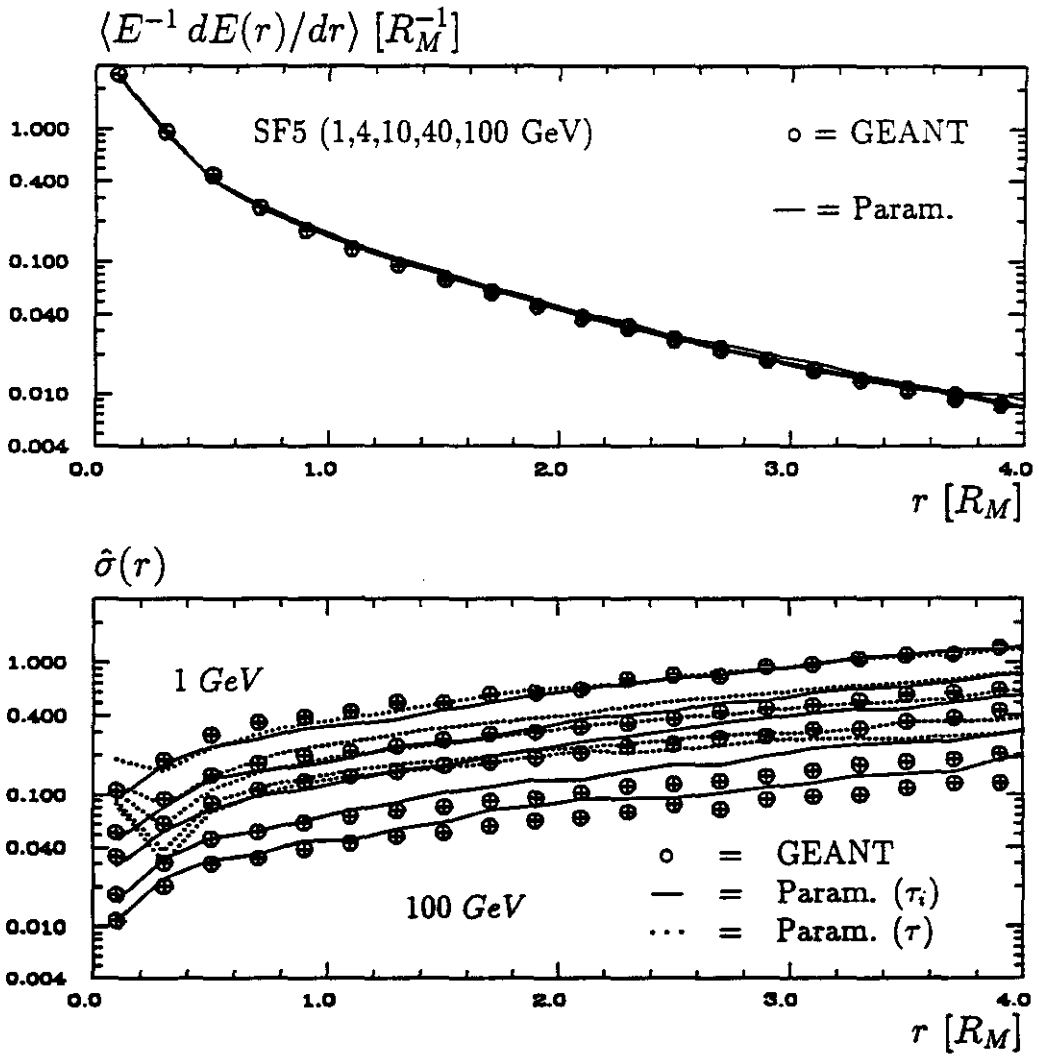
$\langle E^{-1}\, dE(r)/dr \rangle\ [R_M^{-1}]$
SF5 (1,4,10,40,100 GeV)
o = GEANT
— = Param.
1.000
0.400
0.100
0.040
0.010
0.004
0.0
1.0
2.0
3.0
4.0
$r\ [R_M]$
$\hat{\sigma}(r)$
1 GeV
100 GeV
o = GEANT
— = Param. (τ_i)
··· = Param. (τ)
1.000
0.400
0.100
0.040
0.010
0.004
0.0
1.0
2.0
3.0
4.0
$r\ [R_M]$

Figure 13:

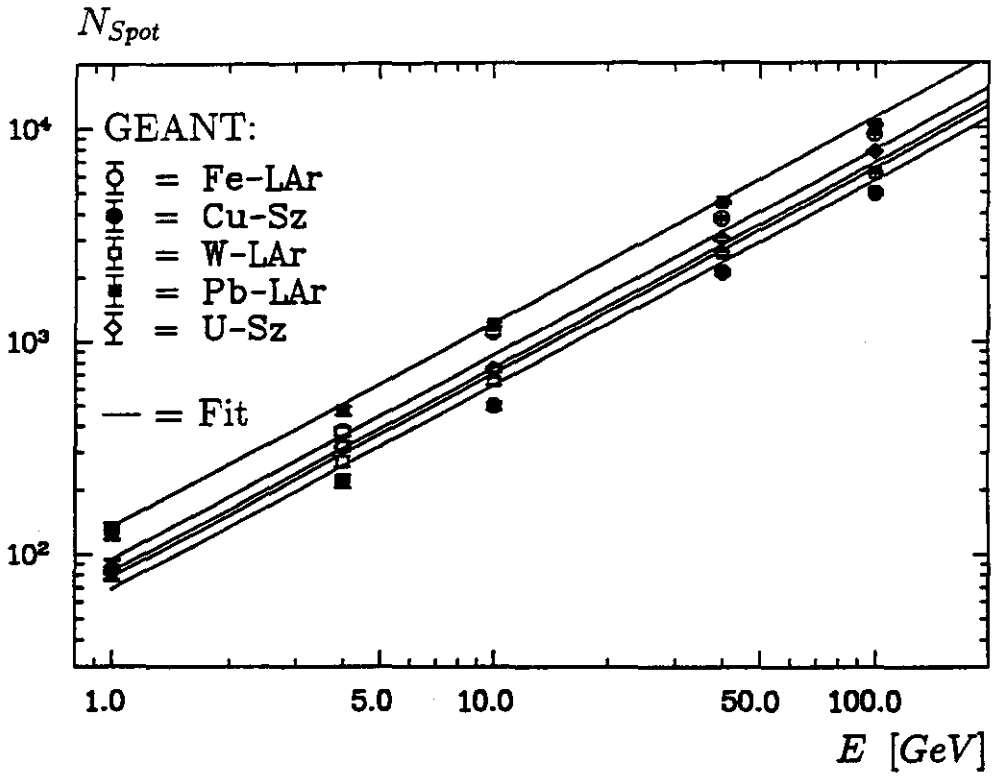
N_{Spot}
GEANT:
= Fe-LAr
= Cu-Sz
= W-LAr
= Pb-LAr
= U-Sz
— = Fit
10^4
10^3
10^2
1.0
5.0
10.0
50.0
100.0
E [GeV]

Figure 14:

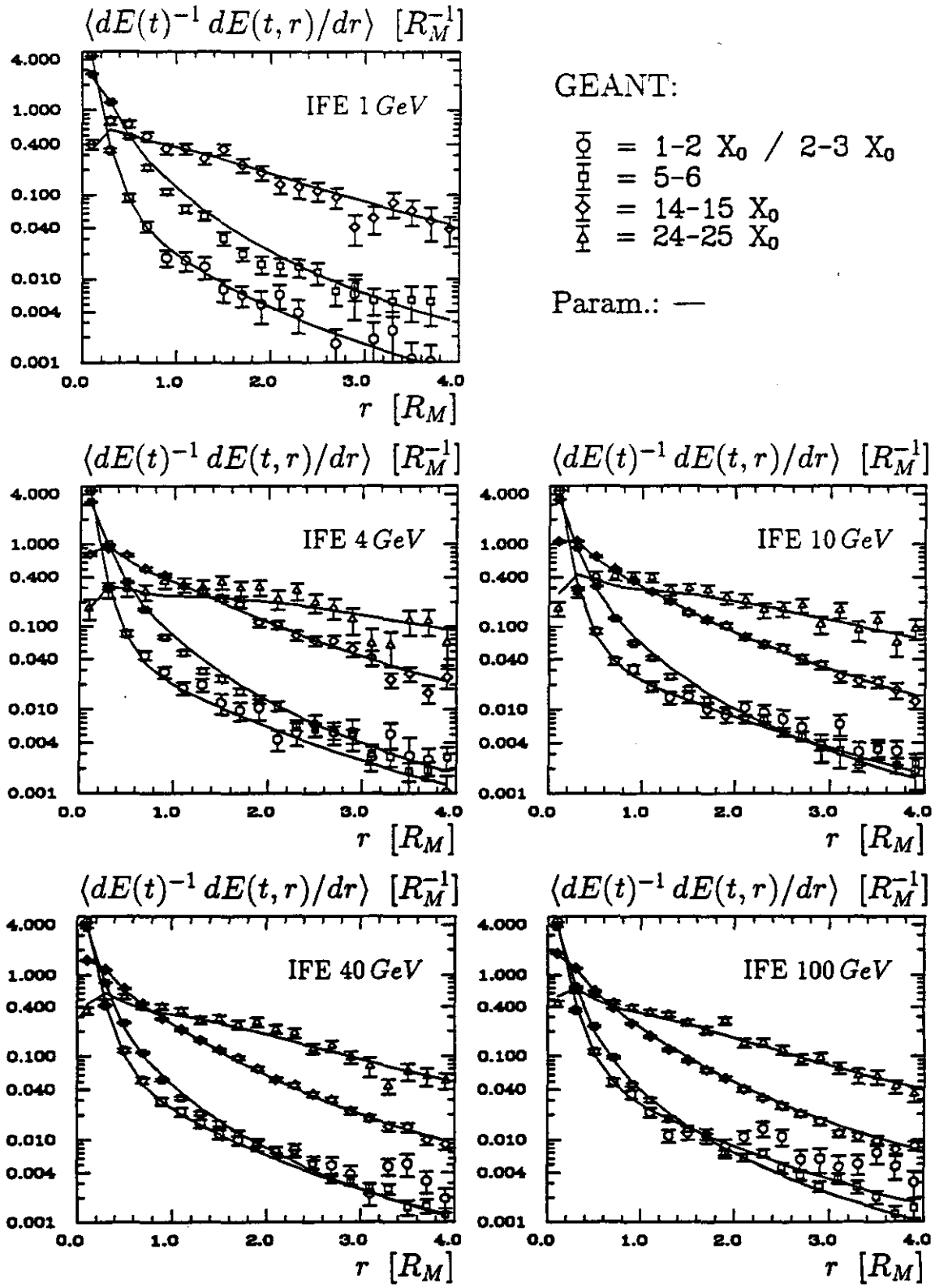
$\langle dE(t)^{-1}\, dE(t,r)/dr\rangle$ $[R_M^{-1}]$
IFE 1 GeV
IFE 4 GeV
IFE 10 GeV
IFE 40 GeV
IFE 100 GeV
r $[R_M]$
GEANT:
= 1-2 X_0 / 2-3 X_0
= 5-6
= 14-15 X_0
= 24-25 X_0
Param.: —

Figure 15:

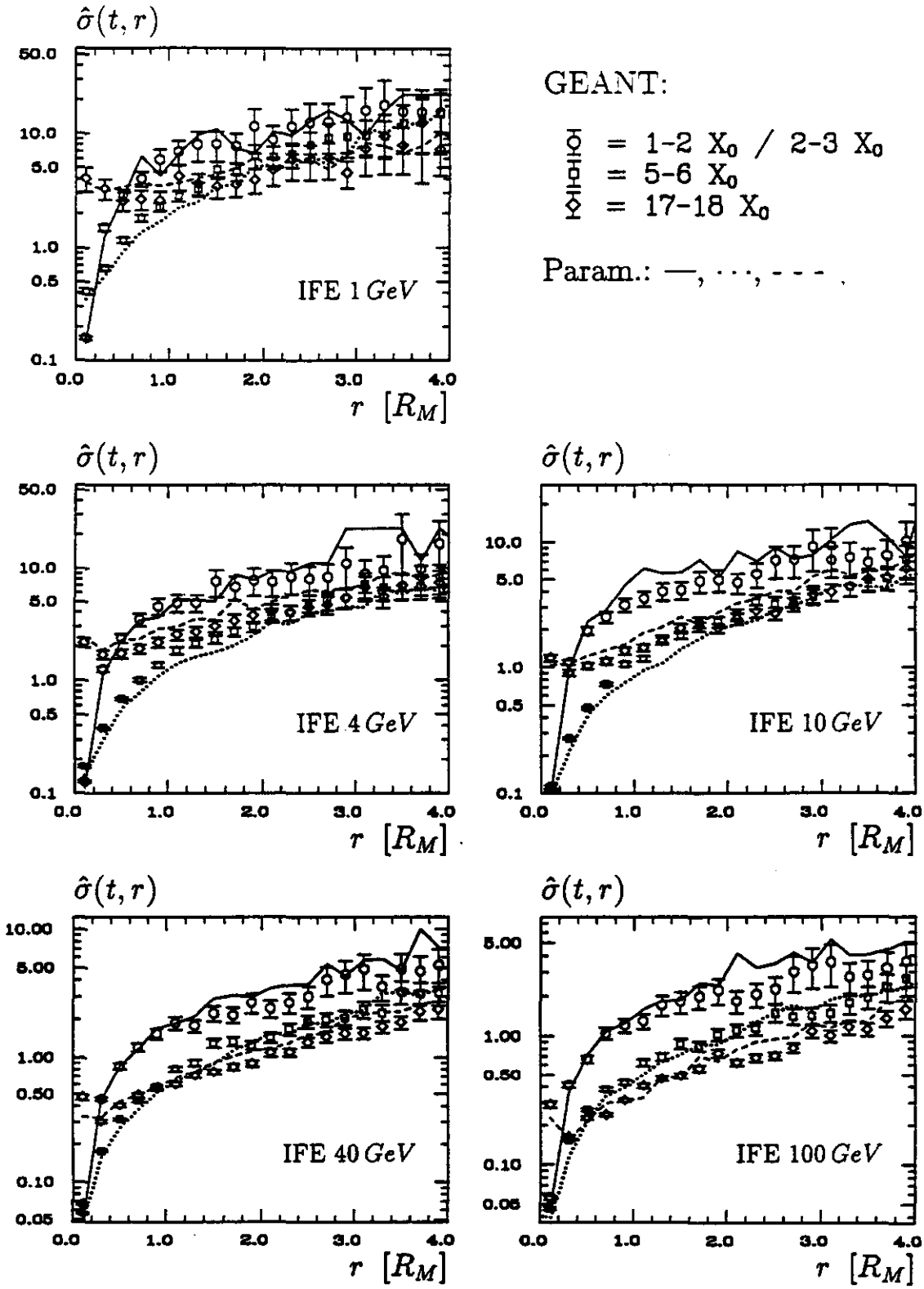
$\hat{\sigma}(t,r)$
GEANT:
= 1-2 X_0 / 2-3 X_0
= 5-6 X_0
= 17-18 X_0
Param.: —, ···, - - - .
IFE 1 GeV
IFE 4 GeV
IFE 10 GeV
IFE 40 GeV
IFE 100 GeV
r $[R_M]$

Figure 16:

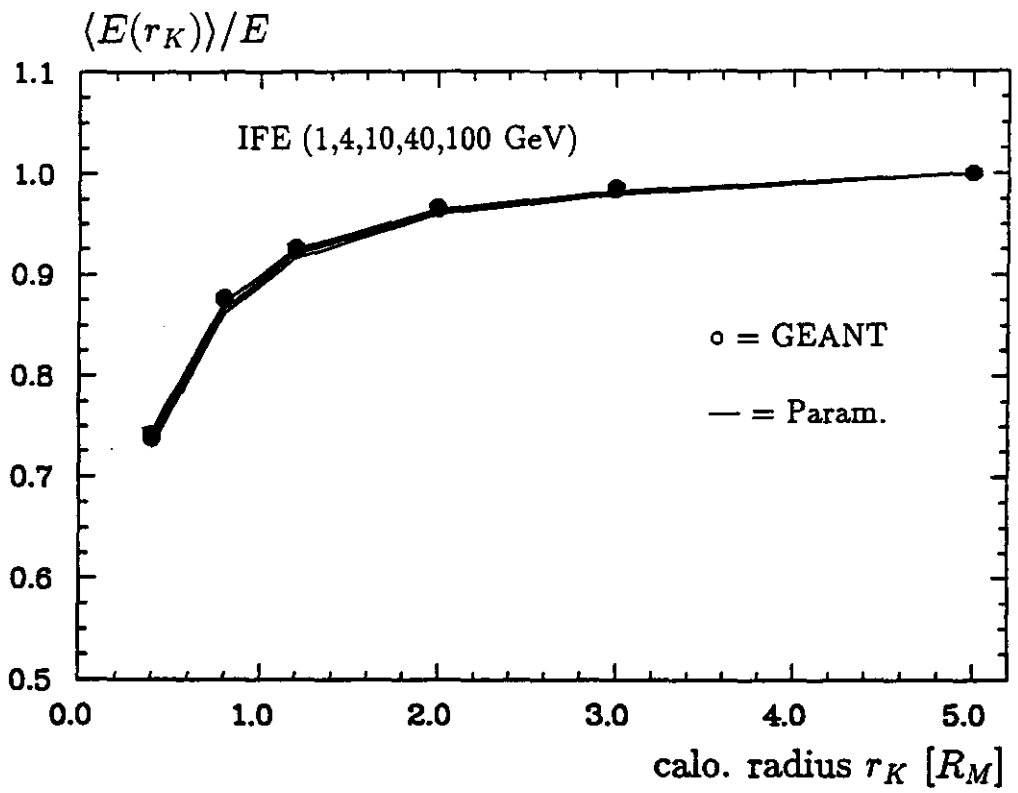
$\langle E(r_K)\rangle/E$
1.1
1.0
0.9
0.8
0.7
0.6
0.5
IFE (1,4,10,40,100 GeV)
o = GEANT
— = Param.
0.0
1.0
2.0
3.0
4.0
5.0
calo. radius r_K $[R_M]$

Figure 17:

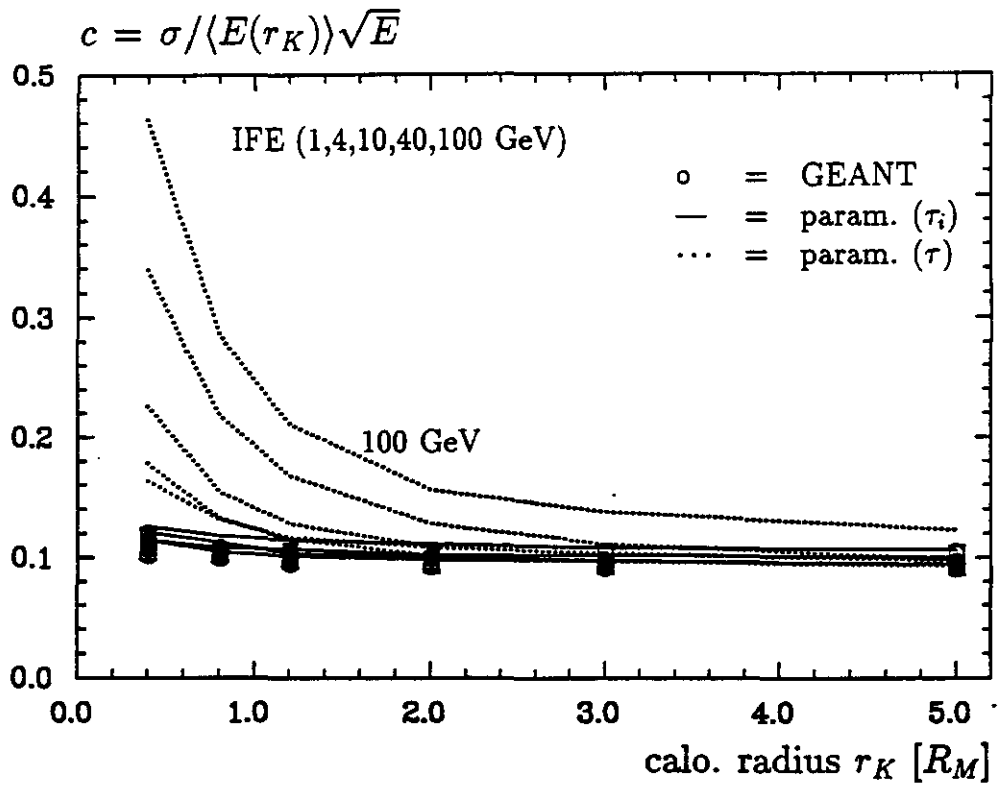
$c = \sigma/\langle E(r_K)\rangle\sqrt{E}$
IFE (1,4,10,40,100 GeV)
o = GEANT
— = param. (τ_i)
··· = param. (τ)
100 GeV
0.5
0.4
0.3
0.2
0.1
0.0
0.0
1.0
2.0
3.0
4.0
5.0
calo. radius r_K [R_M]

Figure 18:

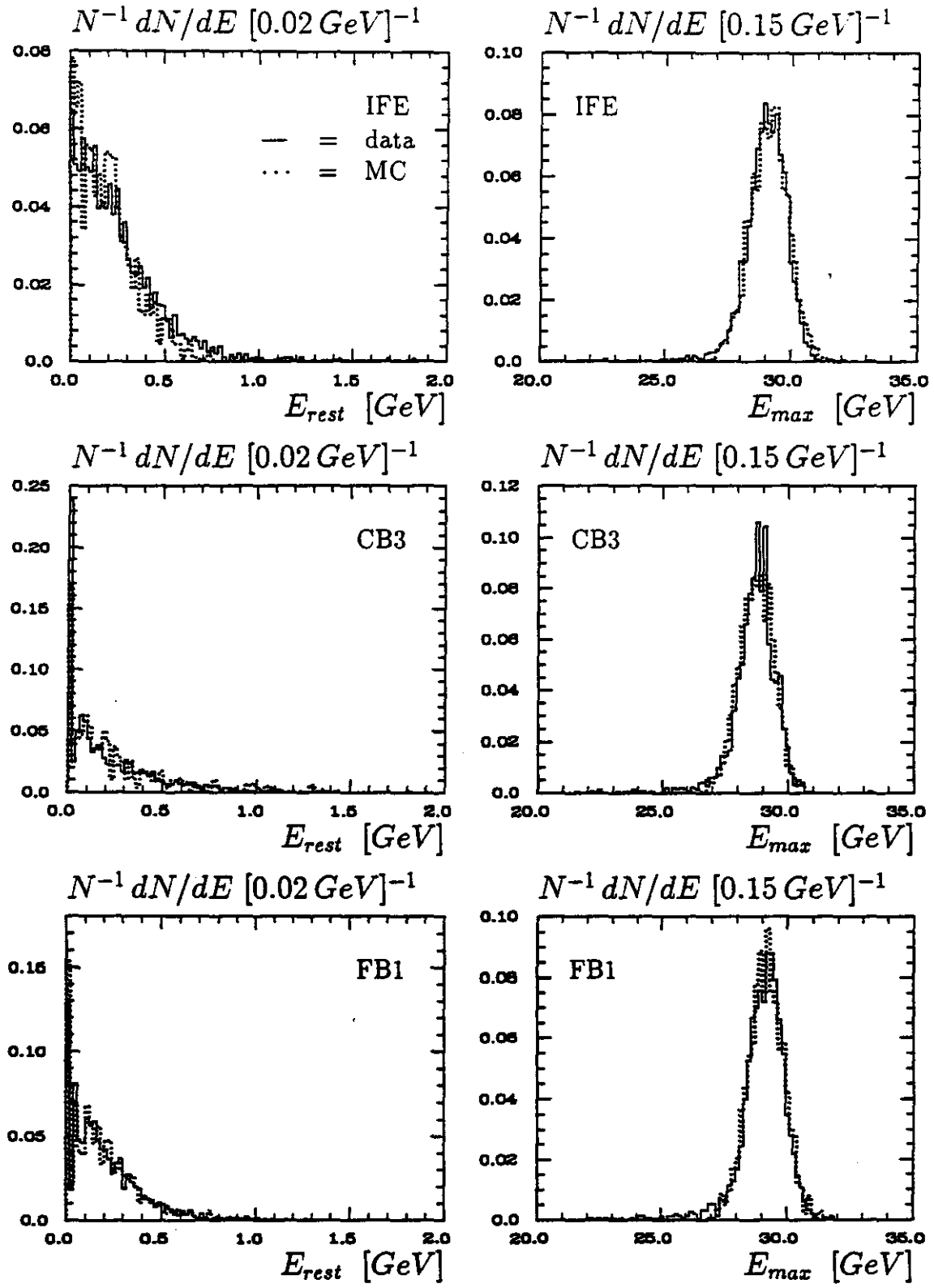
$N^{-1}\,dN/dE\ [0.02\,GeV]^{-1}$
IFE
— = data
··· = MC
E_{rest} [GeV]
$N^{-1}\,dN/dE\ [0.15\,GeV]^{-1}$
IFE
E_{max} [GeV]
$N^{-1}\,dN/dE\ [0.02\,GeV]^{-1}$
CB3
E_{rest} [GeV]
$N^{-1}\,dN/dE\ [0.15\,GeV]^{-1}$
CB3
E_{max} [GeV]
$N^{-1}\,dN/dE\ [0.02\,GeV]^{-1}$
FB1
E_{rest} [GeV]
$N^{-1}\,dN/dE\ [0.15\,GeV]^{-1}$
FB1
E_{max} [GeV]

Figure 19:

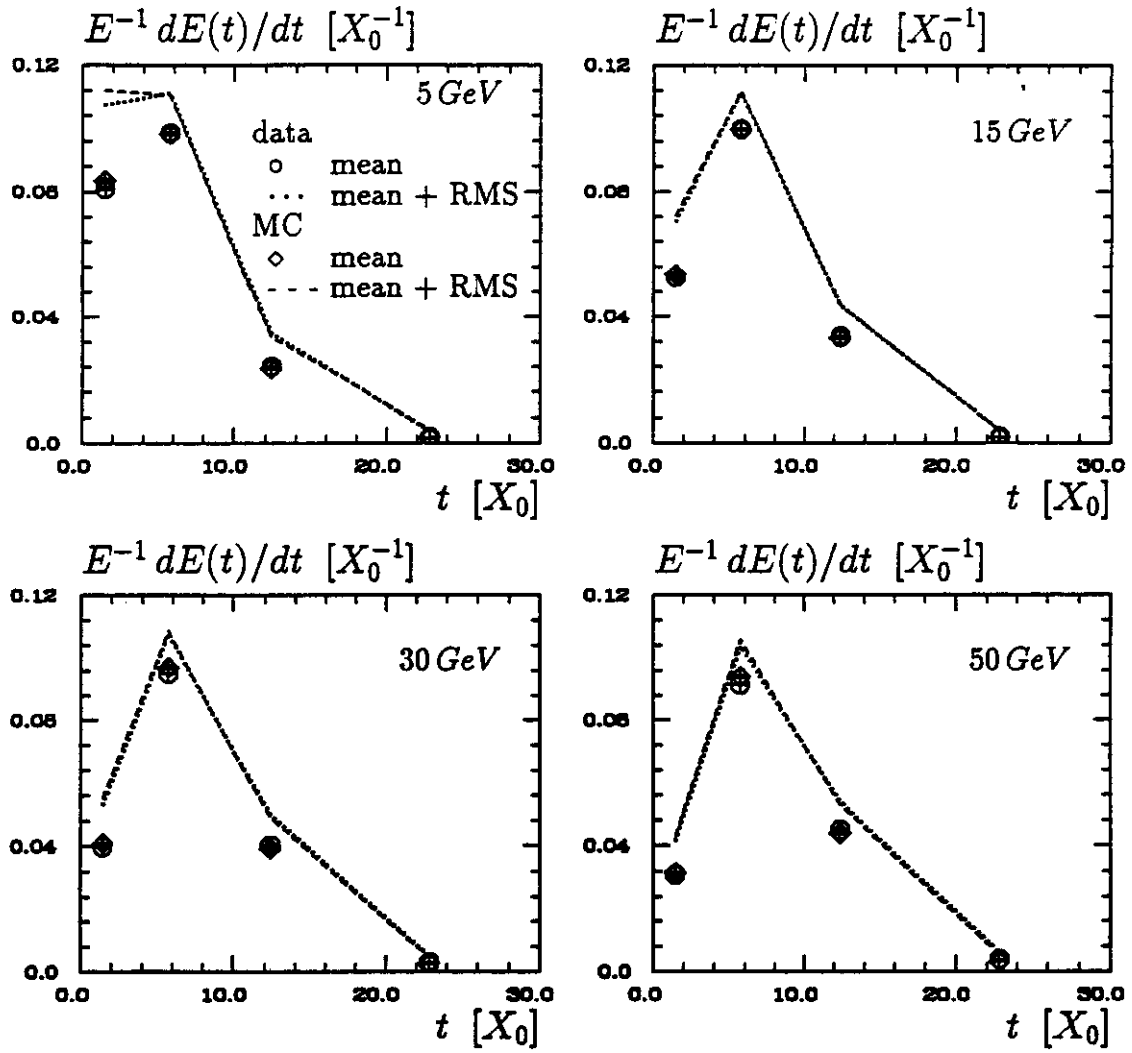
$E^{-1}\,dE(t)/dt\ \ [X_0^{-1}]$
5 GeV
data
mean
mean + RMS
MC
mean
mean + RMS
15 GeV
30 GeV
50 GeV
$t\ \ [X_0]$
0.0
0.04
0.08
0.12
10.0
20.0
30.0

Figure 20:

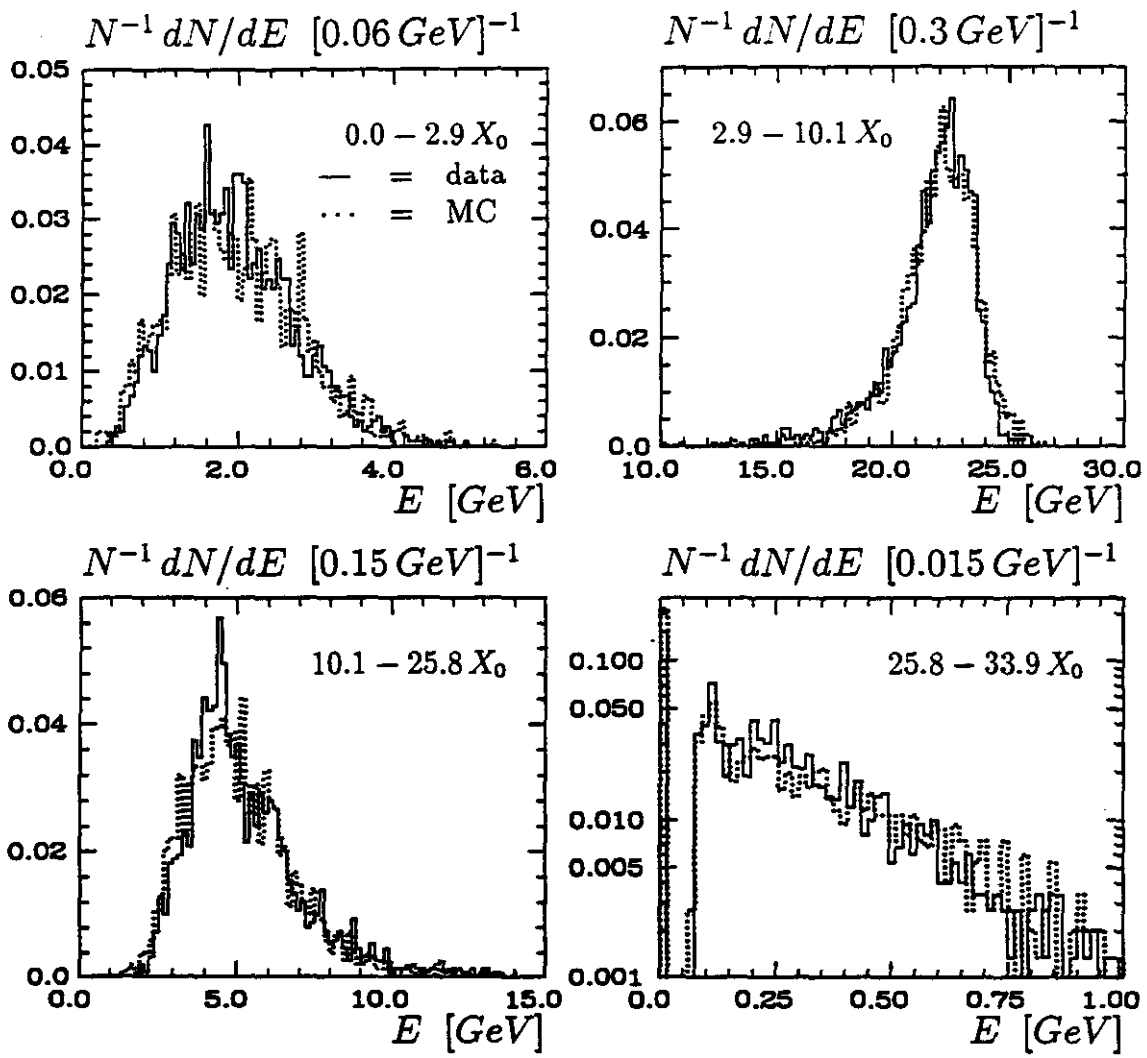
$N^{-1}\,dN/dE\ [0.06\,GeV]^{-1}$
0.05
0.04
0.03
0.02
0.01
0.0
0.0
2.0
4.0
6.0
$0.0 - 2.9\,X_0$
— = data
··· = MC
$E\ [GeV]$
$N^{-1}\,dN/dE\ [0.3\,GeV]^{-1}$
0.06
0.04
0.02
0.0
10.0
15.0
20.0
25.0
30.0
$2.9 - 10.1\,X_0$
$E\ [GeV]$
$N^{-1}\,dN/dE\ [0.15\,GeV]^{-1}$
0.06
0.04
0.02
0.0
0.0
5.0
10.0
15.0
$10.1 - 25.8\,X_0$
$E\ [GeV]$
$N^{-1}\,dN/dE\ [0.015\,GeV]^{-1}$
0.100
0.050
0.010
0.005
0.001
0.0
0.25
0.50
0.75
1.00
$25.8 - 33.9\,X_0$
$E\ [GeV]$

Figure 21:

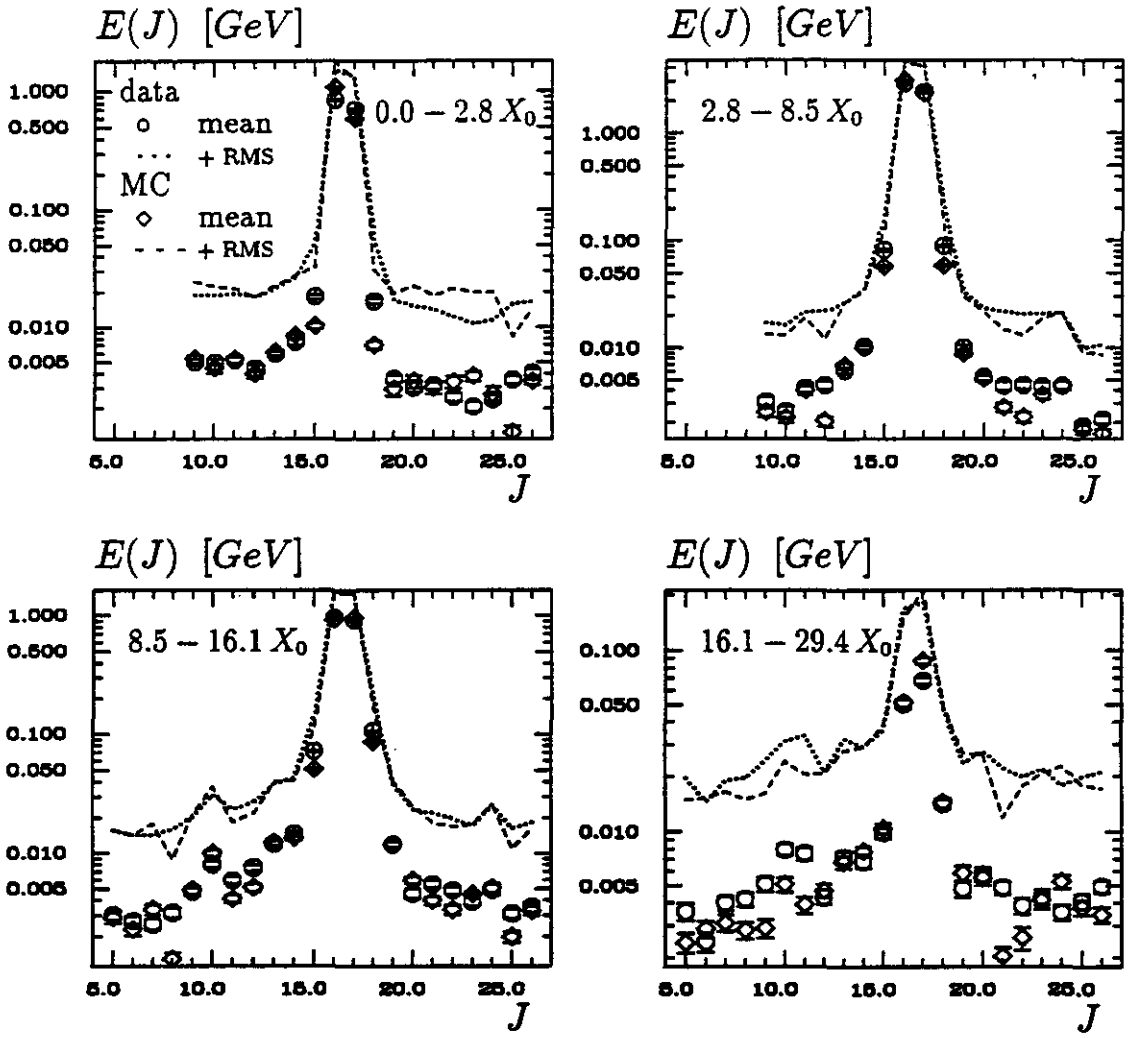
E(J) [GeV]
data
mean
+ RMS
MC
mean
+ RMS
0.0 – 2.8 X0
2.8 – 8.5 X0
8.5 – 16.1 X0
16.1 – 29.4 X0
1.000
0.500
0.100
0.050
0.010
0.005
5.0
10.0
15.0
20.0
25.0
J

Figure 22:

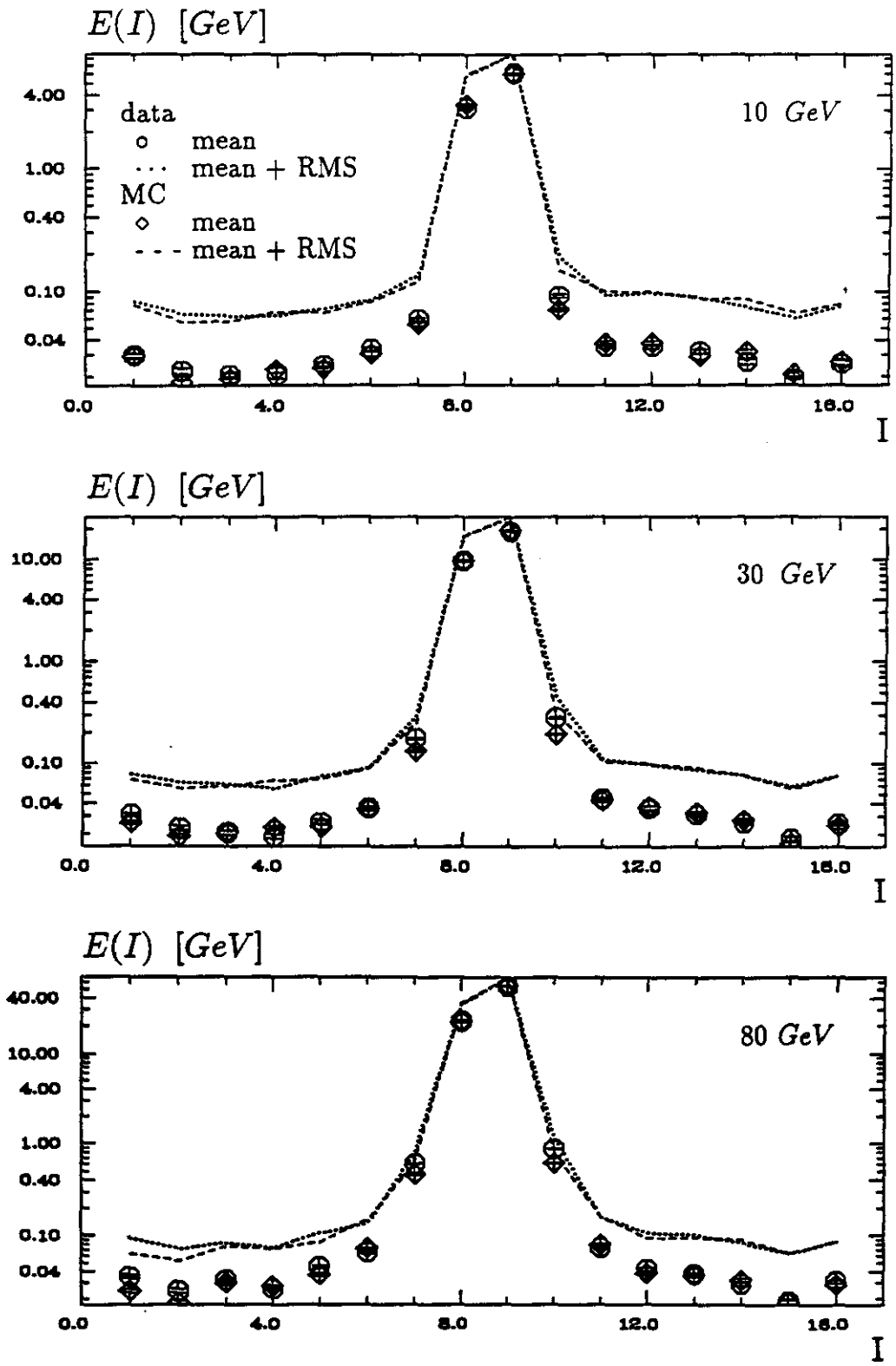
E(I) [GeV]
data
mean
mean + RMS
MC
mean
mean + RMS
10 GeV
4.00
1.00
0.40
0.10
0.04
0.0
4.0
8.0
12.0
16.0
I
E(I) [GeV]
30 GeV
10.00
4.00
1.00
0.40
0.10
0.04
0.0
4.0
8.0
12.0
16.0
I
E(I) [GeV]
80 GeV
40.00
10.00
4.00
1.00
0.40
0.10
0.04
0.0
4.0
8.0
12.0
16.0
I

Figure 23:

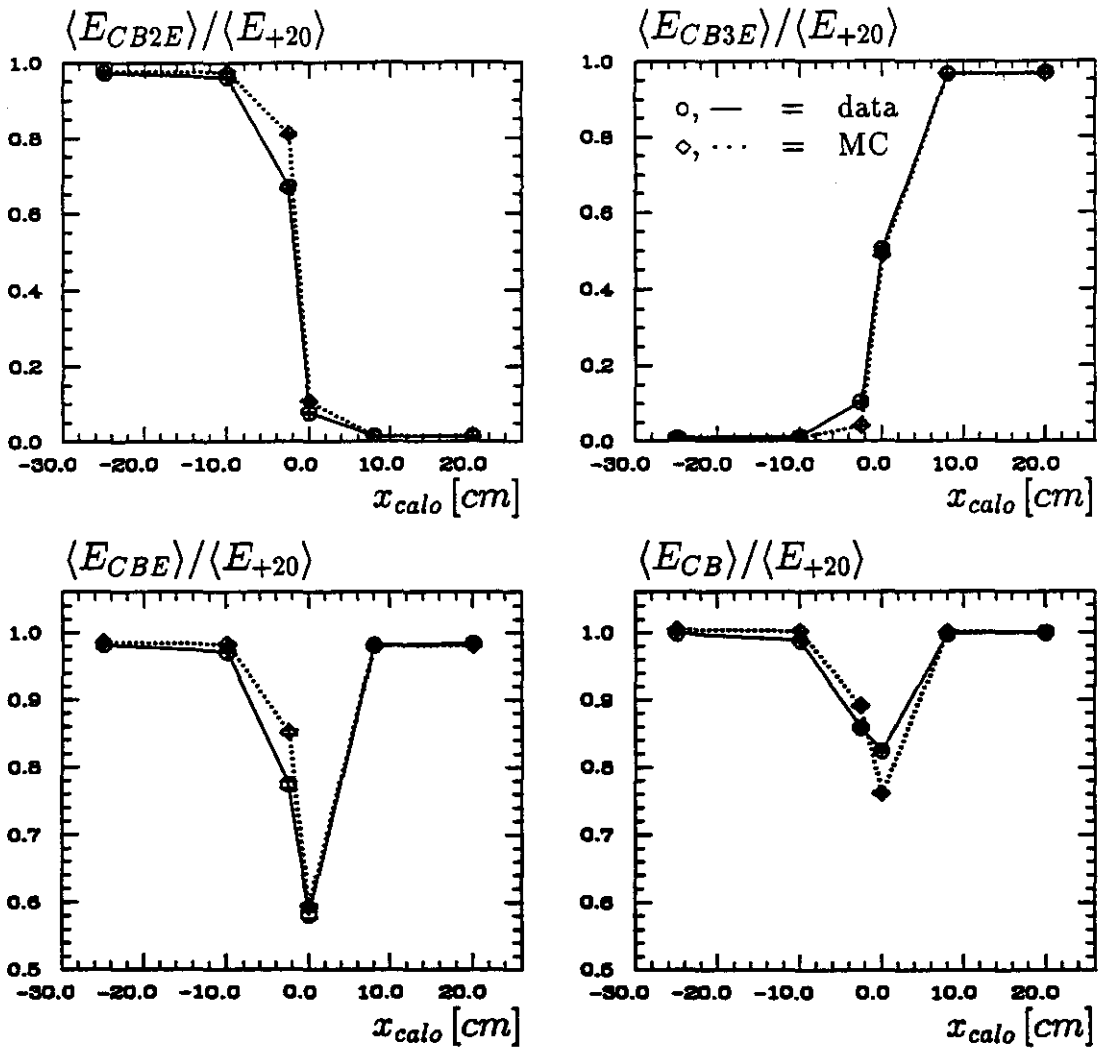
$\langle E_{CB2E}\rangle/\langle E_{+20}\rangle$
$\langle E_{CB3E}\rangle/\langle E_{+20}\rangle$
$\langle E_{CBE}\rangle/\langle E_{+20}\rangle$
$\langle E_{CB}\rangle/\langle E_{+20}\rangle$
o, — = data
◇, ··· = MC
x_{calo} [cm]

Figure 24:

SLAC-PUB-5072
October 1989
(I)

THE FAST SIMULATION OF ELECTROMAGNETIC AND HADRONIC SHOWERS*

G. Grindhammer,[a,b] M. Rudowicz,[b] and S. Peters[b]

[a]*Stanford Linear Accelerator Center, Stanford University, Stanford, CA 94309*

[b]*Max-Planck-Institut für Physik und Astrophysik, Werner-Heisenberg-Institut für Physik, D-8000 München 40*

Presented by G. Grindhammer

Abstract

A program for the fast simulation of electromagnetic and hadronic showers using parameterizations for the longitudinal and lateral profile is described. The fluctuations and correlations of the parameters are taken into account in a consistent way. Comparisons with data over a wide energy range are made.

Invited talk presented at the SSC Workshop on Calorimetry for the Superconducting Super Collider, Tuscaloosa, Alabama, March 13-17, 1989, and Submitted to Nuclear Instruments and Methods.

* Work supported by Department of Energy contract DE-AC03-76SF00515.

1. Introduction

Particle showers in calorimeters and particularly in sampling calorimeters are typically simulated by tracking all secondary particles of the shower down to some minimum energy. The computer time needed for simulations of this type increases linearly with the shower energy and can easily become prohibitive. The parameterization of the energy density distribution of showers has been one method to speed up the simulation.

A simple algorithm for parameterized showers has been successfully used for the simulation of the UA1 calorimeter [1]. The simulation of the longitudinal energy profile of electromagnetic showers was based on fitting the parameters of an ansatz by Longo and Sestili [2] to the mean shower profile. Later, the parameterized simulation was much improved when the shape fluctuations of individual showers were systematically taken into account [3, 4]. We have extended the sophistication reached in the parameterized simulation of electromagnetic showers to hadronic showers by taking into account their individual fluctuations and, in particular, the fluctuation of their π^0 component.

This is of importance for a correct simulation of the e/h response and the energy resolution of a calorimeter, which is of great importance for the experiments being set up at the ep collider HERA and at other currently operating or planned high energy colliders.

The program GFLASH, which we have developed, generates electromagnetic and hadronic showers and computes the visible energy fraction in a geometry defined by the user with the help of GEANT [5]. In addition, GEANT is used for the tracking of particles and the accompanying physics processes, at least until the first inelastic interaction.

2. Procedure

To arrive at a useful ansatz for the longitudinal and lateral energy profiles, and to obtain the necessary parameters, we used the following iterative procedure [6]:

- use/modify an ansatz and fit the parameters to Monte Carlo (MC) data using a detailed simulation of electromagnetic and hadronic showers [5, 7]; and
- compare and fit some of the parameters with experimental data [8].

The MC data were generated for the typical sampling structures of the H1 calorimeter [8, 9] built for the H1 experiment at HERA. The essential materials of this calorimeter are lead (Pb) and liquid argon (LAr) for the electromagnetic and iron (Fe) and LAr for the hadronic modules. Showers in the energy range from 1 to 200 GeV were generated. The parameters, and their fluctuations and correlations, were parameterized as a function of energy, using scales which minimize the dependence on the calorimeter materials.

The simulation of showers in GFLASH has been divided into two steps. First, the spatial distribution of the deposited energy E_{dp} for a shower is calculated for the calorimeter module containing all or part of the shower, taking the fluctuations and correlations of the parameters and their energy dependence into account:

$$dE_{dp}(\vec{r}) \;=\; E_{dp}\; f(z)\,dz\; f(r)\,dr\; f(\phi)\,d\phi \quad . \tag{1}$$

A calorimeter module or a part of it—which may have a complicated, but repetitive, sampling structure—is described by one single effective medium. In the second step, the energy fraction of the deposited energy which is visible in the active medium E_{vs} is computed

$$dE_{vs}(\vec{r}) \;=\; E_{dp}\; \widetilde{mip} \sum_k \frac{\tilde{k}}{\widetilde{mip}}\, c_k\; f_k(\vec{r})\; dV \quad . \tag{2}$$

Here, $\widetilde{mip}$ denotes the sampling fraction for minimum ionizing particles, and $\tilde{e}/\widetilde{mip}$ and $\widetilde{had}/\widetilde{mip}$ are the relative sampling fractions for electrons and hadrons, respectively. The sum is over the electromagnetic ($k = e$) and the purely hadronic ($k = had$) components, taking the distribution functions f_k for the two components and their relative fractions c_k of the energy deposited in the active medium into account. For the calorimeter-dependent sampling fractions $\widetilde{mip}$, $\tilde{e}$, $\widetilde{had}$, and the sampling fluctuations, it is desirable to use measured values.

3. Parameterization of electromagnetic showers

3.1. Longitudinal shower profile

It is well known that the mean longitudinal profile of electromagnetic showers can be described by a Gamma distribution [2]. A realistic simulation, however, requires the simulation of individual showers. Fluctuating the parameters obtained from average profiles does not necessarily lead to a correct description of the fluctuations of individual showers [4]. Assuming that the individual shower profiles can also be approximated by a Gamma distribution

$$f_i(z) \;=\; \frac{x^{\alpha_i - 1}\, e^{-x}}{\Gamma(\alpha_i)} \quad , \qquad \text{with} \qquad x \;=\; \beta_i\, z \quad , \tag{3}$$

the fluctuations can be deduced and reproduced. The index i indicates that the function describes an individual shower i with the parameters α_i and β_i. The shower depth z is measured in units of radiation length [X_0]. The α_i and β_i can be calculated from the first and second moments of the Gamma distribution. They are normal-distributed such that the means μ_α and μ_β, and their fluctuations σ_α and σ_β can be determined and parameterized as a function of energy. The correlation of the α_i and β_i is given by

$$\rho \;=\; \frac{\langle (\alpha_i - \langle\alpha_i\rangle)\;(\beta_i - \langle\beta_i\rangle)\rangle}{\left[\left(\langle\alpha_i^2\rangle - \langle\alpha_i\rangle^2\right)\;\left(\langle\beta_i^2\rangle - \langle\beta_i\rangle^2\right)\right]^{1/2}} \quad . \tag{4}$$

Numerically, $\rho = 0.73$ and is roughly independent of the energy of the shower in the range from 1 to 200 GeV. In the simulation, a correlated pair (α_i, β_i) is generated according to

$$\begin{aligned} \begin{pmatrix} \alpha_i \\ \beta_i \end{pmatrix} \;&=\; \begin{pmatrix} \mu_\alpha \\ \mu_\beta \end{pmatrix} + C \begin{pmatrix} z_1 \\ z_2 \end{pmatrix} \quad , \qquad \text{with} \\ C \;&=\; \begin{pmatrix} \sigma_\alpha & 0 \\ 0 & \sigma_\beta \end{pmatrix} \begin{pmatrix} \sqrt{(1+\rho)/2} & \sqrt{(1-\rho)/2} \\ \sqrt{(1+\rho)/2} & -\sqrt{(1-\rho)/2} \end{pmatrix} \quad , \end{aligned} \tag{5}$$

where z_1 and z_2 are normal-distributed random numbers.

The whole procedure is presented graphically in fig. 1 for 10 GeV e^- showers. The individual and the mean energy profiles of 400 showers, as generated with GEANT and with GFLASH, are shown. In addition, the distribution of the parameters α_i and β_i, and their correlation as obtained from GEANT, are given. A comparison of the GEANT and GFLASH simulation reveals good agreement in the mean profiles (additional energies are compared in fig. 2) and in the individual fluctuations, particularly in the variation of the center of gravity and the shower maximum.

3.2. *Lateral shower profile*

For the description of the lateral energy profile of electromagnetic as well as hadronic showers, we assume only a radial, and no azimuthal dependence. The average radial shower distribution is frequently described by the superposition of two exponentials (see e.g., ref. 10). One of them describes the confined energetic core of the shower and the other the surrounding halo.

In GFLASH, we have used the very simple ansatz

$$f(r) = \frac{2\, r\, R_{50}^2}{(r^2 + R_{50}^2)^2} \quad , \tag{6}$$

for both electromagnetic and hadronic showers, which seems quite adequate, at least as long as the lateral resolution of the calorimeter is of the order of or larger than ~ 1 Molière radius (R_M) for electromagnetic and ~ 0.1 absorption length (λ_0) for hadronic showers. The radius r and the free parameter R_{50} in eq. (6) are in units of R_M (or λ_0 for hadronic showers). Fixed amounts of energy (energy spots) are deposited at radii r, generated according to the radial probability function. To simulate the fluctuations of individual showers, it is necessary to parameterize the mean and the variance (V) of the approximately log-normal distributed parameter R_{50} as a function of shower energy E [GeV] and shower depth z [in units of X_0 or λ_0]:

$$\begin{aligned} \langle R_{50}(E,z)\rangle &= [R_1 + (R_2 - R_3 \ \ln E)\ z]^n \quad , \\ V_{R_{50}}(E,z) &= [(S_1 - S_2 \ \ln E)\ (S_3 + S_4\, z)\ \langle R_{50}(E,z)\rangle]^2 \quad . \end{aligned} \tag{7}$$

This parameterization, with $n = 1$ (2) for hadronic (electromagnetic) showers, describes the increasingly slower growth of the radial extent and of the relative fluctuations $\sqrt{V_{R_{50}}}/\langle R_{50}\rangle$ of a shower with increasing energy. Lateral distributions for 10 GeV e^- showers as a function of depth generated with GEANT and GFLASH are compared in fig. 3. As can be seen, there is reasonable agreement in the description of the hard core and halo of the showers.

3.3. *Sampling fluctuations*

The conversion from the deposited energy to the fraction which is visible in the active part of the sampling structure is performed during the lateral depositioning of the energy spots. In addition, the sampling fluctuations are taken into account.

The visible energy for a spot is computed using the measured sampling fractions $\widetilde{mip}$ and the relative fraction $\tilde{e}/\widetilde{mip}$ (and, in addition, $\widetilde{had}/\widetilde{mip}$ for hadron showers), which may depend on the position of the spot in the calorimeter. The sampling fluctuations are reproduced by depositing a Poisson distributed number of spots $N_s(\ell)$ of energy E_s per longitudinal integration interval ℓ according to the radial probability function. Assuming the energy resolution to be simulated is given by

$$\begin{aligned} \frac{\sigma_{dp}}{E_{dp}} &= \frac{a}{\sqrt{E_{inc}}} \quad , \qquad \text{and with} \\ \sigma_{dp}^2 &= V\left[\sum_\ell E_s\, N_s(\ell)\right] = E_s^2 \sum_\ell V\,[N_s(\ell)] = E_s\, E_{dp} \quad , \end{aligned} \tag{8}$$

we find for the spot energy:

$$E_s = a^2 \quad .$$

4. Parameterization of hadronic showers

It is convenient to imagine a hadronic shower as consisting of a purely hadronic and a π^0 component (mainly π^0's and some η's).The large fluctuations of the relative fractions of the π^0 and hadronic components in a shower lead to

fluctuations in a noncompensating calorimeter ($e/h \neq 1$), which are much larger than the fluctuations of electromagnetic showers alone. A simulation of hadronic showers has to take into account:

- the energy dependence of the fraction of the π^0 component (c_{π^0}) and its fluctuation;
- the response of the calorimeter which, in general, differs for the π^0 and the purely hadronic showers; and
- the different propagation scales, X_0 for the π^0 and λ_0 for the hadronic component.

4.1. *Longitudinal parameterization*

A well-known ansatz for the parameterization of the mean longitudinal energy profile [1] uses the superposition of two Gamma distributions to describe the π^0 and the purely hadronic subprofiles:

$$dE_{dp} = E_{dp}\,[(1-c_{\pi^0})\,\mathcal{H}(x)\,dx + c_{\pi^0}\,\mathcal{E}(y)\,dy] \quad , \tag{9}$$

$$\text{with} \qquad \mathcal{H}(x) = \frac{x^{\alpha_h - 1}\,e^{-x}}{\Gamma(\alpha_h)} \quad , \quad \text{and} \quad x = \beta_h\, s_h \quad ,$$

$$\text{with} \qquad \mathcal{E}(y) = \frac{y^{\alpha_e - 1}\,e^{-y}}{\Gamma(\alpha_e)} \quad , \quad \text{and} \quad y = \beta_e\, s_e \quad .$$

The distance from the shower starting point is given by s_h [λ_0] for the hadronic and by s_e [X_0] for the π^0 component.

We used this ansatz to describe the mean shower energy profile obtained from a simulation of the H1 calorimeter, using GEANT. A satisfactory description of the shower shapes could only be obtained if one allowed the parameter c_{π^0} to decrease with energy which is inconsistent with data [8]. This behavior has also been observed by fitting data with a similar method [11,12]. It is, however, necessary to correctly simulate the π^0 and hadronic subprofiles individually in order to compute their different responses and the fluctuations of individual showers properly. We expected an ansatz containing three terms to accomplish this:

$$dE_{dp} = f_{dp}\,E_{inc}\,\left[c_h\,\mathcal{H}(x)\,dx + c_f\,\mathcal{F}(y)\,dy + c_l\,\mathcal{L}(z)\,dz\right] \quad , \tag{10}$$

$$\text{with} \qquad \mathcal{H}(x) = \frac{x^{\alpha_h - 1}\,e^{-x}}{\Gamma(\alpha_h)} \quad , \quad \text{and} \quad x = \beta_h\,[\lambda_0^{-1}]\;s_h\,[\lambda_0] \quad ;$$

$$\text{with} \qquad \mathcal{F}(y) = \frac{y^{\alpha_f - 1}\,e^{-y}}{\Gamma(\alpha_f)} \quad , \quad \text{and} \quad y = \beta_f\,[X_0^{-1}]\;s_f\,[X_0] \quad ;$$

$$\text{with} \qquad \mathcal{L}(z) = \frac{z^{\alpha_l - 1}\,e^{-z}}{\Gamma(\alpha_l)} \quad , \quad \text{and} \quad z = \beta_l\,[\lambda_0^{-1}]\;s_l\,[\lambda_0] \quad .$$

As before, the first term describes the purely hadronic shower profile. The second term models the subprofile of the π^0 fraction which is produced in the first inelastic interaction(the index f stands for "first"). Its scale is measured in X_0. The third term simulates the subprofile of the π^0 fraction, which is produced in the course of the further development of the shower (the index ℓ stands for "late"). It scales in λ_0. The fraction of deposited energy (f_{dp}) with respect to the energy of the incident particle (E_{inc}) takes the intrinsic losses during the hadronic shower development into account.

Assuming an energy dependence of the form $a + b \ln E$ for the parameters to be fitted, a good description of the mean energy profile was achieved. This can be seen in fig. 4, which shows the results of the fits to the mean shower profiles for different energies simulated with GEANT. However, despite this good agreement, two problems remained. One problem was that one needed two sets of parameters, one for $1 \lesssim E_{inc} \lesssim 5$ and one for $5 < E_{inc}$ [GeV] $\lesssim 200$, and the other problem was that for some of the parameters a normal or log-normal distribution was not a good approximation. Both of these "defects" could be remedied by taking the relative probabilities for the occurrence of the different subprofiles into account.

4.2. *π^0 fluctuations*

To simulate the π^0 fluctuations, it is not sufficient to just fluctuate the average fractions c_h, c_f, and c_ℓ of the deposited energy [see eq. (10)]. The reasons are:

- not every hadronic shower with energy $\lesssim 5$ GeV yields a π^0 in the first inelastic interaction; and
- up to an energy of about 50 GeV, also no "late" π^0 may be produced.

In fig. 5, the relative probabilities for a hadronic shower to have any π^0's $P(\pi^0)$, to have a π^0_f and a π^0_ℓ component $P(\pi^0_f \text{ and } \pi^0_\ell)$, and to have only a π^0_ℓ fraction $P(\pi^0_\ell)$ are shown as simulated by GEANT. We distinguish three classes of hadronic showers according to our ansatz:

1) purely hadronic showers:

   class H with $P(\pi^0) < P \leq 1$,

2) showers containing a π^0_f component:

   class F with $P(\pi^0_f \text{ and } \pi^0_\ell) < P \leq P(\pi^0)$, and

3) showers which in addition to π^0_f also contain a π^0_ℓ component:

   class L with $0 < P \leq P(\pi^0_f \text{ and } \pi^0_\ell)$,

where P is a uniform distributed random number.

Taking these probabilities into account and distinguishing between the three shower classes finally allows us to successfully simulate individual hadronic showers using eq. (10). The fractions c_h, c_f, and c_l are calculated according to:

$$\begin{aligned} c_h(E) &= 1 - f_{\pi^0}(E) \\ c_f(E) &= f_{\pi^0}(E)\,(1 - f^l_{\pi^0}(E)) \\ c_l(E) &= f_{\pi^0}(E)\, f^l_{\pi^0}(E) \end{aligned} \tag{11}$$

$$\text{with} \quad c_h(E) + c_f(E) + c_l(E) = 1 \quad ,$$

$$\text{and} \quad f_{\pi^0} = \left\langle \frac{E_{\pi^0}}{E_{dp}} \right\rangle \quad , \quad f^l_{\pi^0} = \left\langle \frac{E^l_{\pi^0}}{E_{\pi^0}} \right\rangle \quad .$$

The energy dependence of the mean π^0 fractions as obtained from GEANT are shown in fig. 6. The fractional π^0 energy of an individual shower is then given by $f_{\pi^0}/P(\pi^0)$, which is also displayed in fig. 6.

As in the case of electromagnetic showers, individual shower profiles are used to obtain the means, fluctuations and correlations of the parameters f_{dp}, f_{π^0}, $f^l_{\pi^0}$,

α_h, β_h, α_f, β_f, α_l, and β_l. For shower class H, there are three; for class F, there are six; and for class L, there are nine parameters whose means and covariances are parameterized as a function of energy.

The vector of parameters $\vec{x}$ for an individual shower is given by [13]

$$\vec{x} = \vec{\mu} + C\vec{z} \quad , \qquad \text{with} \qquad V = CC^T \quad . \tag{12}$$

The vector $\vec{z}$ contains maximally nine normal-distributed random numbers with variance of one, $\vec{\mu}$ is the vector of the means of the parameters and V is their covariance matrix. A method by Cholesky [14] is used to decompose the n-dimensional symmetric matrix V. To use the more intuitive parameters σ_{ii} and ρ_{ij} instead of the covariance V_{ij}, it is the correlation matrix ρ which is decomposed in GFLASH after the transformation $V = \sigma\rho\sigma^T$ with the diagonal matrix σ.

For the simulation of the lateral shower distribution and the sampling fluctuations, the same functional form and basically the same method are used as for electromagnetic showers.

5. The GEANT–GFLASH interface

The interfacing of GFLASH with GEANT was done for the following reasons:

- Like many other experiments, the H1 collaboration has decided to use GEANT for the description of the detector geometry in its simulation program. With GFLASH implemented in GEANT, it is then very easy for the user to switch between simulations of showers using GEANT/GHEISHA [5,7] or the parameterization algorithm of GFLASH. In addition, in this scheme, GEANT can be used for the first inelastic interaction(s) (for example, until the energies of the secondaries of a very high energy incident particle have cascaded down to the energy range for which the parameterization in GFLASH has been tested), switching to GFLASH for the remaining secondaries.
- When using GFLASH, it is appropriate to describe a calorimeter module of the same type with one medium characterized by a suitable average over the properties of the materials of that module. This considerably reduces the time spent by GEANT in searching for volumes and tracking.

- The major part of the energy of a shower is deposited inside a small cylinder of about one R_M for electromagnetic showers, and less than an λ_0 for hadronic showers. To a good approximation, therefore, the shower development is determined by the medium found at the core of the shower. The "tracking" routines of GEANT are used to provide GFLASH with the geometry and material information it needs.

In fig. 7, we show a simplified schematic of GEANT and the integration of the relevant GFLASH routines (underlined). A trivial change in GTVOL permits attachment of GFLASH.

The routine GTREVE administers the tracking of the primary tracks of the event (prim_tracks) and of the secondary tracks (sec_tracks) generated during tracking by various physics processes. GTRAK, using geometry information (geom_banks), tracks particles through the different volumes. Within a given volume, it is the task of GTVOL to call the particle-type specific routines for the simulation of physical processes. These are the routines GTGAMA for photons, GTELEC for e^+ and e^-, GTNEUT for neutrons, GTHADR for all other hadrons, GTMUON for μ's, and GTNINO for ν's. The energy loss DESTEP calculated in these routines and the generated secondary particles [GKIN (5,NGKINE)] are passed on to the user routine GUSTEP. At this point, GFLASH can be attached. If an inelastic reaction has taken place in a volume belonging to the calorimeter, then this point is taken to be the starting point for the shower development. Whether the ensuing shower development will be parameterized or continued to be simulated in detail can be made dependent on boundary conditions determined by the user. If the shower is to be generated by GFLASH, a "pseudoshower-particle" with the four-momentum of the incident particle (the energy is modified, depending on the incident particle type), initiating the inelastic reaction is created and stored (sec_tracks). The tracking of the original particle is stopped. Standard GEANT routines can be used to track the "pseudoshower-particle" through the detector and to get the material parameters (X_0, λ_0, A, Z, and R_M) necessary for the generation of the longitudinal and lateral shower profiles. This is accomplished by inserting one call to the GFLASH routine GTEMSH (for electromagnetic shower simulation) and one to GTHASH (for hadronic shower simulation)

into the GEANT routine GTVOL. This small change in GTVOL is the only change needed inside a GEANT routine.

After generating the longitudinal energy profile for a shower in GTEMSH or GTHASH, it is integrated in small steps up to the volume boundary. For every integration step energy spots are computed according to the fluctuated lateral distribution for this step and the sampling fluctuations for the volume the spot is in. The visible fraction of the deposited energy of a spot is calculated in GFSPOT after mapping the spot coordinates to read out channel numbers of the calorimeter. The same routine as for the detailed simulation is used for the mapping of the approximately 40000 channels of the H1 calorimeter. Nonsensitive regions of the calorimeter are simulated through the mapping of the energy spots onto those regions. Finally, the visible energy and channel number are stored for digitization (cal_hit_banks in fig. 7).

6. Comparison with data

We compared GFLASH with data from the H1 calorimeter test [8] at CERN using hadron beams. The comparisons shown were made after some of the parameters of GFLASH had been tuned using this data. The longitudinal segmentation of the test calorimeter is shown schematically in fig. 8. The beam enters the EC module (Pb/LAr, 1.13 λ_0, four segments) from the right. Next, the HC (Fe/LAr, 3.76 λ_0, four segments) and the "tail catcher" TC (Fe/LAr, 2.88 λ_0, two segments) with thicker iron plates follow. Superimposed on the drawings are a graphic representation of a 30 GeV π^- shower simulated by GEANT [fig. 8(a)] and the energy spots of GFLASH [fig. 8(b)].

6.1. *Longitudinal and lateral profiles*

The mean longitudinal energy profile for hadronic showers from the experiment and the profile as simulated by GFLASH for different energies are shown in fig. 9 (in linear and log scale) and fig. 10. In addition, the profiles as predicted by GEANT (with GHEISHA7) and by GHEISHA8 [ref. 8] are presented in fig. 9. The excellent agreement of GFLASH with the experimental profile is a consequence of

the refitting of some of the GFLASH parameters. Figure 10 shows the development of a second maximum in the segment HC_2 with increasing energy which is well-simulated by GFLASH. This effect can be understood as follows. The lengths (in λ_0) of EC_4, HC_1, and HC_2 increase such that roughly equal numbers of showers are starting in these segments. However, in units of X_0, due to the difference in the ratios of X_0 to λ_0 for Pb and Fe, the segment HC_1 is shorter than the neighboring segments. While an electromagnetic subshower of a few GeV starting in EC_4 or HC_2 will be almost completely contained there, such a subshower starting in HC_1 will leak some of its energy into HC_2. The correct simulation of this effect by GFLASH indicates a good parameterization of the π^0_f fraction of the shower.

The dependence of the mean lateral profile on the shower depth and energy can be seen in fig. 11 where the lateral charge distribution as a function of depth is shown for one energy, and in fig. 12 where it is plotted for different energies at a fixed depth. There is good agreement between GFLASH and the experiment for the core as well as the halo of the shower.

6.2. Fluctuations of hadronic showers

The total visible energy for the modules EC, HC, and TC (normalized to their respective sampling fractions for minimum ionizing particles) for six different beam energies is compared with the expectations from GFLASH in fig. 13. For the energy range considered, the agreement is good and the asymmetry of the distributions, which is expected for noncompensating calorimeters, is properly simulated. In this comparison of experimental and simulated data, only a single constant relating charge to energy as obtained experimentally with muons was used, and not—as is frequently done—a set of constants which is determined by demanding equality of the means with the incident energy and minimal variances.

The energy resolution of the calorimeter is shown in fig. 14 for pions as a function of energy, together with the results from the simulation. The good agreement here suggests that the intrinsic and sampling fluctuations for the Pb and Fe calorimeters are properly taken into account in GFLASH.

The visible energy seen in the three different modules (EC, HC, and TC) for 30 GeV showers is compared in fig. 15 with results from GEANT and GFLASH.

The good agreement observed for GFLASH indicates a proper handling of the different materials and sampling structures in the simulation. The pattern of slightly too much energy in EC and too little in TC, as generated by GEANT, is a consequence of the shower length of GEANT being too short, as can be noticed in fig. 9.

The first maximum seen in the visible energy in HC is due to showers starting in EC and depositing most of the π^0_f energy there, while the second maximum is due to showers originating in HC. How the visible energy distribution for the HC changes as a function of energy and how this is simulated by GFLASH is shown in fig. 16.

The energy fluctuations and correlations for different calorimeter segments are displayed in fig. 17 for 70 GeV showers. The agreement between GFLASH and the data is quite satisfactory, even for the "long range" (EC vs. TC) correlations.

7. Speed estimate

We used the H1 detector simulation program [15], which is still under development, to provide some preliminary timing information. We took as an example 50 GeV pions which shower in the H1 forward calorimeter [9]. We found the following average times [using an IBM 3090-150E ($\approx$ 3.5 VAX 8600)]: 85 ms for the tracking of the pion from the interaction point through the central and forward tracker volumes to the first inelastic interaction in a calorimeter volume (GEANT), 55 ms for the tracking of the "pseudoshower-particle" (GEANT), and 30 ms for the generation of the energy spots (GFLASH). This indicates that, at least in the context of H1, the time spent on the shower-specific tasks of GFLASH is small compared to the time spent on the geometry-specific tasks of GEANT. The 30 ms for GFLASH includes the time for the tracking of a shower within a volume which is done by GFLASH. Compared to a detailed simulation using GEANT/GHEISHA with standard values for the cutoff energies, we found that the simulation with GFLASH is about 180 times faster. Since neither the detailed nor the parameterized simulation, as such, were particularly optimized for speed, the numbers given above should be taken with caution.

A simulation of the H1 test calorimeter (as shown in fig. 10) by GFLASH and GEANT/GHEISHA leads to the CPU time requirements (using an IBM 3090-180E) as given in Table 1. The times given for GFLASH depend on the parameterization chosen for the number of energy spots as a function of energy, which in turn depends on the geometry and size of the readout channels. In this example, 200 (250) spots were generated for 50 (200) GeV.

Perhaps more important in the comparison of the time required for the detailed and parameterized simulation of showers is their energy dependence. Due to the proportionality of energy and total track length of a shower, the computer time required for simulation with GEANT/GHEISHA increases linearly with energy, while for GFLASH the time is proportional to the shower length which grows only logarithmically with energy.

8. Conclusions

GFLASH* provides a realistic and fast parameterization for the simulation of electromagnetic and hadronic showers in a geometry defined by the user with GEANT. The longitudinal and lateral distribution, their fluctuations and correlations, are modeled in a consistent way. For hadrons, this was made possible by a new ansatz for the longitudinal energy profile consisting of three Gamma distributions: one for the purely hadronic component of the shower, one for the π^0 fraction originating from the first inelastic interaction, and one for the π^0 fraction from later inelastic interactions. The interfacing of GFLASH with GEANT provides great flexibility and ease of use.

Acknowledgments

We are very much indebted to H. Greif for providing us with data tapes and information from the H1 calorimeter test at CERN. We also thank T. Hansl-Kozanecka and D. Groom for their careful reading of this manuscript. One of us (G. G.) would like to thank the SLAC directorate and M. Perl for the hospitality he is enjoying at SLAC.

* GFLASH is available for distribution; please contact one of the authors.

References

[1] R. K. Bock et al., Nucl. Instr. and Meth. **185** (1981) 533;
M. della Negra, Scripta Phys. **23** (1981) 469–479.

[2] E. Longo and I. Sestili, Nucl. Instr. and Meth. **128** (1975) 283.

[3] Y. Hayashide et al., CDF Note 287, Batavia, IL (1985).

[4] J. Badier and M. Bardadin-Otwinowska, ALEPH 87–9, EMCAL 87–1, Geneva (1987).

[5] R. Brun et al., GEANT3 User's Guide, CERN-DD/EE 84-1, Geneva (1986).

[6] M. Rudowicz, Diplomarbeit an der Universität Hamburg; MPI-PAE/Exp. El. 200 (1989);
S. Peters, Diplomarbeit an der Universität Hamburg; MPI-PAE/Exp. El. 202 (1989).

[7] GHEISHA7 as implemented in GEANT; see also H. C. Fesefeldt, PITHA Report 85/02, RWTH Aachen (1985).

[8] H1 Calorimeter Group (W. Braunschweig et al.), DESY 89/022 (1989).

[9] H1 Collaboration, Technical Proposal for the H1 Detector, DESY, Hamburg, 1986.

[10] G. A. Akopdjanov et al., Nucl. Instr. and Meth. **140** (1977) 441–445.

[11] E. Hughes, CERN CDHS Internal Note 4, Geneva (1986).

[12] W. J. Womersley et al., Nucl. Instr. and Meth. **A267** (1988) 49, and erratum **A278** (1989) 447.

[13] F. James, Rep. Prog. Phys. **43** (1980) 1145–1189.

[14] R. Y. Rubinstein, Simulation and the Monte Carlo Method (John Wiley & Sons, New York, 1981).

[15] G. D. Patel et al., H1 Collaboration Internal Note, Hamburg (1988).

Table 1. CPU time requirements (IBM 3090-180E) for the simulation of showers in the H1 test calorimeter.

	Energy	GFLASH	GEANT
π^+	50 GeV	26 ms	8 s
π^+	200 GeV	31 ms	32 s
e^-	50 GeV	10 ms	30 s
e^-	200 GeV	11 ms	110 s

Figure Captions

1. Longitudinal energy profile and parameters for 10 GeV e^- showers.
2. Mean longitudinal energy profile for e^- showers: GEANT (o) and GFLASH (- - -).
3. Lateral energy profile for 10 GeV e^- showers at different depths: GEANT (left) and GFLASH (right).
4. Mean longitudinal energy profile for π^+ showers: FIT (—) and GEANT (o).
5. Relative probabilities for different hadronic shower-classes.
6. Comparison of mean π^0 fractions for π^+-induced showers as a function of the incident energy E_{inc}: f_{π^0} is the mean π^0 fraction from all showers; $f_{\pi^0}/P(\pi^0)$ is the mean π^0 fraction from showers with a π^0 component; and $f_{\pi^0}\, f^l_{\pi^0}$ is the mean "late" π^0 fraction from all showers; GEANT (o, □).
7. Schematic representation of the implementation of GFLASH in GEANT.
8. Simulation of the H1 test calorimeter: (a) GEANT and (b) GFLASH.
9. Mean longitudinal energy profile for 30 GeV π^- showers: experiment (o), GFLASH (···), GEANT311 (- -), and GHEISHA8 (—).
10. Mean longitudinal energy profile for π^- showers: experiment (o) and GFLASH (···).
11. Mean lateral charge profile for 30 GeV π^- showers with shower starting point in HC_1: experiment (—), GEANT (- - -), and GFLASH (···).
12. Mean lateral charge profile in HC_2 for π^- showers with shower starting point in HC_1: experiment (—) and GFLASH (···).
13. Energy distribution for π^- showers for beam energies 10, 30, 50 (top) and 70, 120, 170 GeV (bottom): experiment (—) and GFLASH (···).
14. Energy resolution of the calorimeter ($EC + HC + TC$) for π^- showers: experiment (o) and GFLASH (•).
15. Energy distributions in the modules EC, HC, and TC for 30 GeV π^- showers: experiment (—), GFLASH (···), and GEANT (- - -).
16. Energy distributions for π^- showers in HC for different energies: experiment (—) and GFLASH (···).
17. Energy correlations between different calorimeter modules for 70 GeV π^- showers: experiment (left) and GFLASH (right).

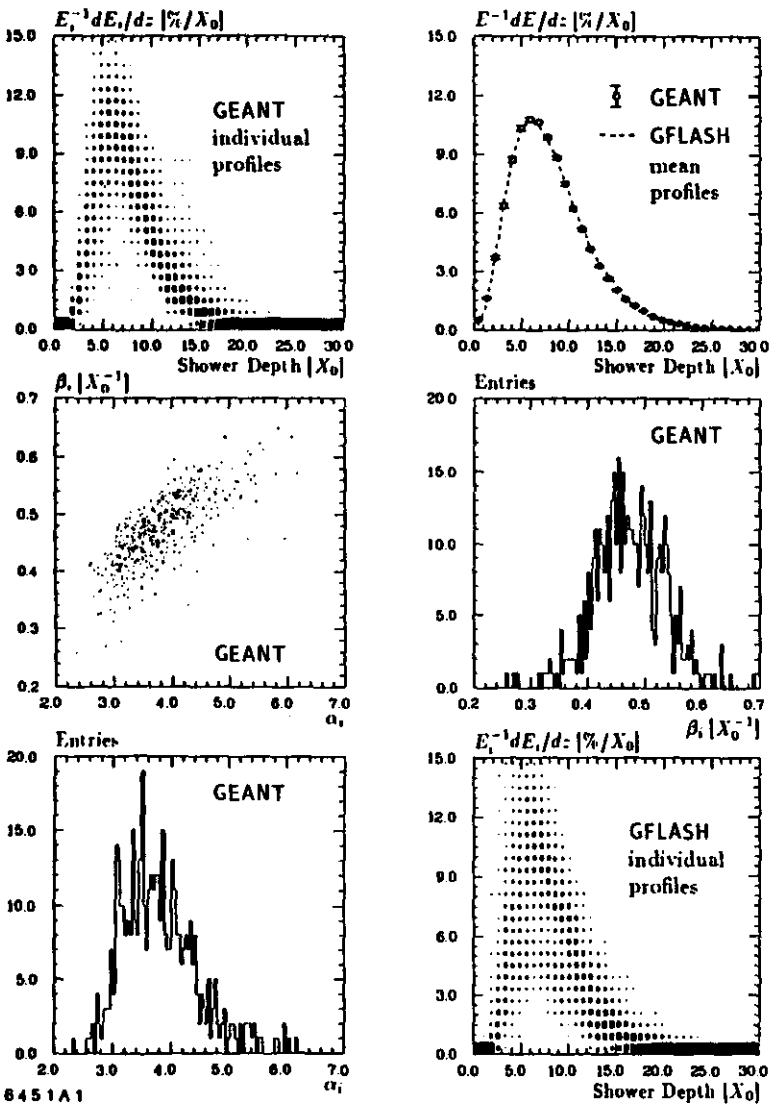
GEANT
individual
profiles
GEANT
GFLASH
mean
profiles
Shower Depth [X_0]
GEANT
Entries
GEANT
GEANT
GFLASH
individual
profiles
6451A1

Fig. 1

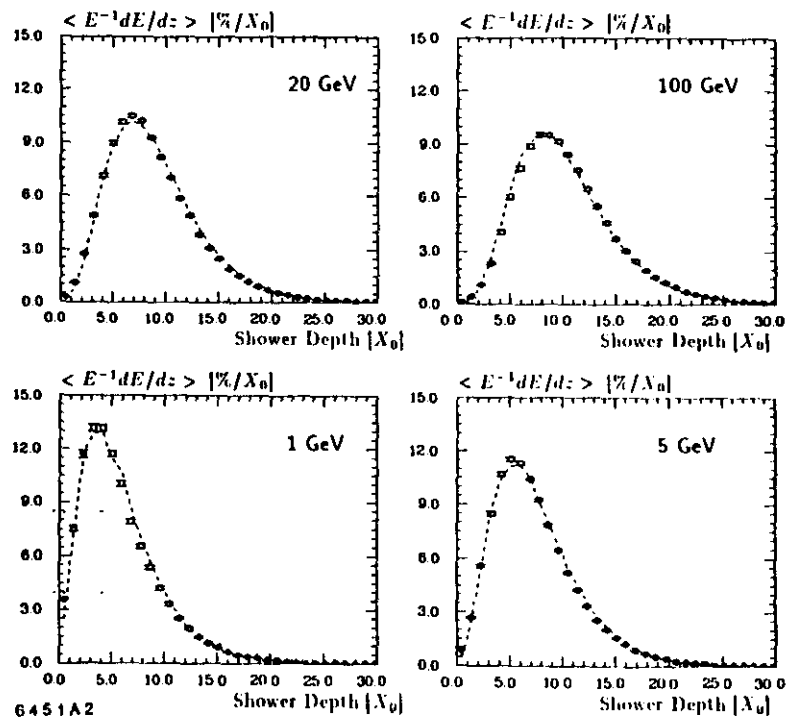
20 GeV
100 GeV
1 GeV
5 GeV
Shower Depth [X_0]
6451A2

Fig. 2

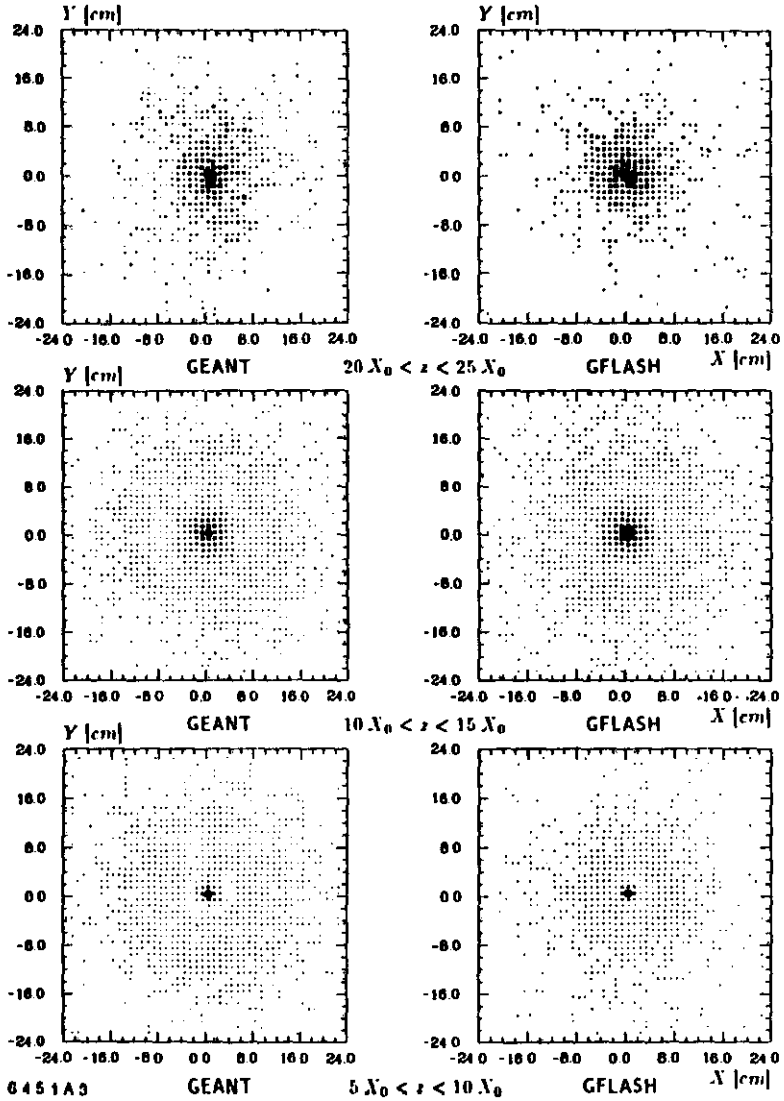
Y [cm]
X [cm]
GEANT
GFLASH
20 X_0 < z < 25 X_0
10 X_0 < z < 15 X_0
5 X_0 < z < 10 X_0
6451A3

Fig. 3

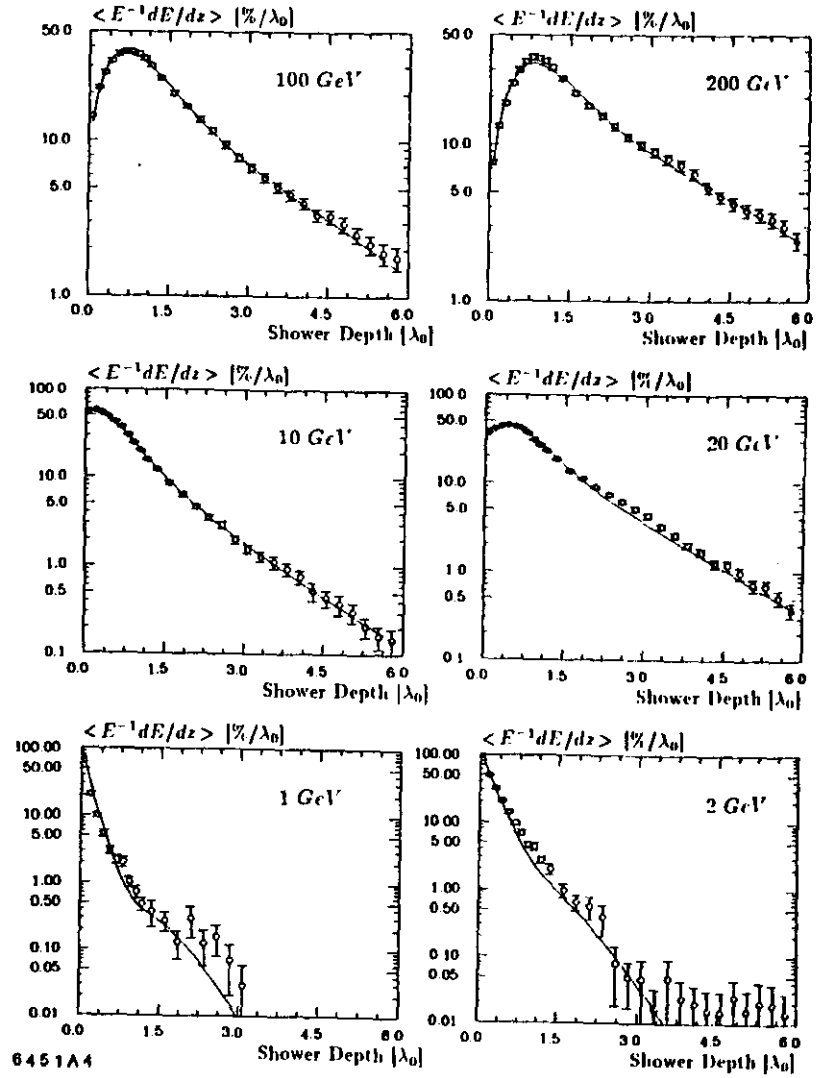
< $E^{-1}dE/dz$ > [%/λ_0]
Shower Depth [λ_0]
100 GeV
200 GeV
10 GeV
20 GeV
1 GeV
2 GeV
6451A4

Fig. 4

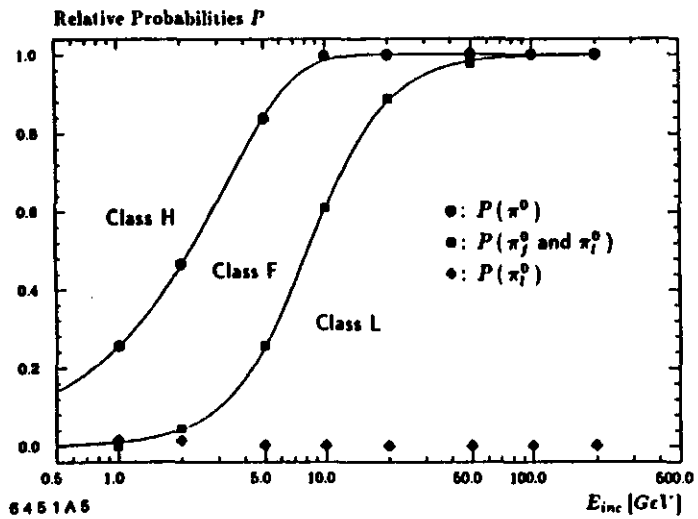
Relative Probabilities P
Class H
Class F
Class L
●: P(π⁰)
■: P(π⁰_f and π⁰_l)
◆: P(π⁰_l)
1.0
0.8
0.6
0.4
0.2
0.0
0.5
1.0
5.0
10.0
50.0
100.0
500.0
E_inc [GeV]
6451A5

Fig. 5

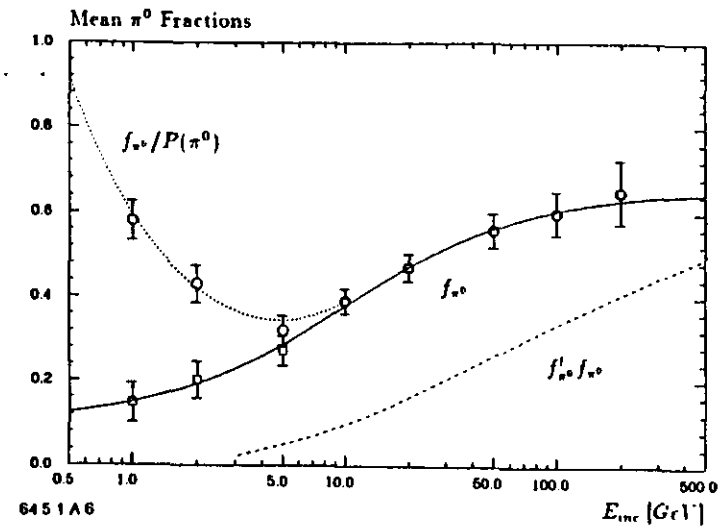
Mean π⁰ Fractions
f_π⁰/P(π⁰)
f_π⁰
f'_π⁰ f_π⁰
1.0
0.8
0.6
0.4
0.2
0.0
0.5
1.0
5.0
10.0
50.0
100.0
500.0
E_inc [GeV]
6451A6

Fig. 6

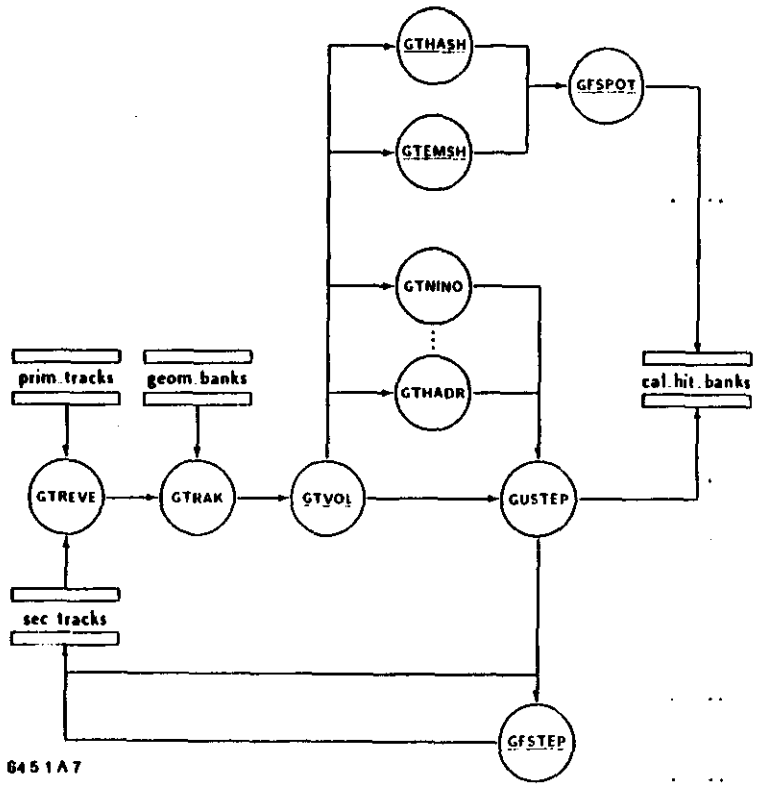
GTHASH
GFSPOT
GTEMSH
GTNINO
GTHADR
prim. tracks
geom. banks
cal. hit. banks
GTREVE
GTRAK
GTVOL
GUSTEP
sec. tracks
GFSTEP
G451A7

Fig. 7

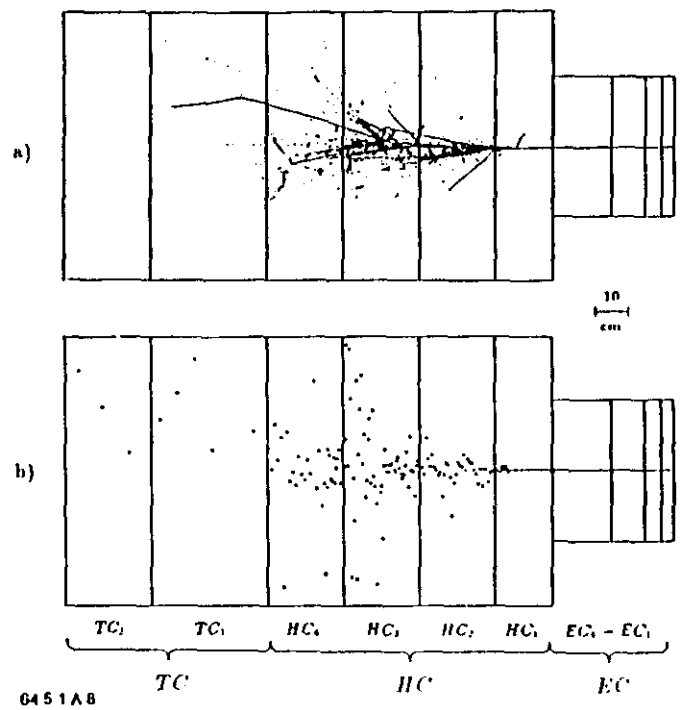
a)
b)
10
cm
TC
HC
EC
G451A8

Fig. 8

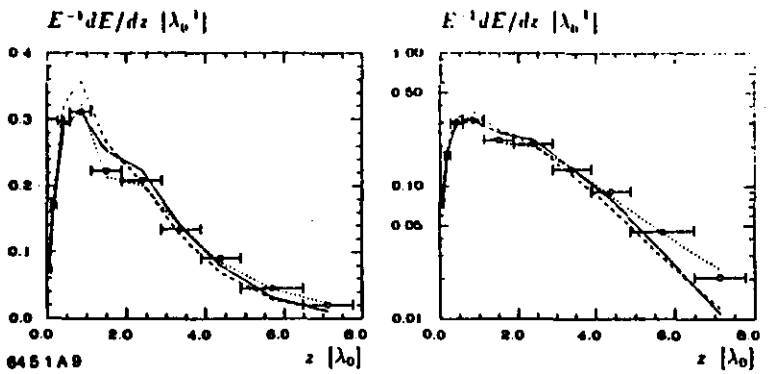
$E^{-1}dE/dz$ $[\lambda_0^{-1}]$
z $[\lambda_0]$
6451A9

Fig. 9

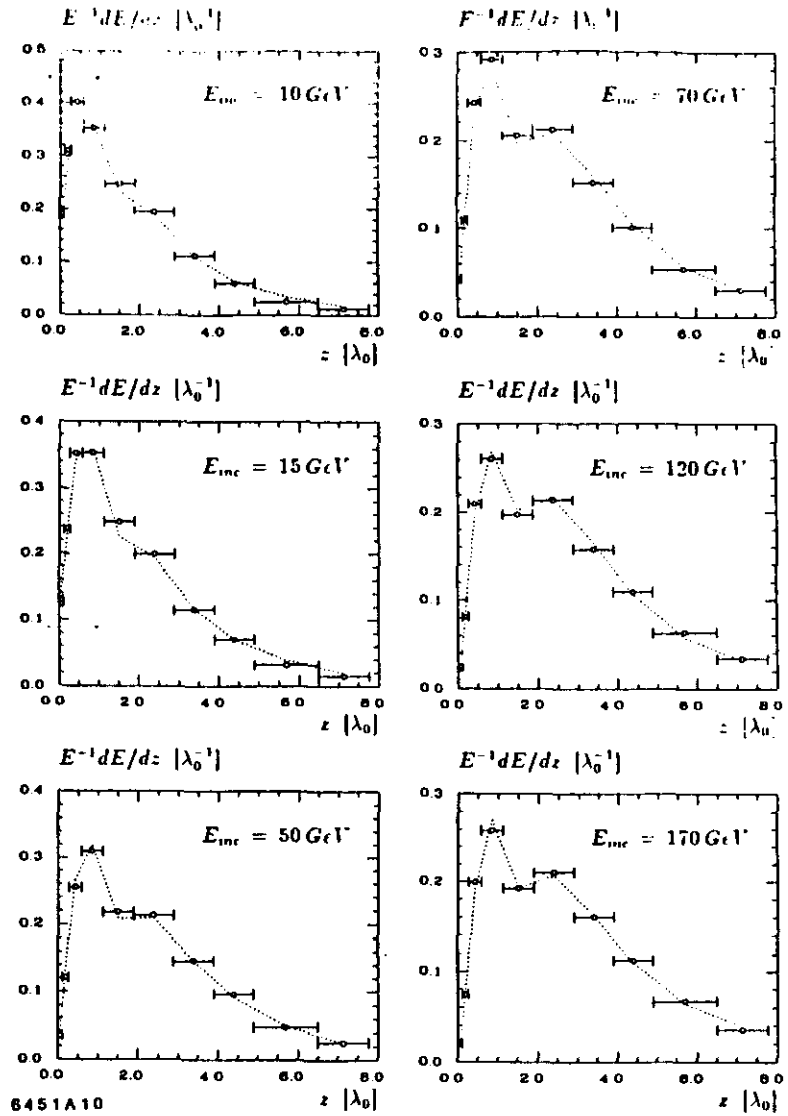
E_{inc} = 10 GeV
E_{inc} = 70 GeV
E_{inc} = 15 GeV
E_{inc} = 120 GeV
E_{inc} = 50 GeV
E_{inc} = 170 GeV
$E^{-1}dE/dz$ $[\lambda_0^{-1}]$
z $[\lambda_0]$
6451A10

Fig. 10

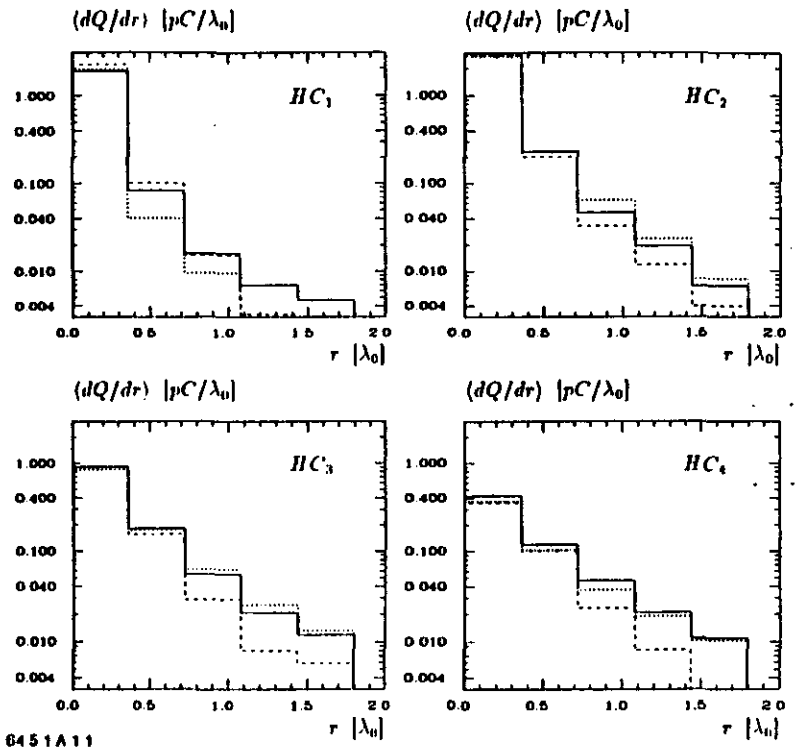
⟨dQ/dr⟩ [pC/λ0]
HC1
HC2
HC3
HC4
r [λ0]
6451A11

Fig. 11

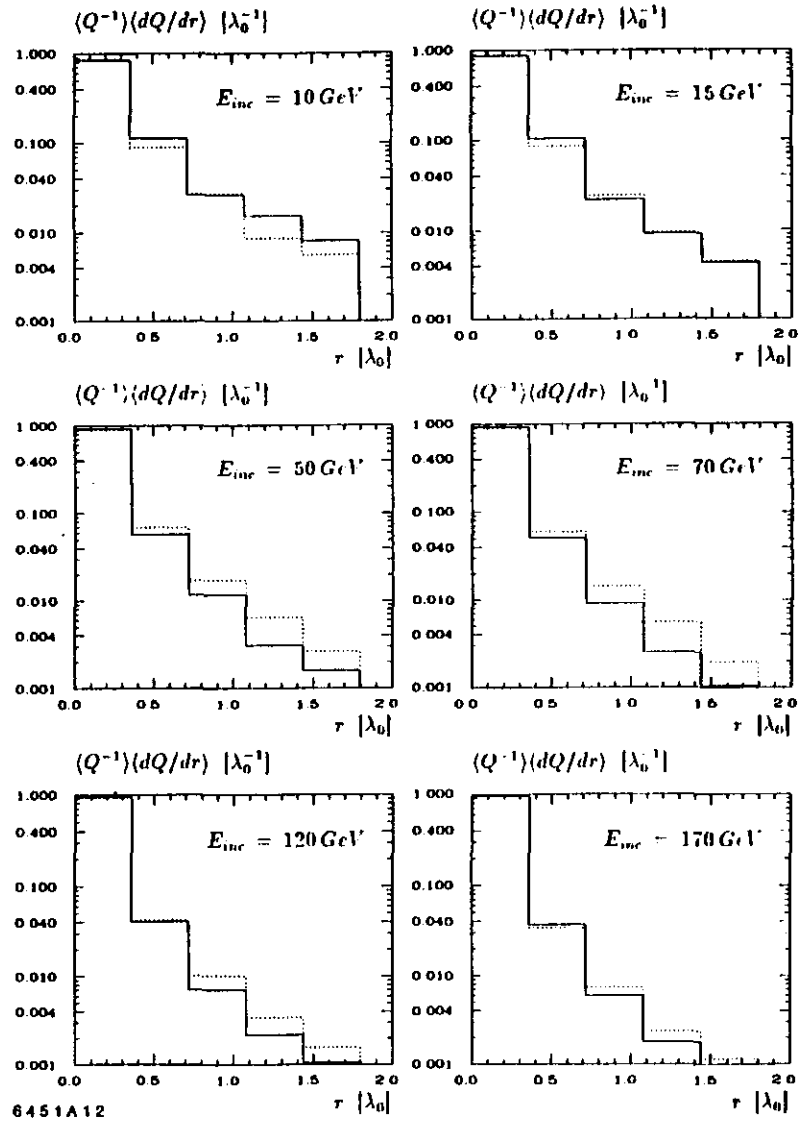
⟨Q⁻¹⟩⟨dQ/dr⟩ [λ0⁻¹]
E_inc = 10 GeV
E_inc = 15 GeV
E_inc = 50 GeV
E_inc = 70 GeV
E_inc = 120 GeV
E_inc = 170 GeV
r [λ0]
6451A12

Fig. 12

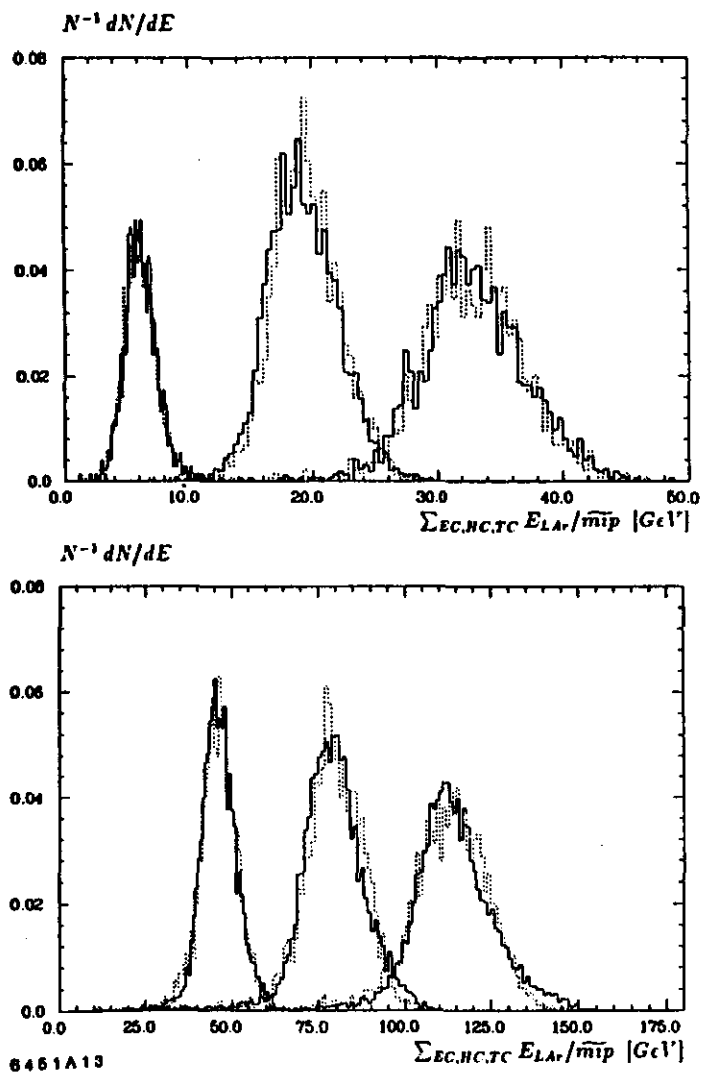
$N^{-1}\,dN/dE$
0.08
0.06
0.04
0.02
0.0
0.0
10.0
20.0
30.0
40.0
50.0
$\sum_{EC,HC,TC} E_{LAr}/\widetilde{mip}$ [GeV]
$N^{-1}\,dN/dE$
0.08
0.06
0.04
0.02
0.0
0.0
25.0
50.0
75.0
100.0
125.0
150.0
175.0
$\sum_{EC,HC,TC} E_{LAr}/\widetilde{mip}$ [GeV]
6451A13

Fig. 13

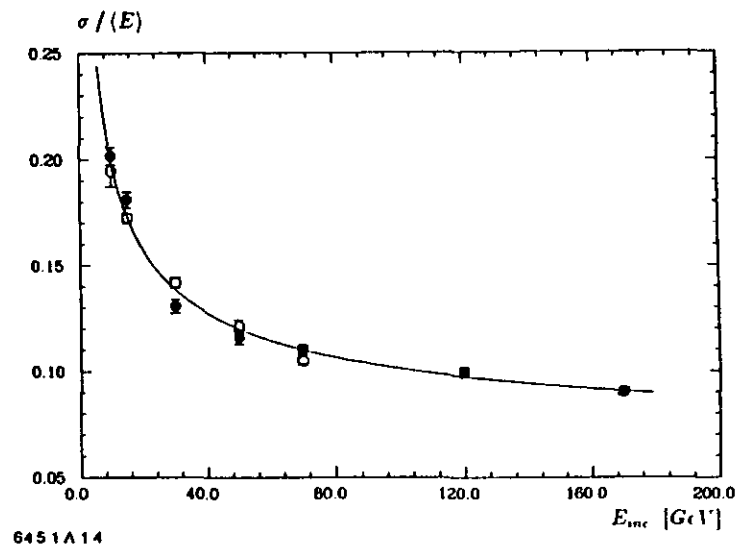
$\sigma/\langle E\rangle$
0.25
0.20
0.15
0.10
0.05
0.0
40.0
80.0
120.0
160.0
200.0
E_{inc} [GeV]
6451A14

Fig. 14

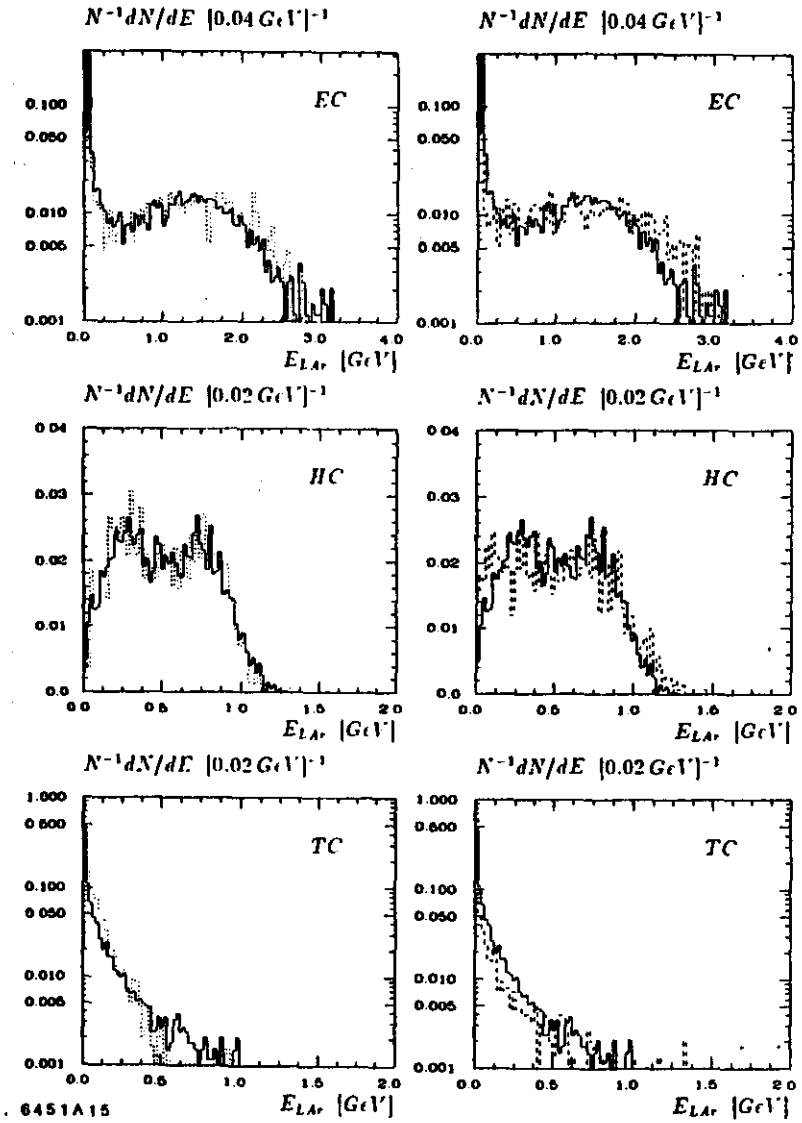
N⁻¹dN/dE [0.04 GeV]⁻¹
EC
N⁻¹dN/dE [0.02 GeV]⁻¹
HC
TC
E_LAr [GeV]
6451A15

Fig. 15

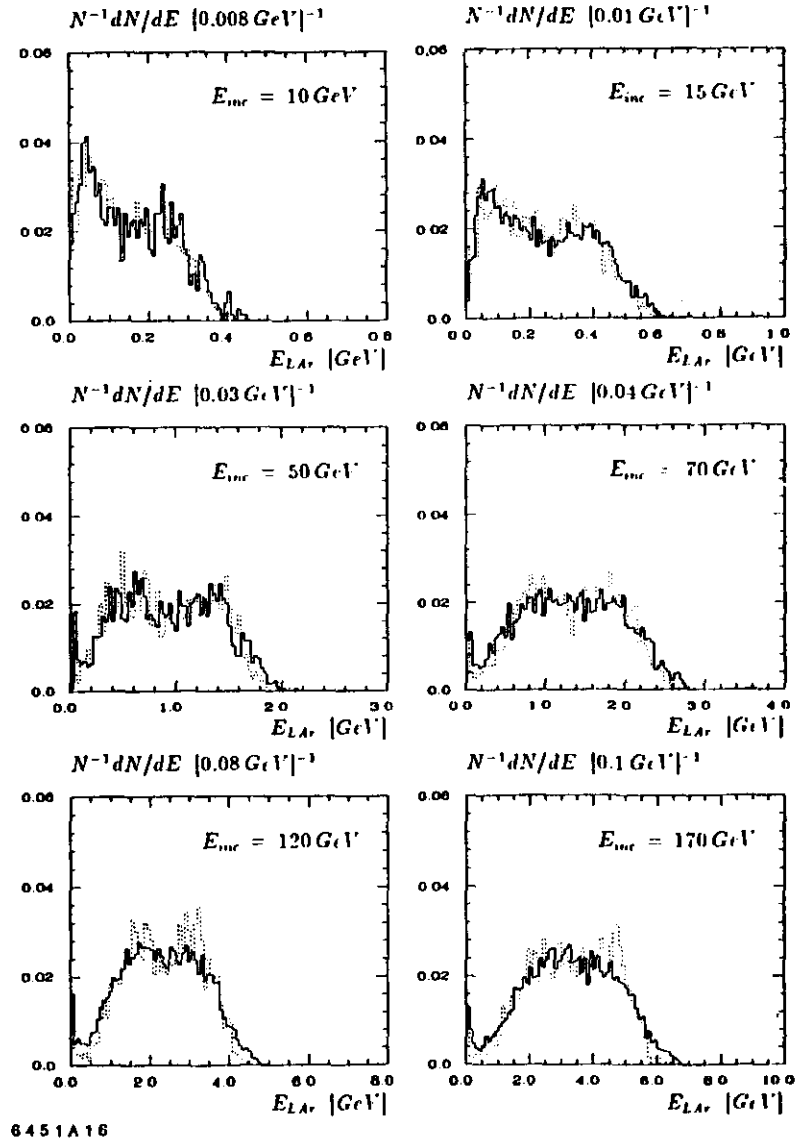
N⁻¹dN/dE [0.008 GeV]⁻¹
N⁻¹dN/dE [0.01 GeV]⁻¹
N⁻¹dN/dE [0.03 GeV]⁻¹
N⁻¹dN/dE [0.04 GeV]⁻¹
N⁻¹dN/dE [0.08 GeV]⁻¹
N⁻¹dN/dE [0.1 GeV]⁻¹
E_inc = 10 GeV
E_inc = 15 GeV
E_inc = 50 GeV
E_inc = 70 GeV
E_inc = 120 GeV
E_inc = 170 GeV
E_LAr [GeV]
6451A16

Fig. 16

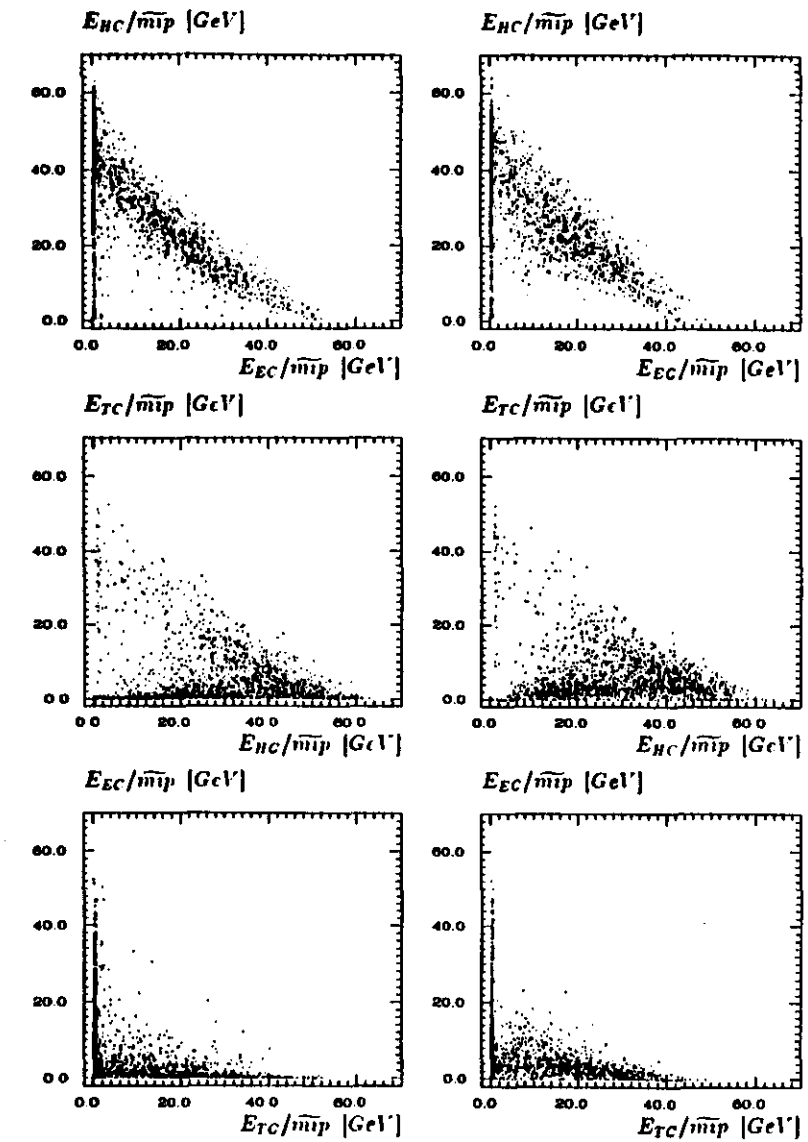
$E_{HC}/\widetilde{mip}$ [GeV]
$E_{EC}/\widetilde{mip}$ [GeV]
$E_{TC}/\widetilde{mip}$ [GeV]
$E_{HC}/\widetilde{mip}$ [GeV]
$E_{EC}/\widetilde{mip}$ [GeV]
$E_{TC}/\widetilde{mip}$ [GeV]
0.0
20.0
40.0
60.0
6451A17

Fig. 17

Software - Standards and Experience
A machine-readable international Journal
published by and for the H1 collaboration

Software Note Number 26 October 1991

Authors: G. Bernardi, W. Hildesheim, M. Kuhlen, M. Rudowicz

Title: "Calibrated Energies" in H1 Detector Simulation

updates:
Jan. 14th, 1992: M. Kuhlen
Sept.21st, 1992: M. Kuhlen

select 0. Introduction

select 1. Simulation

select 1.1. Geometry
select 1.2. Tracking
select 1.3. Energy deposition
select 1.3.1. Visible energy
select 1.3.2. Invisible Energy and Compensation
select 1.3.3. Calibrated energies
select 1.4. Simulation Options
select 1.5. Simulation Output
select 1.6. Performance
select 1.7. Comparison H1FAST vs. detailed simulation

select 2. Reconstruction with "Calibrated Energies"

select 2.1. Overview
select 2.2. Summing up the Hits
select 2.3. The Smearing Step
select 2.3.1. Resolution Functions
select 2.3.2. Smearing and Weighting
select 2.3.3. Dead Material Corrections
select 2.4. Cluster Rescaling
select 2.5. User Options
select 2.6. Status

select 3. Applications

select 3.1. Detector Studies
select 3.2. Physics Analysis
select 3.3. Utilities

select Appendix A: Steering banks
select Appendix B: Bank Descriptions
select Appendix C: Calling Sequence

0. Introduction

This manual describes an approach to simulate the H1 calorimter response at the post reconstruction level, i.e. after calibration, weighting and other correction (for dead materials etc.) procedures have been performed on the data. It has been developed in order to ensure control over the correction procedures in simulation which correspond to the "fully calibrated" detector in reality. The "calibrated energies" are implemented in the framework of H1FAST, where they find their main application for the fast simulation of H1 events. In addition the detailed bookkeeping (detailed H1SIM as well as H1FAST) of energy depositions in this scheme makes it a useful tool for the development of simulation programs and reconstruction algorithms. This note outlines the basic idea and provides the user with the information necessary to use the product.

"Calibrated Energies" is a hybrid approach to detector simulation. The detector simulation is split into two parts, following the hybrid simulation philosophy: Monte Carlo the ugly part, smear the Gaussian part! The first part describes the development of a shower in the calorimeter and its different kinds of energy depositions in the various detector cells with the ususal Monte Carlo method. The outcome is stored for processing in a second step.

The second step applys resolution functions to the energy depositions in order to mimic the actually achieved resolution. These resolution functions have to be determined externally, either from test data or from detailed Monte Carlo studies. The resolution functions describe the well behaved detector response due to e.g. sampling fluctuations, while the Monte Carlo part takes care of intrinsic fluctuations with large tails.

This approach has the advantage that the time consuming first step (shower development) is separated from the second one (smearing). Already produced Monte Carlo data can be easily reprocessed by applying different resolution functions, which is fast compared to the time needed for production.

The word "calibrated" refers to the fact that we shall simulate energies in read out cells directly rather than charge equivalent signals in active layers. There is no need for calibration constants in the Monte Carlo. Furthermore, a complete bookkeeping of all energy depositions in all detector elements has been implemented. The perfect knowledge on the true energy depositions will be used to emulate the correction procedures which work on data and detailed Monte Carlo. The detector response is calibrated in the sense that the mean of the reconstructed energy equals the incident energy.

1. Simulation

1.1. Geometry

We distinguish the active calorimeter parts (= calorimeter stacks for sampling calorimters) from the cracks in between and dead materials in front and behind. The sampling calorimeters are divided into active layers and passive layers (= absorber material). (Note that with this definition, which follows the language in use by H1, an active calorimeter part consists of active and passive layers.) A geometry description which distinguishes between active and passive layers is called detailed. In contrast, in a coarse geometry that distinction is absent, and the stacks are composed of mixtures from the materials in the active and passive layers. Sometimes also the cracks between stacks may be averaged with the stacks into one homogeneous volume. A readout cell consists of one or several subsequent layers of active and passive material.

1.2. Tracking

The tracking mode may be detailed or parametrized. In the detailed tracking mode a particle is tracked through the detector by GEANT. It's reactions are computed step by step, and it's energy losses deposited in the current medium. In case of a parametrized shower development, the energy is deposited in spots according to the shower shape.

1.3. Energy deposition

1.3.1. Visible energy

Energy depositions (hits) are mapped onto readout cells (or dead material cells) via mapping functions and stored in the hit banks. There may be more than one hit per cell. In the conventional scheme charge equivalent energy (E_vis) is simulated. For detailed geometry it is the energy deposited in the active layers, which leads to a signal. Sampling fluctuations are thus simulated intrinsically.

For coarse geometry the energy deposition in the readout cell E_dep is multiplied with a response function (e/mip, h/mip), which is of order and depends in general on the particle type and energy. In H1FAST simulation e/mip is assumed to be a constant, while the actual h/mip is being calculated from the hadron's type and energy. The mip sampling fraction s_mip is applied to go to the E_vis scale:

E_vis = E_dep * (x/mip) * s_mip (with x=e,h).

Sampling fluctuations are applied explicitly to E_dep, because in coarse geometry active and passive layers are not distinguished. The fluctuation is done with a gamma-distribution according to sigma(E)/E = const./sqrt(E). The obtained E_vis corresponds now to the E_vis from detailed simulation.

In order to go from E_vis to the "visible energy on the electromagnetic scale" E_0 in reconstruction, E_vis needs to be multiplied with a scale factor S_em:

E_0 = E_vis * S_em.

In the detailed geometry S_em has to be determined from the Monte Carlo (somewhat surprisingly "calibration constants" for the Monte Carlo appear). In the coarse geometry S_em is known a priori from the constants used in the simulation:

S_em = 1/((e/mip) * s_mip);

the Monte Carlo is intrinsically calibrated. For each event a bank H1FP is written which contains the constants (e/mip), s_mip and in addition (p/mip). The current granularities and tracking modes for each subdetecor are stored in the (undocumented) SIPA bank.

1.3.2. Invisible Energy and Compensation

In hadronic showers a certain fraction of the energy (typically 1/3) does not give rise to a signal in the calorimeter, it is invisible. This may be due to binding energy lost in the break-up of a nucleus, recoil energy of a nucleus, unseen neutrinos or low energy neutrons with small reaction cross section. As a rule of thumb for the H1 liquid argon calorimeter on average 1/3 of the energy of an incident pion is invisible, so pi/e is roughly 2/3. It is the main cause for the fact that the response of non-compensating calorimeters to pion showers is smaller than for for electron showers of same incident energy (pi/e<1). One can try to correct for that, either intrinsically (suppress the electron response, boost the hadron response, increase the neutron cross section, ...), or by software, the so called weighting method. Here one tries to recognize electromagnetic and hadronic shower components and weights them with appropriate factors such that pi/e = 1. One may also think of weighting as estimating the invisible part.

1.3.3. Calibrated energy

In addition to E_vis, the "calibrated energies" are computed for each hit in a readout cell. These are the unfluctuated electromagnetic, hadronic, invisible and hadronic-visible energies. Unfluctuated means that sampling fluctuations have not been applied, the energies are not smeared. The electromagnetic energy E_em is the total energy deposition by electrons and photons, the hadronic energy E_had is the energy deposition by charged hadrons, and the invisible energy E_inv comprises all energy depositions that do not give rise to a signal in the calorimeter, e.g. energy lost in the break_up of a nucleus. The hadronic-visible energy E_vh in coarse geometry is the hadronic energy deposition multiplied with its particle and energy dependent response factor, E_vh = E_had * (h/mip).

The total energy lost in the read-out cell is given by

E_tot = E_em + E_had + E_inv.

Note that with our definitions E_vis + E_inv is not E_tot. E_tot is defined as the difference between the measurable energy of incoming and outgoing particles for any reaction or volume. We define the measurable energy to be the energy which has the potential of giving a calorimeter signal. For particles it is the kinetic energy, for antiparticles the kinetic energy plus twice its rest mass. By definition, it is a conserved quantity in a calorimeter. In practice, this relation is used to calculate the invisible energy per reaction. With this definition, E_inv may be negative. An example is the case of a stopping neutron undergoing a neutron capture with emerging photons. The incoming measurable energy is 0 (kinetic energy has run down), the outgoing measureable energy is >0 (photon energy).

Storing this information allows for complete book keeping of all energy depositions anywhere in the detector. In addition, particles escaping the detector are recorded in leaving particle banks. All incident energy is thus accounted for. The energy sum over all calorimeter cells in all subdetectors and dead detector regions and the leaving particles yields the incident energy. The hit banks contain the following information (Please note the subtle difference in the meaning of the words E_vis and E_vh for detailed and coarse geometry!)

A) detailed geometry

1) E_vis visible energy in active layer as described above
2) E_em electromagnetic energy in readout cell (unfluct.)
3) E_had hadronic energy in readout cell (unfluct.)
4) E_inv invisible energy in readout cell (unfluct.)
5) E_vh hadronic energy in active layer
6) tracking history word ITRHIS

From this we can extract:

e.m. energy in active layer: E_vis - E_vh
had. energy in active layer: E_vh
e.m. energy in absorber : E_em - (E_vis - E_vh)
had. Energy in absorber : E_had - E_vh

B) coarse geometry

1) E_vis vis. energy in readout cell as described above (fluct.)
2) E_em electromagnetic energy in readout cell (unfluct.)
3) E_had hadronic energy in readout cell (unfluct.)
4) E_inv invisible energy in readout cell (unfluct.)
5) E_vh hadronic-visible energy in readout cell (unfluct.)
6) tracking history word ITRHIS

(for the location of the words in the different banks please consult the DDL)

Coded in the bits of the tracking history word ITRHIS is apart from other useful information the type of the deposited invisible energy:

bit on	means
9	secondary particle created in an interaction in the detector
10	energy lost in break-up or recoil of nucleus
11	particle stopped by GEANT due to long elapsed life time
12	neutrino energy
13	low energy neutrons (H1FAST doesn't track neutrons below 50 MeV)

1.4. Simulation Options

In principle for each subdetector many combinations of granularities and tracking modes are possible (steerable via the steering bank OSGD) not all of which are sensible or supported. Steering parameters for H1FAST come through the GFCP bank. In order to make life easier for the user, there are five levels of simulation detail predefined in the OTTO (Our Tricky Tracking Options) steering bank (overriding OSGD), going from the slowest and most detailed tracking level to the fastest with full shower parametrization. Levels 3-5 are considered as fast options (the realm of H1FAST), with 3 being the standard level. In OTTO also GHEISHA or FLUKA can be chosen for hadronic reactions. GHEISHA is considered the standard H1 choice.

level 1: Detailed shower tracking using GEANT on the detailed detector geometry. Active and passive layers are distinguished, so sampling fractions and fluctuations are simulated intrinsically via energy depositions in active layers.

level 2: Same as level 1, but with higher energy cut-offs for the tracking of low energy particles.

level 3: Uses a coarse geometry with averaged materials in the sensitive volumes, and a detailed description of the dead materials. Hadronic shower particles are tracked by GEANT. Electromagnetic showers are parametrized if they do not extend over cracks, and tracked in detail otherwise. In order to simulate sampling fluctuations, the energy depositions are fluctuated explicitly. In the tail catcher (IRON) however, tracking and granularity are detailed at present.

level 4: In addition to level 3, all "slow" hadronic secondary particles (energy < 10 % of mother particle) are parametrized in a continuum shower.

level 5: Full parametrization for electromagnetic and hadronic showers.

1.5. Simulation Output

1.5.1. Hit banks

The hit banks for Argon, BEMC and Plug calorimeters are ARHT, BRCT and PRDT. Energy depositions in the tail catcher (IRON) are stored together with the dead energies in the ARWT bank using the generalized mapping function. The following table shows the information content for the different hit banks, which are relevant for calibrated energies.

	location in bank			
information	ARHT	BRCT	PRDT	ARWT
channel #	1	1	1	1
ITRHIS	3	16	3	3
E_vis	2	8	2	2 *)
E_inv	5	18	5	5
E_em	6	19	6	6
E_had	7	20	7	2-6
E_vh	8	21	8	-
E_tot	5+6+7	18+19+20	5+6+7	2+5

*) Word 2 in ARWT means E_em + E_had

1.5.2. Digi Banks

The standard H1SIM digi module produces the digi banks ARCE, BRCE, PRDE and IRTE for Argon, BEMC, Plug and IRON from the hit banks. They contain E_vis per readout cell (exception: IRON gives # of streamers at present). The digi banks are input to the standard H1REC algorithms and the trigger module. For calibrated energies they are not used. However it is possible to recreate these banks by smearing the perfect energies. This will be discussed in the reconstruction chapter.

1.6. Performance

As a cross check of the book keeping of energy depositions we compare the incident energy (E_inc) with the sum of all perfect energies deposited in all calorimeters and dead materials and the leaving energy (E_sum). The following tables give the offset and sigma of the distribution E_sum - E_inc, the maximal deviation max(|E_sum-E_inc|) and the simulation time per event t. Large deviations point to a bug.

10 GeV pi+ in CB2 (GHEISHA)

simul. level	offset (%)	sigma (%)	max dev (%)	sample	t/evt. (sec)
1	+1.4	0.7	+4	1000	11.3
2	-0.6	0.3	-2	1000	2.7
3	0.0	0.13	+0.6	1000	1.0
4	+0.2	0.5	+2	1000	0.45
5	0.0	0.1	-0.4	166	0.36

NC events Q**2 = 500 GeV2

simul. level	offset (%)	sigma (%)	max dev (%)	sample	t/evt. (sec)
1			<0.7	12	292.7
2			-0.35	60	75.0
3			-0.23	141	31.9
4			-0.23	168	26.8
5			-0.30	19	14.3

The precision of the book keeping for levels 1-5 is sufficient for physics analysis preparation requiring an absolute calibration of 1 %. The book keeping for the FLUKA option does not work, and no effort is made at present to fix it.

1.7. Comparison H1FAST vs. detailed simulation

While the energy response can be adjusted after simulation with H1FAST in the calibrated energy scheme, a wrong shower shape cannot be corrected after simulation. It has to be satisfactory before extqnsive simulation of physics events commences! Therefore a few words on the status of H1FAST simulation are in order at this place.

Direct comparisons of simulation output (visible energy on the electromagnetic scale) in detailed (level 1) and H1FAST mode (level 3) have been performed by various people (J.Gayler, S.Peters, M.R., M.K. for the liquid argon, J.Ferencei, H.P. Kasselmann, C. Pichler and P.Reimer for the BEMC and M.Seidel for the Plug; unfortunately the iron has not been studied yet). Most important, H1FAST has been checked extensively against CERN test beam data by S. Peters and M. Rudowicz. These studies show a good to excellent description of the longitudinal and lateral shower shapes, of the energy response and resolution, of the response over cracks, and of e/pi separation estimators. Weighting algorithms need to be checked with the latest version.

So far the only discrepancy worth mentioning is the multiplicity of hit cells above the readout threshold, which is about 10 % too low for em. showers. However, the missing cells contain only little energy and lie in the peripheral shower region, where only 5 % of the total shower energy is deposited.

2. Reconstruction with "Calibrated Energies"

2.1. Overview

In reconstruction response functions are applied to the "perfect energies" from simulation in order to obtain the desired detector resolution. That proceeds in several steps. First, all the hits from the different tracks in each cell are summed up. Then, the summed energies are smeared, depending on the subdetector and the user option for resolution, weighting, etc.. Dead corrections are emulated by adding the energies from the dead material cells to the closest and hottest active cells. The dead energies can also be smeared to have a handle on the degradation of resolution in the crack regions. Finally, a relation between cells with true energy deposition and reconstruction clusters is set up, so it is possible to rescale the reconstruction clusters with the "calibrated" energy.

2.2. Summing up the Hits

```
Module: ESUMHT
Input : ARHT  BRCT  PRDT  ARWT
Output: EANG  EBNG  EPNG  EING  EWNG
        EAEG  EBEG  EPEG  EIEG  EWEG
```

The module ESUMHT sums up the hits from the hit banks for each cell. The result are parallel banks ExNG and ExEG for each subdetector (x=A,B,P,I,W for Argon, BEMC, Plug, Iron and dead material), containing the cell numbers and the 4 energy types E_inv, E_em, E_had, E_vh. Hits from the ARWT banks are written into the EING/EIEG banks, if they are in the iron, and into the EWNG/EWEG banks, if they are in the dead material.

2.3. The Smearing Step

Module: EWGHT, calls ESMEAR, EDEADC, ECLUST, ECALIB

```
input:  EAEG, EBEG, EPEG, EIEG, EWEG,
        EANG, EBNG, EPNG, EING, EWNG,
        ANGR, BNGR, PNGR, INGR,
        AEFR, BEFR, PEFR, IEFR,
        RCLX, RCLU

output: EAFR, EBFR, EPFR, EIFR, EWFR,
       (EASG, EBSG, EPSG, EISG, EWSG,) optional for the output list
        EAFX, EBFX, EPFX, EIFX,
        ECLX, ECLC
```

It is planned to split this module into two.

2.3.1. Resolution Functions

The main cause for a finite resolution in the H1 calorimeters are sampling fluctuations. They are due to statistical fluctuations in the number of shower particles crossing an active layer, so the relative energy resolution is proportional to 1/sqrt(N) or 1/sqrt(E).

Therefore the resolution functions are chosen such that the energy resolution scales like sigma(E)/E = c/sqrt(E). Each bit of energy deposition is smeared using a gamma distribution with the parameter beta=1:

$$f(x,\mathrm{alpha},\mathrm{beta}) = \frac{x^{\mathrm{alpha}-1}\, e^{-x/\mathrm{beta}}}{\mathrm{gamma}(\mathrm{alpha})\ \ \mathrm{beta}^{\mathrm{alpha}}} \quad .$$

The parameter alpha is used to adjust the resolution.
The gamma distribution has the
following required features: it vanishes for negative values, it is continuous, the variance equals the mean, and the sum of two gamma distributed random variables is again gamma distributed. For large means of course the gamma distribution becomes Gaussian. It has been shown that sampling fluctuations can be described quite well with this ansatz. However, it is not guaranteed that this relatively simple ansatz can be used for all response functions. They may be refined with increased knowledge of the real detector performance.

2.3.2. Smearing and Weighting

```
Routine ESMEAR
Input : EAEG EANG EBEG EPEG EIEG EWEG
Output: EASG      EBSG EPSG EISG EWSG
```

For each cell a smeared energy $\bar{E}$ is constructed from the 4 "perfect" energies E_inv, E_em, E_had and E_vh, depending on the user's options in steering bank ESMS (sensible choices are default). A bar indicates fluctuated (=smeared) energies. The smeared energies are stored in the banks ExSG parallel to ExNG. It is possible to simulate energy on the electromagnetic scale (A), weighted energy (B), or total energy (C), corresponding to the different levels of reconstruction.

A) energy on electromagnetic scale (EMC and HAC unweighted, BEMC).

(It is foreseen to create the digi banks ARCE, BRCE, PRDE and IRTE from this energy. ESMEAR has already been prepared for that).

$$\bar{E} = \bar{E}_em + \bar{E}_vh_em$$

with E_vh_em = E_vh / (e/mip) to bring it to the e.m. scale.
(Careful with detailed geometry, E_vh has different meaning!
We set E_vh_em = E_had * (p/mip) / (e/mip).)

B) weighted energy (EMC and HAC weighted)

$$\bar{E} = \bar{E}_em + \bar{E}_vh_em + \bar{E}_miss$$

with E_miss = E_tot - E_em - E_vh_em, E_tot = E_em + E_inv + E_had

C) total energy (Iron and Plug and dead cells)

$$\bar{E} = \bar{E}_tot$$

The smearing constants c for all types of energies and for each subdetector can be set also in bank ESMS. The default values reflect the best of our knowledge. It is worth mentioning that the Argon smearing constants (EMC and HAC) could be chosen such that the same constants describe the weighted and the unweighted detector. The weighted detector resolution has been set to sigma(E)/E = 50%/sqrt(E). The unweighted detector is approximately described by sigma(E)/E = sqrt(0.484**2/E + 0.097**2).

Energies which are deposited by particles which are not part of a shower (muons, pions before first interaction ...) should not be be fluctuated. That is ensured in the usual simulation path (creation of ARET), but not yet in ESMEAR.

2.3.3. Dead Material Corrections

```
Routine EDEADC
Input : EASG EBSG EPSG EISG EWSG
        EANG EBNG EPNG EING EWNG
Output: EAFR EBFR EPFR EIFR
```

The smeared energies from the dead cells (EWSG) are added to the corresponding active cells (ExSG) in order to emulate dead corrections. The result is stored in the final ExFR banks(parallel ExNG). Dead energies which have been used for the correction are set 0 in the EWFR bank. This pseudo dead correction is implemented for the Argon (routine EPDEAD), but not yet for the BEMC, plug and tailcatcher.

2.4. Cluster Rescaling

```
Routine ECLUST (cluster assignment)
Input : EANG EBNG EPNG EING RCLX RCLU ANGR BNGR PNGR INGR
Output: EAFX EBFX EPFX EIFX ECLX

Routine ECALIB (scale factors)
Input : RCLU AEFR BEFR PEFR IEFR EAFR EBFR EPFR EIFR
        RCLX
        ECLX
Output: ECLC
```

The final objects of the reconstruction for analysis are clusters and their associated cells. They are created from the visible cells (ARCE etc.), not from the perfect ones (EAEG, EANG, ...). Our task is to scale the reconstruction clusters and cells to the right scale with desired resolution using the final "calibrated" energies (EAFR, ...), derived from the perfect ones (EAEG,...). Unfortunately, the set of legal reconstruction cells (set R: visible cells associated to a cluster, e.g. ANGR cells with positive cell #)) is not identical to the set of cells in which energy had really been deposited (set T, e.g. EANG cells), because noise may add cells, and the noise cuts may kill cells.

If we want to rescale the reconstruction clusters, we have to assign all T cells to exactly one cluster. There is a large overlap with the R cells, so for most of the T cells the assignment is just as for the R cells. The rest is assigned to the cluster for which d/log(E_cl) is smallest. E_cl is the cluster energy, d the distance from the cell to the cluster centre. The assignment criterion has not yet been studied carefully, contributions are welcome. The cluster assignment is stored in a bank ECLX (parallel RCLX), which points to the pointer banks ExFX, which points to the cluster cells in ExNG (uff).

In the final step for each cluster its "calibrated" energy is determined by summing over all its associated T cells. The ratio between the "calibrated" energy and the "reconstruction" energy of the cluster is stored in the ECLC bank (parallel RCLU). It is the factor with which to scale the energies of reconstruction clusters and cells in order to go to the "calibrated energy scale".

2.5. User Options

The different levels of smearing, weighting and corrections are controlled via the steering bank ESMS, which is listed in the appendix. Basically the following options exist:

resolution:	standard / perfect / user
weighting:	standard / no / perfect / user
dead correction:	standard / no / perfect / user

"user" means the user has to define a value for the smearing resolution constant. Sensible choices are default (=standard).

2.6. Status

The product is tested and ready for use in analysis preparation (= field test). It has already been used for the development of reconstruction algorithms in the calorimeters. Known deficiencies are:

*) Missing dead corrections for BEMC, Plug, Iron -> subdetector resp.
*) tuning of crack corrections -> needs study of crack resol.
*) tuning of smearing parameters in Iron and Plug -> check resol.
*) study cell - cluster assignment (2.4.)
*) recreate digi banks from smeared energy banks
*) no smearing of energies from primary particles in ESMEAR
*) in rare cases dead energies cannot be assigned to a hot neighbour cell and its energy is lost.

3. Applications

3.1. Detector Studies

The knowledge about the true energy depositions in each detector cell allows Monte Carlo studies of the underlying calorimeter physics. It has proven to be a useful tool for the development of dead material corrections and of weighting algorithms. In Monte Carlo containment cuts can be easily performed.

3.2. Physics Analysis

The main application is the fast simulation of the H1 calorimeter. It is easy to change the smearing and correction resolutions, so they can be set to the best of the current knowledge without a new simulation.

The influence of detector resolution on kinematic variables (x,y,Q**2,...) can be investigated. Migration can be studied and correction procedures for the data can be developed. It also allows a wide range of systematic studies, e.g. effects of the detector granularity, uncertainties in resolution and calibration, biases introduced by cluster algorithms and weightings etc..

3.2. Utilities

All new banks are described in the DDL language and can be printed using H1PRNT. A routine H1FMES calculates the "measurable energy" (see definition in 1.3.3) from the particle type and energy. For event reconstruction (e.g. Jacquet-Blondel) an inverse mapping function EMAPI gives the space point xyz for each subdetector and channel number (unfortunately not available for dead materials).

Appendix A: Steering Banks

```
ESMS       ! 'calibrated Energies' SMearing Steering bank
*             ===========#=========##=======#============
*
* smearing option as a function of the subdetector:
* ------------------------------------------------
*   Etot(smeared) = Eem(smeared) + Ehad(smeared) + Einv(smeared)
*   Evis(smeared) = Eem(smeared) + Ehad(smeared)
*
*   delta_Eem/Eem    = a/sqrt(Eem)
*   delta_Evh/Ehad   = b/sqrt(Ehad)
*
*   1 = with smearing default
*   2 = with smearing choosen by the user
*       put 0.00 for no smearing in a subdetector
*   3 = no smearing at all, perfect signal
*   em-argon  had-argon BEMC      PLUG    IRON
*   1         1         1         1       1         (default)
    1         1         1         1       1         ! word 1-5 user
* the user smearing values for the electromagnetic fraction (a)
*   0.1       0.198     0.1       0.56    0.50      (default)
    0.1       0.198     0.1       0.56    0.50      ! word 5-10
* the user smearing values for the hadronic fraction (b)
*   0.178     0.464     0.178     1.00    1.00      (deault)
    0.178     0.464     0.178     1.00    1.00      ! word 10-15
*
* weighting option as a function of the subdetector:
* -------------------------------------------------
*
*   delta_Einv/Einv = c/sqrt(Einv)
*
*   0 = no weighting, visible energy simulated Evis=Eem+Ehad
*   1 = weighting with default resolution (c=default)
*   2 = weighting with resolution by user (c=optional)
*   3 = perfect weighting Etot=Eem+Ehad+Einv
*   weighting only for argon-calorimeter meaningful (2,3)
*   em-argon  had-argon BEMC      PLUG    IRON
*   1         1         0         1       1         (default)
    1         1         0         1       1         ! word 15-20
* user values for weighting (c)
*   0.178     0.950     0.00      1.00    1.00      (default)
    0.178     0.950     0.00      1.00    1.00      ! word 20-25
*
* dead correction as a function of the subdetector:
* ------------------------------------------------
*
*   word 26 dead correction option, word 27 smearing of dead energy
*   0 = no dead correction
*   1 = with dead correction, smearing of dead energy with default
*   2 = with dead correction, smearing of dead energy with user choise
*   3 = with dead correction, no smearing of dead energy, perfect
*   1                                                   (default)
    1                                                   ! word 26
*   1.00                                                (default)
    1.00                                                ! word 27
```

Appendix B: Bank Descriptions

x = A, B, P, I, W for Argon, BEMC, Plug, Iron, dead material

The Ex.. banks contain all channels with true energy depos. (set T)

The Ex banks of one subdetector are parallel to each other:
ExNG || ExEG || ExSG || ExFR || ExFX

ExNG contains all cells of set T

1	Nchan	I	channel number

ExEG perfect energy bank
parallel to ExNG, which contains channel numbers.
scale is 500 keV/unit
packed, use IFRB16

1	Einv	I	invisible energy
2	Eem	I	electromagn. energy
3	Ehad	I	hadronic energy
4	Evh	I	hadronic visible energy

ExSG smeared energy

1	Esmear	F	smeared cell energy (GeV)

ExFR final "calibrated energy"

1	Esmear	F	smeared cell energy (GeV), w. dead mat. corr.

ExFX pointer bank

1	Inext	I	pointer to next cell in cluster

==========

The cluster banks ECLX, ECLC are parallel to the reconstr. cl. banks
ECLX || ECLC || RCLU || RCLX

ECLX points to perfect energy cells belonging to this cluster

1	NCHA	I	# of cells in LAr
3	NCHI	I	# of cells in TC
5	NCHB	I	# of cells in BEMC
7	NCHP	I	# of cells in plug
2	AGFX	I	pointer to 1st channel in lAr
4	IGFX	I	pointer to 1st channel in Iron
6	BGFX	I	pointer to 1st channel in Bemc
8	PGFX	I	pointer to 1st channel in Plug

ECLC contains "calibration factors" for final rec. cluster and cell energies to go to "calibrated energies"

1	cala	F	"calibration factor" for argon cells
2	cali	F	"calibration factor" for iron cells
3	calb	F	"calibration factor" for BEMC cells
4	calp	F	"calibration factor" for Plug cells
5	calcl	F	"calibration factor" for cluster energy

==========

H1FP H1FAST Parameter Bank

Rows 1-5 contain simulation parameters for EMC, HAC, Iron, Plug, BEMC used in case of coarse geometry.
Column 1 contains s_mip, column 2 e/mip and column 3 p/mip.

1	RSFMIP	F	sampling fraction of mip s_mip
2	EBYMIP	F	e/mip
3	PBYMIP	F	p/mip

Appendix C: Calling Sequence

```
 1   0   ESUMHT            module steering: sum up calorimeter hits
 2   1      MODULS
 3   1      ENESUM         sum for each calorimeter hit bank
 4   2         BKFMT
 5   2         BKTOW
 6   2         WBANK
 7   2         NWSOFT
 8   2         BKFRW
 9   2         BLIST
10   2         WDROP
11   1      MODULF

 1   0   EWGHT              module steering: smearing
 2   1      MODULS
 3   1      EWINIT         initialization of options and parameters
 4   2         UGTBNK
 5   2         ERRLOG
 6   1      ESMEAR         perform the smearing for each subdetector
 7   2         BKTOW
 8   2         BKFMT
 9   2         UCOPY
10   2         NBSOFT
11   2         ESAMPF      smear cell energy with gamma distribution
12   2         WBANK
13   2         BKFRW
14   2         BLIST
15   2         WDROP
16   1      EDEADC         perform dead corrections
17   2         BKFMT
18   2         BLIST
19   2         BKTOW
20   2         BKFRW
21   2         EPDEAD      dead corrections for the Argon
22   3            ERRLOG
23   3            NBSOFT
24   3            AWFIL
25   4               AWFFIL
26   4               AWPFIL
27   4               AWRFIL
28   4               AWZFIL
29   4               ERRLOG
30   3            EPDFIL
31   4               ERRLOG
32   4               NWSOFT
33   4               AWCRAK
34   5                  AWZFIL
35   5                  AWPFIL
36   5                  AWRFIL
37   3            EWCORR
38   4               SORTIL
39   1      ECLUST         cluster assignment for cells
40   2         BKFMT
41   2         VZERO
42   2         ECLOSE      find closest cluster for a given cell
43   3            EMAPI    inverse mapping for all calorimeters
44   4               ARINIT
45   4               VZERO
46   4               NBSOFT
47   4               AVCGEN
48   4               ICONT2
49   4               PMAPI
50   2         BLIST
51   1      ECALIB         scaling of rec. clusters with calib. ener.
52   2         BKFMT
53   2         BLIST
54   1      MODULF
```

GFLASH Version 1.4, January 07, 1993.

Authors (Institute): BITNET/EARN Address:
M. Kuhlen (MPI) H1KMKU AT DHHDESY3
G. Grindhammer (MPI) F36GGG AT DHHDESY3
S. Peters (DESY) F36PET AT DHHDESY3
M. Rudowicz (MPI)
Mailing Address: DESY - FH1K
Notkestr. 85
D - 2000 Hamburg 52

-- PREFACE --

Users of this program are encouraged to contact one of us in order to be informed about updates, bugs found, etc.
We of course would like to hear from anybody who has discovered a bug or wants to make a suggestion or an addition to the program.
If you use GFLASH for a talk or publication, we would appreciate your crediting the program.

Since the first release of GFLASH work has been concentrated on its development as one of the simulation options for the H1 detector at HERA, in Hamburg. In this version of GFLASH (1.4) all mayor features used in H1 are made available to the public. In addition new parameterizations of electromagnetic showers are implemented, which cover a wide range of possible calorimeter configurations. Full hadronic shower parametrization is not supported any more. Instead the concept of "partial parametrization" as used in H1 has been introduced. In this concept hadrons are always tracked individually. Electromagnetic showers are only parametrized if they don't cross boundaries between calorimeter stacks. The energy loss of real particles on an averaged geometry is handled by GFLASH consistently. The interface and routines for full hadronic shower parametrization are kept for convenience (users may build their own system from this).

---

0. -- CONTENTS --

---

1. INTRODUCTION
2. HOW TO RUN GFLASH WITH GEANT
3. OVERVIEW ON FUNCTIONS AND SUBROUTINES
4. GFLASH DETAILS
   4.1 Overview on COMMON blocks
   4.2 Geometry
   4.3 Steering
   4.4 Electromagnetic shower parametrization
   4.5 Hadronic shower parametrization
   4.6 Tracking of real particles
   4.7 Termination of real particles
   4.8 Book keeping of energy
5. TESTRUN OUTPUT (FOR COMPARISON)

---

1. -- INTRODUCTION --

GFLASH is a program for fast calorimeter simulation with parametrized

electromagnetic (and hadronic) showers inside GEANT. In order to reproduce typical signalstructures correlations between the parametrized physical quantities are taken into account. GFLASH is the standard option for Monte Carlo mass production for physics events in the H1 detector at the e-p collider HERA at DESY, Hamburg.

The basic idea of interfacing parametrized simulations a la GFLASH with GEANT was to define two new "physics" processes, one for "electromagnetically" and one for "hadronically" showering particles. GEANT tracks a particle up to the first inelastic interaction (the start of the shower) and from then on searches only for the next volume boundary. At the first inelastic reaction the incident particle is stopped, and a "pseudo shower" particle with the momentum of the incident particle is stored in the temporary stack of GEANT. For the definition of the two types of "pseudo shower" particles the GEANT variables IPART and ITRTYP are used:

```
    ipart = 51 ("eshowino")
          = 50 ("hshowino")

   itrtyp = 12  em-pseudo shower track
          = 14 had-pseudo shower track
```

Once a "pseudo particle" is created, GFLASH takes over control and the "pseudo shower" is tracked in small steps within a volume. The energy to be deposited in each of the steps in the given medium is computed and energy spots are deposited perpendicularly to the "pseudo shower" track according to the radial distribution for this shower.

In addition to "shower tracking" the energy loss of real particles (e+-,gammas,hadrons,muons) is handled by GFLASH, if they are tracked on a coarse geometry (average GEANT mixture). This allows to perform "partial parametrizations" where only parts of the shower energy (eg. only electromagnetic (sub)showers) are parametrized depending on user defined conditions.

The current version of GFLASH allows up to 5 calorimeter types with different media, to be defined by the user.

Information concerning the parameterizations, comparisons with data and GEANT/GHEISHA and other related information can be found in:

(1) "THE FAST SIMULATION OF ELCTROMAGNETIC AND HADRONIC SHOWERS"
SLAC-PUB-5072, October 1989, published in NIM A290(1990) 469-488
(2) "THE PARAMETERIZED SIMULATION OF ELECTROMAGNETIC SHOWERS"
in preparation
(3) ""CALIBRATED ENERGIES" IN H1 DETECTOR SIMULATION"
H1 Software Note Number 26, October 1991
and in german only:
(4) MPI-PAE / Exp.E1. 200, January 1989
(5) MPI-PAE / Exp.E1. 202, June 1989
(6) MPI-PhE / 92-13, September 1992
(7) MPI-PhE / 92-14, September 1992

---

2. -- HOW TO RUN GFLASH WITH GEANT --

The file GFLASH14, distributed together with this manual, contains a complete example program with all necessary GFLASH and GEANT routines to make a test run on your computer.

To run GFLASH, materials with effective A and Z values, radiation and

absorption length, and an effective density, have to be defined (GEANT mixture).

In addition the user has to input material and geometry dependent parameters for each calorimeter in the subroutine GFPARM. The service routine GFCPAR may be used to calculate some the neccessary parameters. In addition a function that maps space points to calorimeter types rsp. read out cells has to be provided by the user (GFMAP in the example).

GFLASH steering parameters are also defined in GFPARM (for details see section 4.3).

At initialization GFLASH has to be called once from the subroutine UGINIT.

The main interface to GEANT is coded in GUSTEP. (See example in the file GFLASH14 for details).

In the example we have calculated the neccessary information for for two calorimeter modules (a lead/liquid argon and an iron/liquid argon calorimeter) of the H1 detector. These modules where put together in a beam acting as electromagnetic (EMC) and hadronic (HAC) calorimeter respectivly:

```
                    beam ---->  |EMC|HAC|
```

The user has to provide data cards for the input of the kinematics and other GEANT parameters (see section 5). The calorimeter geometry described above is coded in the subroutine UGEOM.
For the comparison, we ran GFLASH jobs under different conditions. What the different conditions are, and how the output should look like can be seen at the end of this manual (section 5).

---

3. -- OVERVIEW ON FUNCTIONS AND SUBROUTINES --

```
 3.1 standard GEANT stuff:
     MAIN, GUTREV, GUTRAK, GUHADR, GUPHAD, GUFLD
 3.2 specific GEANT stuff:
     UGINIT  -- call GFLASH at initialization
     UGEOM   -- geometry definition
     GUSTEP  -- main interface to GFLASH
 3.3 GFLASH stuff, calling sequence:
     X GUSTEP
     0   GFINV  ---------- book keeping of invisible energies
     1      GFLMES ------- calc. measurable energ. (acc.f. rest masses)
     0   GFLASH ---------- main GFLASH steering routine
     1      GFPARM ------- input calorimeter and steering parameters
     1      GFSECO ------- handling of secondaries, decision on param.
     1      GFLMES
     2         GFSAME ---- test if em-shower will be contained in stack
     3            GFMAP -- map space points to geometry
     1      GFTERP ------- terminate protons below GFLASH cut
     2         GFMAP
     1      GFTERG ------- terminate gammas below GFLASH cut
     2         GFSAMP ---- apply sampling fluctuations
     3            GFSF  -- calculate fluctuated energy
     1      GFELOS ------- handle E.-loss of real particles on ave.geo.
     2         GFRESP ---- calculate hadronic response factors
     2         GFSAMP
     3            GFSF
     1      GFEMSH ------- track "e-showinos" (perform parametrization)
     2         GFSAMP
     3            GFSF
```

```
    2         GFDEPO  --- (see below)
    3            GFMAP
    1      GFSHOW ------- track "h-showino" (hadronic parametrization)
    2         GFINHA ---- get intrinsic parameters for one shower
    3            GFCHOL - Cholesky decomposition of covariance matrix
    2         GFSAMP
    1      GFDEPO ------- spot deposition, scaling with samp. fract.
    2         GFTEST ---- (see below)
```

3.4 Random numbers

```
    These generators use the GEANT random number generator GRNDM
    FUNCTION GFRN ------- One uniform random number
    SUBROUTINE GFNORR --- gaussian random number
    FUNCTION GFRGAM ----- gamma distributed random number
```

3.5 Routines used to produce some output for the example run

```
    GFTEST  -- perform energy sums
    GFCPAR  -- calculates material and geometry dep. parameter
    GUKINE  -- unpack event kinematics
    GUOUT   -- perform energy sums
    UGLAST  -- print some numbers (test output)
```

---

4. -- GFLASH DETAILS --

The most important features of GFLASH are detailed in the following. Please refer also to the inline documentation in the example.

4.1 Overview on COMMON blocks ----------

```
--- *** GFLRUN -> GFLASH run dependent parameters
        PARAMETER ( NGFCAL = 5 )
        COMMON /GFLRUN/
       +         ISSAMP(NGFCAL),IFLASH(2,NGFCAL),CFLASH(4,NGFCAL)
       +        ,RSPMIP(NGFCAL),PBYMIP(NGFCAL),EBYMIP(NGFCAL)
       +        ,SAMELM(3,NGFCAL),SAMHAD(3,NGFCAL),FLUHAD(3,NGFCAL)
       +        ,RLTHAD(NGFCAL)
       +        ,ECRIT(NGFCAL),SFREQ(NGFCAL),EBM(NGFCAL)
       +        ,RMX(235),NSTRTR(8)
  -> NGFCAL: number of GFLASH calorimeters
  -> ISSAMP: =1 for sampling calorimeters
  -> IFLASH,CFLASH: GFLASH steering options (see sect. 4.3)
  -> RSPMIP,PBYMIP,EBYMIP: energy scaling functions( see sect. 4.2)
  -> SAMELM,SAMHAD,FLUHAD: energy fluctuations (see sect. 4.2)
  -> RLTHAD: nuclear absorption lengths, used in full hadronic
             shower param. as lateral scale.
  -> ECRIT,SFREQ,EBM: geometry dependent parameter used for em shower
             parameterization (see sect. 4.2).
  -> RMX,NSTRTR: Used internally in hadronic shower parametrization.

--- *** GFLSHW -> GFLASH shower dependent parameters
        COMMON /GFLSHW/
       +         JCALOR,JCSENS
       +        ,ROTMAT(3,2),EINC,XLNE,EDP,PINC,XLNP,H1EINV
       +        ,ALPHA(0:4),BETA(0:4),FRAC(0:4),ISHAD,IPC
       +        ,ZINLX(0:3),ZCONV(0:3)
       +        ,ARTIMS,PAR(4)
  -> JCALOR: identifier of actual calorimeter (1,...,5)
  -> JCSENS: sensitive calorimeter flag. If equal to 1 we are in
             the mixture.
  -> ROTMAT: rotation matrix to convert shower reference into
             detector reference.
  -> EINC,XLNE,PINC,XLNP: energy, momentum and their logarithms
             of the incoming particle.
  -> H1EINV: invisible energy in first hadronic interaction (used
```

```
            in full hadronic shower param. only.
  -> ALPHA,BETA,FRAC,IPC,ZINLX,ZCONV,PAR: actual shower parameter for
            hadronic shower parameterization.
  -> ISHAD:  flag that indicates electromagnetic (0) and
            hadronic (1) shower development.
  -> ARTIMS: used for averaging of the lateral scale in case of
            boundary crossings.

--- *** GFLOUT -> GFLASH output of energy spots
        PARAMETER ( NSPMAX = 5000 )
        COMMON/GFLOUT/ NGFSPO,GFSPOT(3,NSPMAX),GFEN(6,NSPMAX)
  -> NSPMAX: dimension of spot arrays.
  -> NGFSPO: actual number of spots sampled.
  -> GFSPOT(3,*): spot coordinates x,y,z.
  -> GFEN(6,*): spot energy (see sect. 4.8 for details)

--- *** GFLAGS -> GFLASH various flags
        PARAMETER (NESHOW=51, NHSHOW=50)
        COMMON/GFLAGS/ IGFLAG, IGFSTP, GFCLOW, GFCHIG
      +               ,GFCGAM, GFCELE, GFCMUO, GFCPIO, GFCPRO, GFCNEU
  -> NESHOW,NHSHOW: GEANT particle codes for showinos
  -> IGFLAG: act. parametrization flag=IFLASH(1,JCALOR)(see sect. 4.3)
  -> IGFSTP: act. GFLASH stopping flag=IFLASH(2,JCALOR)(see 4.3, 4.7)
  -> GFCLOW,GFCHIG: actual energy range in which parameterizations
            are allowed (see 4.3).
  -> GFCGAM,GFCPRO,GFCNEU: energy cut below which gammas, protons
            and neutrons are terminated (see 4.3, 4.7 for details).
  -> GFCELE,GFCMUO,GFCPIO: actually not used.

4.2 Geometry ------------------------------------------------------------
Related routines: UGEOM, GFCPAR, GFMAP, GFPARM

-UGEOM: Definition of the coarse geometry
 The GEANT medium number is used to define the GFLASH calorimeter
 JCALOR:
 ==== Dependence of JCALOR on NUMED  ====
    subdetektor       NUMED    JCALOR
  in the example
      EMC              301        1
      HAC              302        2
   not used            303        3
   not used            304        4
   not used            305        5

-GFCPAR: Service routine to calculate calorimeter parameter
    SUBROUTINE GFCPAR(N,Z,A,D,X0,RHO,DEDX,
   +        W,RM,EC,ZEFF,AEFF,X0EFF,RMEFF,RHOEFF,ECEFF,SF,EMIP,RMIP)
      PURPOSE: Calculate material and geometry dependent parameters
               to be used with parametrized simulations on average
               geometries (mixtures).
      INPUT: N, D (CM), X0 (G/CM**2), RHO (G), DEDX (MEV/(G/CM**2))
             N=number of layers, for each layer: Z=charge number
             A=atomic weight, D=width, X0=radiation length
             RHO=density, DEDX=dE/dx of mip's
             It is assumed that the first array elements (N=1) contains
             the values of the read out layer.
      OUTPUT:for each layer:W=proportion by weigths, RM=Moliere radius
             EC=critical energies.
             for the mixture: xEFF=effective material parameters,
             SF=1./sampling frequency, EMIP=approx value of e/mip
             RMIP=sampling fraction for mip's

-GFMAP: map space point (x,y,z) to calo.-typ NCALO and cell numbers.
 This mapping function is needed to find the appropriate scaling
```

functions (eg. e/mip) for spot energies. It is also used to evaluate geometrical constraints on em shower parameterization and proton termination. In more elaborated simulations this function should return a channel number in addition (it should reflect the read out geometry).

-GFPARM: main user routine to input calorimeter parameter
The following parameters have to prepared by the user for each calorimeter JCALOR:
(some of them may be calculated by GFCPAR)

```
   RSPMIP(JCALOR)    : sampling fraction of minimum ion. particles
   EBYMIP(JCALOR)    : ratio sampl. fract. of electrons to sf.(mip's)
   PBYMIP(JCALOR)    : ratio sf.(pure hadronic comp.) to sf.(mip's)
                       This global factor is only used in the case of
                       full hadronic shower parametrization.

   SAMELM(1,JCALOR) : sampling fluctuations for elm showers acc. to
                       Sigma/E = SAMELM/sqrt(E)
   SAMELM(2,JCALOR) : act. not used
   SAMELM(3,JCALOR) : act. not used

   FLUHAD(1,JCALOR) : intrinsic fluctuations for had showers acc. to
   FLUHAD(2,JCALOR) : Sigma/Edp = fh(1,j)/sqrt(Einc)
   FLUHAD(3,JCALOR) :                        + fh(2,j)/Einc + fh(3,j)
                       (only used in case of full hadronic shower
                       parametrization).

   SAMHAD(1,JCALOR) : sampling fluctuations of pur had component
                       acc. to Sigma/E = SAMHAD/sqrt(E)
   SAMHAD(2,JCALOR) : act. not used
   SAMHAD(3,JCALOR) : act. not used

   RLTHAD(JCALOR)    : conv.length for lateral spreading of had sh.

   ECRIT(JCALOR)     : effective critical energy in MeV calculated
                       according to GFCPAR.
   SFREQ(JCALOR)     : sampling frequency calculated according to
                       GFCPAR. Only valid if d=d_a+d_p < 2 X_0
                       (d_a,d_p=width of active/passive layers).
                       Set to zero if d > 2X_0.
                       (set to 0 if it is not a sampling calorimeter)
   EBM(JCALOR)       : 1.-EBYMIP(JCALOR)
                       (set to 0 if it is not a sampling calorimeter)
```

4.3 Steering ----------
Related Routines: GFPARM, GFLASH, GFSECO, GFSAME

- GFPARM: The following steering parameters have to provided by the user:

```
  ISSAMP: Calorimeter type flag
    =1 means sampling calo, =0 means homogenous calo.

  IFLASH(1,JCALOR): parametrization flag
    = 0  no parameterized showers, det. tracking on coarse geom.
    = 1  only param. elmag. showers, if they fit into one stack
         (JCSENS = 1, and shower fits into stack)
    = 2  only param. elmag. showers, if they start inside a stack
         (JCSENS = 1)
    = 3  param. elmag. + had. showers, if they start inside a stack
         (JCSENS = 1)
    = 4  param. elmag. + had. showers, everywhere in calo-like det.
         (JCALOR .NE. 0)
         (the energy window defined in CFLASH is ignored in this case)
```

Usage in H1: By default H1 runs with IFLASH(1,JCALOR)=1. Thus electromagnetic showers are only parametrized if they do not cross boundaries (eg. cracks, dead material in front of calor.). Hadrons are always tracked individiually.

IFLASH(2,JCALOR): low energy track stopping flag
= 0 no termination of particles by GFLASH
= 1 stop neutrons if kinetic energ. below GFCNEU
= 2 1 + terminate gammas if energy below GFCGAM according to the algorithm in GFTERG.
= 3 1 + 2 + terminate protons if kinetic energy below GFCPRO and if they are expected to range out within the current read out cell.
Usage in H1: By default H1 runs with IFLASH(2,JCALOR)=3. The particle termination is optimized for the H1 calorimeter.

GFCNEX(JCALOR) : GFCNEU: low energy cut for neutron stopping
GFCGAX(JCALOR) : GFCGAX: low energy cut for gamma termination
GFCPRX(JCALOR) : GFCPRX: low energy cut for proton termination

CFLASH(1,JCALOR) : low energy cut for param. em showers
CFLASH(2,JCALOR) : high energy cut for param. em showers
CFLASH(3,JCALOR) : low energy cut for param. had showers
CFLASH(4,JCALOR) : high energy cut for param. had showers
IF energy of showering particle is outside GFLASH window,
THEN secondary particles are tracked by GEANT

-GFLASH: Depending on the flags and cuts given in GFPARM GFLASH will call the appropriate routines.

-GFSECO: In GFSECO the secondaries are handled and the final decision on parametrized or individual tracking is performed. In case of parametrizations, "showinos" will be generated and stored in the GEANT particle stack. Effects of rest masses will be taken into account.
Electromagnetic showers will only be parametrized, if a bremsstrahlungs process has occured.

-GFSAME: Is called from GFSECO to test, if 90% of a given electromagnetic shower will be contained within the same stack the shower is supposed to start in. (Uses GFMAP).

4.4 Electromagnetic shower parametrization

Related routines: GFEMSH, GFSAMP

In GFEMSH the shape of a parametrized electromagnetic shower is calculated and the shower is "tracked" through a volume.
Sampling fluctuations are applied (GFSAMP) and energy spots are distributed according to the actual shape parameter.

The physics of electromagnetic shower parametrization has been totally revised since the last release of GFLASH.
The main improvements are:
- The parametrization depends now on the calorimeter geometry and materials used. They are therfor valid for various calorimeter types.
- The radial profiles have been improved with respect to both, their average behaviour and shape fluctuations.
- Correlations between longitudinal and radial shape fluctuations are taken into account.

For more details please refer to refs (2) and (6).

4.5 Hadronic shower parametrization

Related Routines: GFSHOW, GFINHA, GFCHOL, GFSAMP

In GFINHA and GFCHOL the shape of a parametrized hadronic shower as well as the intrinsic losses and fluctuations are calculated and the shower is "tracked" through a volume in GFSHOW.
Sampling fluctuations are applied (GFSAMP) and energy spots are distributed according to the actual shape parameter.
The energy spots are scaled with a global response factor (PBYMIP in GFPARM) to account for (pur) hadronic sampling fractions.

No improvements have been developed in the hadronic shower parametrization since the last release of GFLASH because it is no longer used in H1. The parametrizations implemented are very H1 specific and it is not recommended to use them for other calorimeters. Users should instead develop their own parametrizations. GFSHOW may be used as guidance and interface.
In addition the detailed book keeping of energies in GFLASH (see section 4.8) provides the user with a powerful tool to develop hadronic shower parametrizations.
For more details on hadronic shower parametrization please refer to refs (1), (4) and (5).

4.6 Tracking of real particles

Related Routines: GFELOS, GFSAMP, GFRESP

If real particles are tracked individually through the coarse geometry the effect of the sampling has to be simulated explicitly.

The continous energy loss is distributed along the trajectory of the particles (GFELOS).

In case of electrons, photons and hadrons sampling fluctuations will be applied on the energy loss (GFSAMP). (Sampling fluctuations will also be applied in homogenous calorimeters -> the user has to choose a small input value in GFPARM).

Hadronic sampling fractions depend on the kinectic energy and the mass of the particle: had/mip = had/mip(E_k,m).
The user has to provide this response functions in the subroutine GFRESP. In the example we have tabulated the integrated response had/mip(E_k,m) * f(BIRK) / E_k for heavy ionizing particles, from which the actual had/mip can be calculated (see GFRESP). The lost energy E_dep will be scaled to visible hadronic energies according to E_vh = E_dep * had/mip(E_k,m).
(GFRESP will also be called in homogenous calorimeters)

For more details please refer to refs (3) and (7).

4.7 Termination of real particles

Related routines: GFLASH, GFTERG, GFTERP

To speed up the individual tracking of hadronic showers, GFLASH allows for an early termination of neutrons, gammas and protons. Depending on the steering flags in GFPARM the following options are available:

IFLASH(2,*)=1:Neutron with kinetic energy below GFCNEU are stopped. Their energy is regarded as invisible (see next section)
IFLASH(2,*)=2:In addition to neutron stopping gammas with energies below GFCGAM are terminated. Their energy will be deposited as one spot. The spot coordinates are choosen randomly according to an exponential distri-

bution (GFTERG).

IFLASH(2,*)=3: In addition to neutron and gamma termination protons with energies below GFCPRO will be terminated, if they are expected to range out within the current read out cell (GFTERP). Their kinetic energy is kept in DESTEP. GFCPRO should be choosen according to the read out granularity.

For more details please refer to ref (3).

4.8 Book keeping of energy ----------
Related routines: GFDEPO, GFINV, GFLMES

GFLASH provides a very detailed book keeping of all energies. At H1 this detailed knowledge is used eg. to test the integrity of the Monte Carlo and to optimize weighting procedures for the non compensating calorimeters.
For all energy depositions the array GFEN(6,NGFSPO) containing 6 different kinds of energy and the array GFSPOT(3,NGFSPO) containing the spot coordinates are filled. These energies will partly be scaled with sampling fractions in the subroutine GFDEPO. In GFDEPO the user has to decide where to store the energy.

In hadronic interactions the energy used to break up nuclei is counted in GFINV. Energies from neutrinos and stopped neutrons are also counted as invisible as well as the energy of particles that are leaving the experimental set up. Effects of rest masses are taken into account properly (GFLMES).

After beeing processed by GFDEPO GFEN(6,NGFSPO) contains the the following information:
(muon energies are counted as "hadronic" with had/mip=1

```
 GFEN(1,*)  visible hadronic energy (fluctuated)
            E_vis = E_dep_had * had/mip * mip
 GFEN(2,*)  visible electromagnetic energy (fluctuated)
            E_vis = E_dep_elm * e/mip * mip
 GFEN(3,*)  invisible energy (unscaled, unfluctuated)
            E_inv = energy from nucl. break up, neutrinos,
                    stopped neutrons, leaving particles, ...
 GFEN(4,*)  deposited electromagnetic energy (unscaled, unfluctuated)
            E_dep_elm
 GFEN(5,*)  deposited hadronic energy (unscaled, unfluctuated)
            E_dep_had
 GFEN(6,*)  deposited hadronic energy (scaled, unfluctuated)
            E_vh = E_dep_had * had/mip
```

Using this information we can calculate various quantities. To name but a few:

- The total signal:
  E_calo_vis = GFEN(1) + GFEN(2)
- The unscaled signal:
  E_calo_dep = GFEN(4) + GFEN(5)
- The global response factor for hadrons:
  GFEN(6) / GFEN(5)
- The "measurable" energy E_mes:
  E_mes = GFEN(3) + GFEN(4) + GFEN(5)
  Note: E_mes is defined as all energy which has the potential to be measured. It acts therfor as something like a conserved quantity in calorimetry. It's value is in general not identical with the total energy of the in incoming particle but depends on the particle type. Depending on the particle type, the rest mass may convert into measurable energy. In case of hadrons

this effect is not negligable. Let p be the momentum of the incoming particle and m its mass. E_tot = sqrt(p**2 + m**2) denotes the total energy. The following table shows how E_mes is calculated for different particles:

initial particle	E_mes	Reason
pi+,pi-	E_mes = E_tot	initial particle decays
p,n	E_mes = E_tot - m	initial particle comes to rest
anti-p,anti-n	E_mes = E_tot + m	initial particle annihilates

Usually the understanding of the response functions (x/mip, saturation) and the sampling fluctuations of a given calorimeter increases with time. Keeping the above information after the simulation step allows for quick retuning of cell energies at the recontruction level avoiding the time consuming detector simulation. Using GFEN(4,*) and GFEN(5,*) new sampling fractions and saturation factors may be applied to the cell energies. Fluctuation is done with help of GFSAMP,GFSF at the cell level.

Warning: Neutrons should always be terminated by GFLASH to get E_mes correctly. Reason: The kinetic energy of neutrons is lost if they are stopped by GEANT (GTNEUT). The "lowest level" simulation in GFLASH should therfor be IFLASH(1,*)=0, IFLASH(2,*)=1 and CUTNEU (the GEANT neutron cut) well below GFCNEU (CUTNEU<=GFCNEU/10.).

4.8 Summary

To summarize: The most important user routines in GFLASH are -

- GFPARM: input of steering parameter
  input of material and geometry dependent parameter
- GFMAP: provide GFLASH with a mapping function reflecting the detector geometry at the cell level.
- GFRESP: provide GFLASH with hadronic response factors for individual tracking on coarse geometry.

5. -- TESTRUN OUTPUT (FOR COMPARISON) --

We ran the GFLASH example with the following sets of data cards:

```
LIST
TRIG 5000
RUNG 1
RNDM 123 456
KINE ip  0.  0. 0.  0. 0. 10.    ! ip =1,2,3,9,14,15,...
CUTS 0.001 0.001 0.001
ANNI 1
BREM 1
COMP 1
DRAY 1
PAIR 1
PHOT 1
HADR 1
DEBU 1 10000 100
SWIT 0  0  0
TIME 5. 5. 1
STOP
```

The data card KINE is used to input the particle type and the kinematics. In GUKINE this card is interpreted as:

KINE ip x. y. z. p_x. p_y. p_z.

A subset of the output produced for various incident particles and steering options can be seen down below.
(The recommended options are IFLASH(1,*)=1 and IFLASH(2,*)=3)

Three kinds of energies are given in the output:

1. the reconstructed energy on the electromagnetic scale, ie. all energy has been reconstructed assuming it to be electromagnetic energy. Due to intrinsic losses in hadronic shower development this number will not sum up to the incident energy.
2. The visible energy in the two calorimeters and their sum.
3. A decomposition of the energy (using the detailed book keeping in GFLASH). The measurable energy E_mes (see sect 4.8 for a definition) should sum up to following values:

initial particle	initial momentum	E_mes
pi-	10 GeV	E_mes = E_tot = 10.00097 GeV
p	10 GeV	E_mes = E_tot - m = 9.1065 GeV
anti-p	10 GeV	E_mes = E_tot + m = 10.982 GeV

(at this momentum the rest mass effects for e-, e+ and even pions are negligible).
Comparing the expected values for E_mes with the output below shows deviations at a level well below 1 permille (0.05% typically)

```
%%%%%%%%%%%%%%%%%%%%%%%%%%%%%%%%%%%%%%%%%%%%%%%%%%%%%%%%%%%%%%%%%%%%%%%%%%%%%%%%
%%% recommended steering options: gammas e-, e+, pi-, p, anti-p      %%%
%%%%%%%%%%%%%%%%%%%%%%%%%%%%%%%%%%%%%%%%%%%%%%%%%%%%%%%%%%%%%%%%%%%%%%%%%%%%%%%%

 Gamma p=10 GeV IFLASH(1,*)=1, IFLASH(2,*)=3

 ***** DATA CARD CONTENT     KINE 1  0. 0. 0.  0. 0. 10.
  ****************  GFLASH STEERING  *********************
  ********   EMC  **   HAC  **   NN   **   NN   **   NN
  IFLASH1     1         1         0         0         0
  IFLASH2     3         3         0         0         0
++++++++++++++   GFLASH test output   ++++++++++++++

-total reconstructed energy (em-scale) (GeV) -------
   mean ........................  9.992 +-  0.0055
   sigma / mean ................  3.91%

-visible energies (GeV) ---------------------------
   total ......................... 0.7926 +- 0.00044
   EMC........................... 0.7917 +- 0.00044
   HAC........................... 0.0009 +- 0.00003

-energy decomposition (GeV) -------- mean ---- RMS -
   electromagnetic E_elm .........  9.989     0.1114
   hadronic E_had ................  0.000     0.0000
   invisible E_inv ...............  0.000     0.0000
   geometrical losses E_geo ......  0.008     0.0104
   E_calo = E_elm+E_had+E_inv ....  9.989     0.1114
   E_mes = E_calo+E_geo ..........  9.996     0.1298

++++++++++++++++++++++++++++++++++++++++++++++++++++
          **** TIME TO PROCESS ONE EVENT IS =    0.0289 SECONDS

%%%%%%%%%%%%%%%%%%%%%%%%%%%%%%%%%%%%%%%%%%%%%%%%%%%%%%%%%%%%%%%%%%%%%%%%%%%%%%%%

 Positron p=10 GeV IFLASH(1,*)=1, IFLASH(2,*)=3

 ***** DATA CARD CONTENT     KINE 2  0. 0. 0.  0. 0. 10.
```

```
  ****************  GFLASH STEERING  *********************
  ********   EMC  **   HAC  **   NN   **   NN   **   NN
  IFLASH1     1         1         0         0         0
  IFLASH2     3         3         0         0         0
++++++++++++++   GFLASH test output   ++++++++++++++

-total reconstructed energy (em-scale) (GeV) -------
   mean ........................  9.993 +-  0.0054
   sigma / mean ................  3.84%

-visible energies (GeV) ---------------------------
   total ........................ 0.7928 +- 0.00043
   EMC........................... 0.7922 +- 0.00043
   HAC........................... 0.0006 +- 0.00002

-energy decomposition (GeV) -------- mean ---- RMS -
   electromagnetic E_elm .........  9.990     0.1149
   hadronic E_had ................  0.000     0.0000
   invisible E_inv ...............  0.000     0.0000
   geometrical losses E_geo ......  0.008     0.0105
   E_calo = E_elm+E_had+E_inv ....  9.990     0.1149
   E_mes = E_calo+E_geo ..........  9.996     0.1306

++++++++++++++++++++++++++++++++++++++++++++++++++++
          **** TIME TO PROCESS ONE EVENT IS =    0.0245 SECONDS

%%%%%%%%%%%%%%%%%%%%%%%%%%%%%%%%%%%%%%%%%%%%%%%%%%%%%%%%%%%%%%%%%%%%%%%%%%%%

 Electron p=10 GeV IFLASH(1,*)=1, IFLASH(2,*)=3

 ***** DATA CARD CONTENT     KINE 3  0. 0. 0.  0. 0. 10.
  ****************  GFLASH STEERING  *********************
  ********   EMC  **   HAC  **   NN   **   NN   **   NN
  IFLASH1     1         1         0         0         0
  IFLASH2     3         3         0         0         0
++++++++++++++   GFLASH test output   ++++++++++++++

-total reconstructed energy (em-scale) (GeV) -------
   mean ........................  9.990 +-  0.0054
   sigma / mean ................  3.85%

-visible energies (GeV) ---------------------------
   total ........................ 0.7926 +- 0.00043
   EMC........................... 0.7920 +- 0.00043
   HAC........................... 0.0005 +- 0.00002

-energy decomposition (GeV) -------- mean ---- RMS -
   electromagnetic E_elm .........  9.989     0.1141
   hadronic E_had ................  0.000     0.0000
   invisible E_inv ...............  0.000     0.0000
   geometrical losses E_geo ......  0.008     0.0108
   E_calo = E_elm+E_had+E_inv ....  9.989     0.1141
   E_mes = E_calo+E_geo ..........  9.996     0.1307

++++++++++++++++++++++++++++++++++++++++++++++++++++
          **** TIME TO PROCESS ONE EVENT IS =    0.0245 SECONDS

%%%%%%%%%%%%%%%%%%%%%%%%%%%%%%%%%%%%%%%%%%%%%%%%%%%%%%%%%%%%%%%%%%%%%%%%%%%%

 Pion-    p=10 GeV IFLASH(1,*)=1, IFLASH(2,*)=3

 ***** DATA CARD CONTENT     KINE 9  0. 0. 0.  0. 0. 10.
  ****************  GFLASH STEERING  *********************
  ********   EMC  **   HAC  **   NN   **   NN   **   NN
```

```
  IFLASH1     1          1          0          0          0
  IFLASH2     3          3          0          0          0
++++++++++++++   GFLASH test output   ++++++++++++++

-total reconstructed energy (em-scale) (GeV) -------
   mean ........................... 6.853 +-  0.0196
   sigma / mean .................. 20.23%

-visible energies (GeV) ----------------------------
   total ......................... 0.5005 +- 0.00150
   EMC............................ 0.2814 +- 0.00289
   HAC............................ 0.2190 +- 0.00240

-energy decomposition (GeV) -------- mean ---- RMS -
   electromagnetic E_elm .........  3.367     1.8361
   hadronic E_had ................  2.844     1.0619
   invisible E_inv ...............  3.406     1.1901
   geometrical losses E_geo ......  0.377     0.8908
   E_calo = E_elm+E_had+E_inv ....  9.620     0.8983
   E_mes = E_calo+E_geo ..........  9.997     0.1023

++++++++++++++++++++++++++++++++++++++++++++++++++++

          **** TIME TO PROCESS ONE EVENT IS =    0.2145 SECONDS

%%%%%%%%%%%%%%%%%%%%%%%%%%%%%%%%%%%%%%%%%%%%%%%%%%%%%%%%%%%%%%%%%%%%%%%%%%%%%%%%

 Proton   p=10 GeV IFLASH(1,*)=1, IFLASH(2,*)=3

 ***** DATA CARD CONTENT     KINE 14 0. 0. 0.  0. 0. 10.
  ****************  GFLASH STEERING  *********************
  ********   EMC  **   HAC  **   NN   **   NN   **   NN
  IFLASH1     1          1          0          0          0
  IFLASH2     3          3          0          0          0
++++++++++++++   GFLASH test output   ++++++++++++++

-total reconstructed energy (em-scale) (GeV) -------
   mean ........................... 7.380 +-  0.0220
   sigma / mean .................. 21.10%

-visible energies (GeV) ----------------------------
   total ......................... 0.5316 +- 0.00163
   EMC............................ 0.2583 +- 0.00258
   HAC............................ 0.2733 +- 0.00225

-energy decomposition (GeV) -------- mean ---- RMS -
   electromagnetic E_elm .........  2.448     1.1425
   hadronic E_had ................  4.137     1.0034
   invisible E_inv ...............  1.910     1.1406
   geometrical losses E_geo ......  0.603     0.9332
   E_calo = E_elm+E_had+E_inv ....  8.497     0.9398
   E_mes = E_calo+E_geo ..........  9.100     0.1019

++++++++++++++++++++++++++++++++++++++++++++++++++++
          **** TIME TO PROCESS ONE EVENT IS =    0.2510 SECONDS

%%%%%%%%%%%%%%%%%%%%%%%%%%%%%%%%%%%%%%%%%%%%%%%%%%%%%%%%%%%%%%%%%%%%%%%%%%%%%%%%

 Anti-Proton   p=10 GeV IFLASH(1,*)=1, IFLASH(2,*)=3

 ***** DATA CARD CONTENT     KINE 15 0. 0. 0.  0. 0. 10.
  ****************  GFLASH STEERING  *********************
  ********   EMC  **   HAC  **   NN   **   NN   **   NN
  IFLASH1     1          1          0          0          0
```

```
  IFLASH2     3          3          0          0          0
+++++++++++++   GFLASH test output   +++++++++++++

-total reconstructed energy (em-scale) (GeV) -------
   mean ........................... 8.568 +-  0.0222
   sigma / mean .................. 18.32%

-visible energies (GeV) ----------------------------
   total ......................... 0.6229 +- 0.00171
   EMC............................ 0.3344 +- 0.00318
   HAC............................ 0.2883 +- 0.00261

-energy decomposition (GeV) -------- mean ---- RMS -
   electromagnetic E_elm .........  3.619     1.6993
   hadronic E_had ................  4.075     1.2076
   invisible E_inv ...............  2.775     1.2376
   geometrical losses E_geo ......  0.505     0.8502
   E_calo = E_elm+E_had+E_inv .... 10.471     0.8595
   E_mes = E_calo+E_geo .......... 10.977     0.1276

++++++++++++++++++++++++++++++++++++++++++++++++++
          **** TIME TO PROCESS ONE EVENT IS =    0.2976 SECONDS

%%%%%%%%%%%%%%%%%%%%%%%%%%%%%%%%%%%%%%%%%%%%%%%%%%%%%%%%%%%%%%%%%%%%%%%%%%%%
%%%  other steering options for pions %%%%%%%%%%%%%%%%%%%%%%%%%%%%%%%%%%%%
%%%%%%%%%%%%%%%%%%%%%%%%%%%%%%%%%%%%%%%%%%%%%%%%%%%%%%%%%%%%%%%%%%%%%%%%%%%%

 Pion-     p=10 GeV IFLASH(1,*)=0, IFLASH(2,*)=1

 ***** DATA CARD CONTENT     KINE 9  0. 0. 0.  0. 0. 10.
  ****************  GFLASH STEERING  ********************
  ********   EMC  **   HAC  **   NN   **   NN   **   NN
  IFLASH1     0         0         0         0         0
  IFLASH2     1         1         0         0         0
+++++++++++++   GFLASH test output   +++++++++++++

-total reconstructed energy (em-scale) (GeV) -------
   mean ........................... 6.829 +-  0.0194
   sigma / mean .................. 20.08%

-visible energies (GeV) ----------------------------
   total ......................... 0.4989 +- 0.00149
   EMC............................ 0.2812 +- 0.00288
   HAC............................ 0.2176 +- 0.00239

-energy decomposition (GeV) -------- mean ---- RMS -
   electromagnetic E_elm .........  3.388     1.8276
   hadronic E_had ................  2.808     1.0422
   invisible E_inv ...............  3.453     1.1860
   geometrical losses E_geo ......  0.343     0.8461
   E_calo = E_elm+E_had+E_inv ....  9.652     0.8530
   E_mes = E_calo+E_geo ..........  9.995     0.1005

++++++++++++++++++++++++++++++++++++++++++++++++++
          **** TIME TO PROCESS ONE EVENT IS =    0.7013 SECONDS

%%%%%%%%%%%%%%%%%%%%%%%%%%%%%%%%%%%%%%%%%%%%%%%%%%%%%%%%%%%%%%%%%%%%%%%%%%%%

 Pion-     p=10 GeV IFLASH(1,*)=0, IFLASH(2,*)=3

 ***** DATA CARD CONTENT     KINE 9  0. 0. 0.  0. 0. 10.
  ****************  GFLASH STEERING  ********************
  ********   EMC  **   HAC  **   NN   **   NN   **   NN
  IFLASH1     0         0         0         0         0
```

```
  IFLASH2     3          3          0          0          0
+++++++++++++   GFLASH test output   +++++++++++++
-total reconstructed energy (em-scale) (GeV) -------
   mean ........................... 6.850 +-  0.0199
   sigma / mean ................... 20.59%

-visible energies (GeV) ----------------------------
   total ......................... 0.4996 +- 0.00152
   EMC............................ 0.2770 +- 0.00291
   HAC............................ 0.2225 +- 0.00243

-energy decomposition (GeV) -------- mean ---- RMS -
   electromagnetic E_elm .........  3.350     1.8168
   hadronic E_had ................  2.873     1.0619
   invisible E_inv ...............  3.405     1.1984
   geometrical losses E_geo ......  0.365     0.9445
   E_calo = E_elm+E_had+E_inv ....  9.630     0.9496
   E_mes = E_calo+E_geo ..........  9.995     0.0924

++++++++++++++++++++++++++++++++++++++++++++++++++++
          **** TIME TO PROCESS ONE EVENT IS =    0.4528 SECONDS
```

Addendum:

The version 1.41/00 of GFLASH provides one additional feature compared to vers. 1.40/01: The introduction of a 'tracking history word' ITRHIS in the COMMON GFTHIS.

Single bits in this word may be used to store information about the particles history. The word is cleared in the subroutine GFTREV which contains a modified copy of the GEANT routine GTREVE. GFTREV is called from GUTREV instead of GTREVE if th program is running in GFLASH mode.

GFLASH uses bit number 9 to distinguish primary hadrons which have not yet initiated a hadronic shower from those, which are part of an hadronic cascade. No sampling fluctuations are applied to the energy loss of primary hadrons (see GFELOS). This ensures a correct detector response for punching particles.

Other bits in ITRHIS maybe introduced by the user according to their needs.

++

C U R R E N T S T A T U S O F G F L A S H 1.4 I N S I G E M

++

1. STATUS:

GFLASH 1.4 has been interfaced to SIGEM to be used in all calorimeters of baseline 2. The calorimeters are described by GEANT mixtures. The following changes to the original code are mentioned:

- Mixture definitions:
  Geant mixtures have been defined for all GEM calorimeters according to the needs of GFLASH.

- Calorimeter dependent steering and material parameters:
  The calorimeter dependent parameters needed by GFLASH have been moved to user words in the tracking media definition. Most of the parameters are calculated from the GEANT media definitions. The subroutines GFCPAR and GFBEBL have been introduced for this purpose. GFBEBL calculates sampling fractions for heavy ionizing particles and stores them in tables which are readable by GFLASH. Consequently, GFLASH is steered completely by the geometry.

  GFPARM is called to update the corresponding GFLASH COMMON every time a new medium is entered. The subroutines GFLASH, GFSAMP and GFRESP have been recoded correspondingly.

  Parameters that are hard to calculate, eg. sampling fluctuations or k_B factors to be applied with Birk's Law, have to be introduced inline. For all calorimeters a default set of parameters has been established which is used if no user action is taken.

- Mapping function:
  The mapping routine GFMAP tests if a number of given points is located in the same volume as VECT(1..3) (GEANT particle vector). The GEANT routine GINVOL is used for this purpose. GFMAP is called from GFSAME and GFTERP where decisions on parameterization and proton termination are taken.

- spot deposition and hit recording:
  All energy depositions in calorimeter volumes are handled by the subroutine SIFHIT (The original routine GFDEPO has been removed). For every single energy spot GMEDIA is called to find the corresponding medium number. Visible energies are calculated applying the appropriate sampling fractions for electrons (individually tracked hadrons have been scaled already during tracking by GFRESP). The energies are stored in the same way as in detailed GEANT simulation, including however in addition invisible, unscaled and unfluctuated energies for a possible later reprocessing.

2. FURTHER DEVELOPMENT:

The following topics are crucial to the further development:

- Mapping function:
  In the long range a unique mapping function should be developed representing the detector at the cell level. This function should be used for both the scaling and hit deposition (currently done in SIFHIT) and the determination of geometrical constraints (currently GFMAP). The current approach in GFMAP is sufficient to put constraints on electromagnetic shower parameterization (call from GFSAME) but is too crude for proton termination (call from GFTERP),

where cell information is needed.
The spot deposition mechanism in SIFHIT may turn out to be too slow for a fast Monte Carlo.

- Calorimeter dependent parameters:
  The default calorimeter dependent GFLASH parameters which are not calculated automatically are to some extend 'educated guesses'. They have to be defined with more care using measured values or detailed GEANT studies. The most important parameters of this category are the electromagnetic and hadronic sampling fluctuations and k_B factors (Birk's Law).

- Transition from the calorimeter region to other subdetectors:
  Decisions have to be made about how to handle parametrized showers which are leaking out of calorimeters into subdectors which are not defined via GEANT mixtures. Should e.g. leaking showers produce hits in the muon system?

- ... (this space left intentionally free)